12-1995

Expression and characterization of two alternatively spliced isoforms of rat type I receptor for inositol 1,4,5-trisphosphate

Doris Da May Lin
Yale University.

Expression and Characterization of Two Alternatively Spliced Isoforms of Rat Type I Receptor for Inositol 1,4,5-Trisphosphate

A Dissertation

Presented to the Faculty of the Graduate School

of

Yale University

in Candidacy for the Degree of

Doctor of Philosophy

by

Doris Da May Lin

Dissertation Director: Dr. William S. Agnew

December 1995

To my parents

Daniel & Judy Lin

with love

ACKNOWLEDGMENTS

This thesis will never be completed without the help from many of my mentors and friends. First, I thank my advisor Dr. William Agnew for his teaching, confidence, and support. He has led me to seeing Science from the eyes of a child - with awe, curiosity, imagination, and pure admiration for Nature - and has given me an environment to freely explore all that interested me. In the Agnew lab I have been fortunate to work with a fun and wonderful group of people, both in the past and the present. I thank Chinwe Ukomadu and Sunil Hingorani for teaching me biochemical techniques used in this project; Mark Emerick for his inspiring example of a thoughtful and disciplined scientist, and his devotion to many hours of discussion; Jerry Potts, Megan Stephan, Sally Tomiko, and Jim Trimmer for their help and encouargement; Maureen Peters, Said Bendahou and Melissa Regan in the Baltimore lab for all the attention and warmth during the short, frantic time I spent there toward the end of my thesis work.

I owe many thanks to members of my thesis committee, Len Kaczmareck, Sue Hockfield, Laurie Roman and Fred Sigworth, for their valuable guidance, criticism and support, especially after Bill has relocated the lab to Hopkins. The entire Neuroscience community and Physiology Department at Yale have also been graciouly supportive.

Dr. Sue Hockfield and the members of the entire lab, from whom I have learned all I know about immunohistochemistry, provided a friendly setting outside the Agnew lab. Dr. Ann Cornell-Bell, an undaunted scientist who always approaches science with enthusiasm and makes every task enjoyable, has most selflessly offered me much of her time and lab equipment for performing calcium imaging studies. I am grateful to Dr. Fred Sigworth for his evaluation of this work, and the many constructive suggestions in the data analysis.

Special thanks are due to Dr. Laurie Roman, who has been meticulously and tirelessly reading, critiquing my drafts, and has continually encouraged me. I have also made home away from my own in the labs of Kaczmareck, Sigworth, Roman, Moczydolowski and Forbush. I appreciate the friendship everyone has so generously offered throughout my graduate training at Yale, making these years all the more memorable.

Finally, the work would not be possible without the financial assistance from the M.D.-Ph.D. program. I am grateful to Marybeth Brandi for making my student life worriless and pleasant.

TABLE OF CONTENTS

LIST OF ILLUSTRATIONS

LIST OF TABLES

Chapter 1.

Introduction

Cells have evolved sophisticated systems to generate calcium signals in response to extracellular cues. The calcium signaling pathway plays an important role in many cellular processes, including fertilization and embryonic development, cell proliferation and transformation, neuroendocrine secretion, smooth muscle contraction, as well as neuromodulation and neuronal signaling (Balla & Catt, 1994; Berridge, 1993). One system involves inositol 1,4,5-trisphosphate (IP_3), which was established as a second messenger leading to mobilization of cellular calcium (Berridge & Irvine, 1984). IP_3 operates through specific receptors on intracellular membranes which resemble in many structural and functional features the calcium release channels (ryanodine receptors) of muscle. Since the purification and cloning of the IP_3 receptor, studies have provided some insight as to how IP_3 and its receptor function to generate complex calcium waves and oscillations.

The phosphoinositide second messenger cascade

In many cell types the binding of neurotransmitters, hormones, growth factors, or antigens to cell surface receptors results in activation of phospholipase C via either a G protein-dependent or a tyrosine kinase-linked mechanism (Berridge, 1987). Hydrolysis of a minor membrane phospholipid, phosphatidylinositol 4,5-bisphosphate (PIP_2) results in liberation of diacylglycerol and IP_3. Diacylglycerol remains membrane-bound and together with calcium activates protein kinase C. IP_3, released into the cytosol, triggers the release of calcium from intracellular stores and, perhaps by coupling with IP_4

or another second messenger, also promotes an influx of calcium from the extracellular medium (Fadool & Ache, 1994; Shirakawa & Miyazaki, 1994).

In addition to IP_3 and IP_4, other metabolites of the phosphoinositides may have additional roles as second messengers (Bansal & Majerus, 1990; Hokin, 1985). Figure 1-1 illustrates a simplified view of this signaling pathway. For simplicity the multitude of other cellular components; e.g., the surface receptors, GTP-binding proteins, phospholipase C, IP_3 receptor, and PKC have been omitted. Each component has multiple isoforms or isoenzymes. Despite the molecular heterogeneity, all these cellular components converge to a common theme of linking extracellular cues with a wide range of cellular activities through the phosphoinositide second messengers.

Calcium signaling

It is through calcium that IP_3 influences many cellular processes. Calcium plays an intimate role mediating cytoskeletal remodeling, stimulation of gene expression, excitation-contraction in muscles, stimulus-secretion coupling in secretory cells, and even cytotoxicity leading to apoptosis (Augustine & Neher, 1992; Connor *et al.*, 1990; Ebashi & Endo, 1968; Kennedy, 1989; Morgan & Curran, 1986; Neher, 1993; Nicotera *et al.*, 1992). It is therefore no surprise that cellular calcium levels are exquisitely controlled. At rest the intracellular free calcium is kept at 10^{-7} M, whereas the level is about 10^{-3} M in the external milieu and intracellular stores (Sambrook, 1990). Upon stimulation, the cytosolic calcium rises to 1.6×10^{-6} M, although the effective concentration of calcium near the active release site (e.g., adjacent to the membrane surface) may exceed 10^{-5} M (Nakayama & Kretsinger, 1994). Such fine regulation of intracellular calcium concentration is achieved by various cellular components: numerous cytosolic calcium-binding proteins (e.g., calmodulin, parvalbumin, calbindin, and calretinin) in addition to the intracellular membrane-bounded compartments (including endoplasmic

Figure 1-1. **The phosphoinositide second messenger cascade.** Phospholipase C (PLC) is activated through two major, or possibly three pathways. The first involves a GTP-binding protein (G) linked to various 7-membrane-spanning receptors (R). The surface receptor agonists include angiotensin II, vasopressin, bradykinin, serotonin, histamine, noradrenalin, glutamate, acetylcholine, TRH and TSH. The second pathway involves tyrosine kinase-linked receptors which are activated by antigens or growth factors such as PDGF and EGF. The third possibility is elevated $[Ca]_i$ caused by calcium influx through a channel on the plasma membrane. Upon activation, PLC hydrolyzes phosphatidylinositol 4,5-bisphosphate (PIP_2) in the plasma membrane to produce inositol 1,4,5-trisphosphate (IP_3) and diacylglycerol (DAG). IP_3 diffuses into the cytoplasm and activates calcium release from intracellular stores by binding to and activating IP_3 receptors on internal membranes. DAG, sometimes together with calcium, is an activator of protein kinase C (PKC). IP_3 is further metabolized both by kinases into higher intermediates (such as IP_4, IP_5 and IP_6, not shown in figure) and by phosphatases. Eventually IP_3 is dephosphorylated to inositol, which is the precursor for PIP_2. Lithium is an uncompetitive inhibitor of inositol monophosphatase as well as the $Ins(1,4)P_2/Ins(1,3,4)P_3$ 1-phosphatase.

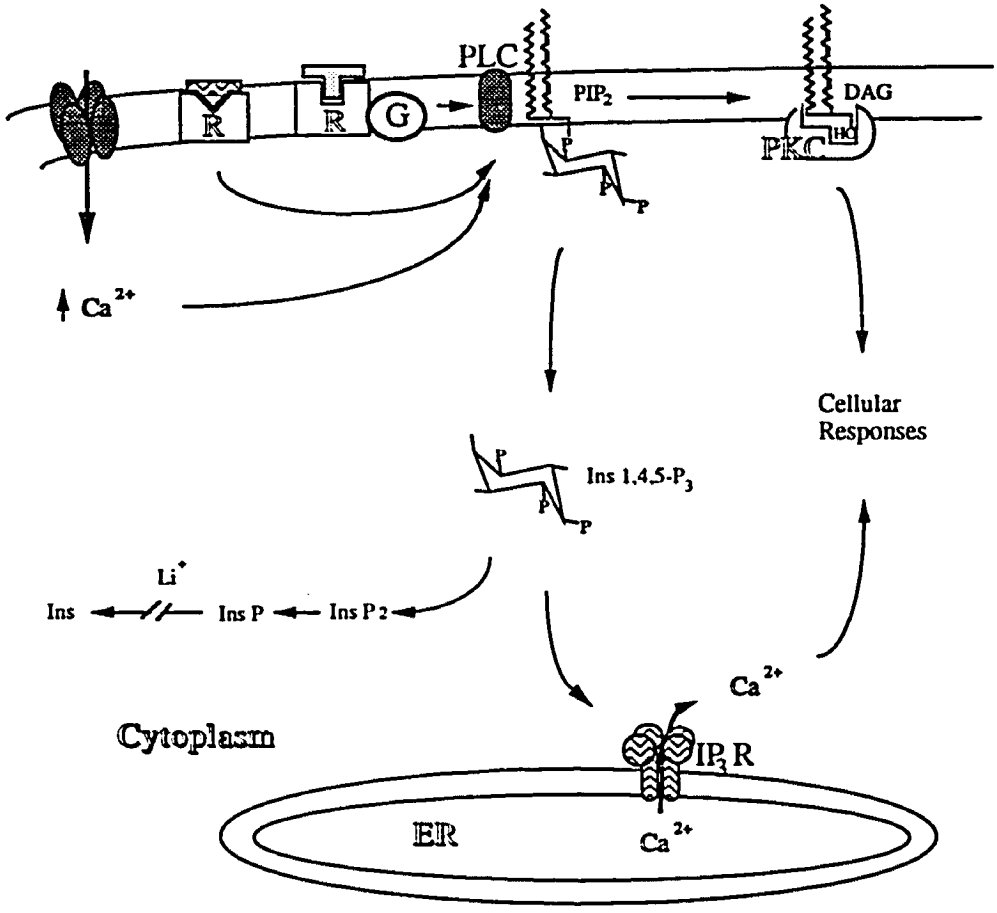

reticulum/sarcoplasmic reticulum, mitochondria, and nucleus) serve as a high-capacity calcium buffer. There are calcium channels residing on the surface membrane: voltage-gated channels in excitable cells and receptor-operated channels in both excitable and non-excitable cells (Bertolino & Llinas, 1992; Tsien & Tsien, 1990). In addition, ligand-gated calcium channels including the ryanodine receptor and IP_3 receptor are found in the non-mitochondrial intracellular organelles. Finally the calcium ATPases, which are located on the plasma membrane as well as the intracellular membranes of endoplasmic reticulum (ER) or sarcoplasmic reticulum (SR), extrude calcium across the plasma membrane or facilitate the reuptake into intracellular compartments to restore the low resting level in cytosol.

In many cell types, activation of the IP_3 system not only results in transient calcium mobilization, but triggers oscillatory patterns of calcium release which may spread in waves throughout the cell, and, in some cases, to neighboring cells that are coupled by gap junctions (Boitano *et al.*, 1992; Finkbeiner, 1992; Sanderson *et al.*, 1994). These waves may in part be propagated by calcium-induced calcium release, perhaps mediated by calcium-release channels homologous to the ryanodine receptor of skeletal muscle. The intercellular calcium waves provide a means for long-range signal propagation. The mechanism for the oscillatory calcium release is not completely understood, but may reflect a complex pattern of receptor activation, inactivation, and reactivation (Berridge, 1992; Meyer & Stryer, 1991). Calcium oscillations have been postulated to encode a frequency-modulated signal in response to increasing agonist concentrations, as opposed to one that is dependent of amplitude (Meyer & Stryer, 1991).

Ryanodine receptor and IP_3 receptor

Both the ryanodine receptor and the IP3 receptor are representative of a class of intracellular channels involved in mobilization of calcium in cells. They share many common structural and functional properties. The ryanodine receptor is classically considered the calcium-activated, caffeine- and ryanodine-sensitive calcium release channel in muscle cells (Fleischer & Inui, 1989; Meissner, 1994). Another second messenger, cyclic ADP-ribose has recently been shown to activate ryanodine receptor and has been proposed to be an endogenous agonist in non-muscle cells (Galione, 1993; Lee *et al.*, 1994). The subtype of ryanodine receptor in skeletal muscle forms the prominent "foot processes", a tetragonal structure seen with freeze-fracture and negative-staining EM (Block & Franzini, 1988; Lai *et al.*, 1989). These foot processes span the junctional gap between two separate but closely apposed membrane systems, the transverse-tubule (t-tubule) and SR. Together with the t-tubule dihydropyridine receptor, the ryanodine receptor provides the structural and functional basis for excitation-contraction coupling in skeletal muscles (Anderson *et al.*, 1989; Saito *et al.*, 1988). In cardiac muscles and perhaps many other cell types including neurons the ryanodine receptor operates through a calcium-induced calcium release (CICR) mechanism.

In skeletal muscle cells only the ryanodine-sensitive calcium stores play an important role in mobilizing intracellular calcium stores. In contrast, in the *Xenopus* oocyte the IP3-induced calcium release (IICR) dominates. In many other cells, however, both ryanodine and IP3 receptors coexist. Cerebellar Purkinje neurons contain both receptors. Ellisman and coworkers have demonstrated with immunogold electron microscopy that the two receptors have overlapping but different intracellular distributions in the avian Purkinje neuron. While both receptors are found throughout the intracellular compartments of the axon, soma and dendritic shafts, only IP3 receptors are present in dendritic spines (Ellisman *et al.*, 1990; Walton *et al.*, 1991). This

suggests that the calcium signal in various neuronal compartments has different mechanism of generation, likely subserving different functions.

Primary structure of the cerebellar IP3 receptor

The IP3 receptor was first cloned from mouse cerebellum by Mikoshiba and coworkers (Furuichi *et al.*, 1989). The protein with which they were working, designated P400, had been identified originally as a particularly abundant cerebellar protein that was an exceptionally good substrate for phosphorylation by the catalytic subunit of cAMP-dependent protein kinase (PKA) (Maeda *et al.*, 1988; Mikoshiba *et al.*, 1985). It was after developing methods for its cloning and expression that the identity of the protein was revealed (Furuichi, 1989; Maeda *et al.*, 1990).

The primary structure of the cerebellar IP3 receptor is similar, and indeed homologous, to that of the ryanodine receptor located in SR of the skeletal muscle. The open reading frame of gene encodes a polypeptide of 2749 amino acids, with a molecular weight of 313 kD. Inspection of the primary sequence (see Figure 1-2) reveals a large hydrophilic segment extending from the amino-terminus to residue 2276 (i.e., more than 80% of the polypeptide length). This is followed by six or eight hydrophobic segments, each sufficiently long to span the membrane bilayer. A hydrophilic carboxyl-terminus runs from residue 2589 to 2749. Thus, the protein consists of an extremely elaborate hydrophilic amino terminus shown by immunocytochemistry to lie in the cytoplasm, followed by a small integral membrane domain of 313 residues about 10% of the entire subunit, and finally a short carboxyl terminal tail also located in the cytoplasm (Figure 1-2).

By measuring IP3 binding to various truncated forms of the receptor, Mignery and coworkers localized the IP3 binding region to the N-terminal one-fourth of the receptor (Mignery & Sudhof, 1990; Sudhof *et al.*, 1991). By photoaffinity labeling the

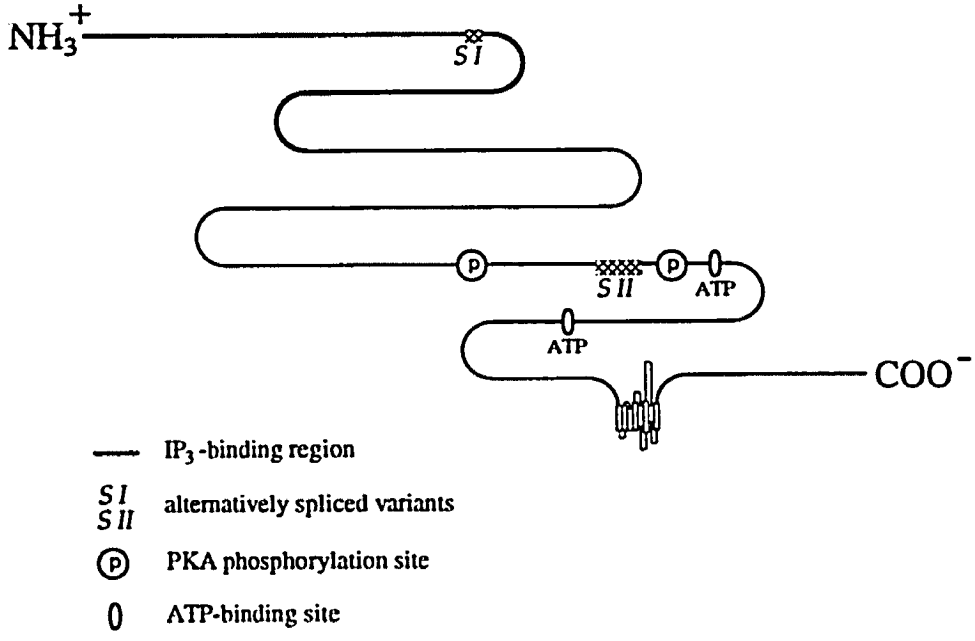

Figure 1-2. Schematic illustration of the $InsP_3$ receptor subunit.

binding domain was further refined to residues 476-501 (Mourey *et al.*, 1993). This places the ligand-recognition site some 1400 amino acids away from the transmembrane region. The extensive interim sequence contains sites for ATP interaction as well as phosphorylation by a number of kinases. This segment is dubbed the "coupling region" which transduces the IP_3-binding event to channel opening, likely by means of an extensive conformational change (Mignery & Sudhof, 1990).

Analogous to the ryanodine receptor, the IP_3 receptor forms a tetrameric complex. Gel-filtration column chromatography gives an estimated molecular weight for the native IP_3 receptor of ~1,000 kD, consistent with a complex of four 260-kD subunits (Supattapone *et al.*, 1988b). This tetrameric arrangement is further supported by chemical cross-linking studies (Maeda *et al.*, 1991). Each receptor molecule forms a characteristic four-leaf clover (or quatrefoil) structure reminiscent of the foot structure of the ryanodine receptor (Maeda, 1988).

Molecular heterogeneity

Soon after the cloning of the first mouse cerebellar receptor, many more receptor variants were discovered (Blondel *et al.*, 1993; De Smedt *et al.*, 1994; Kume *et al.*, 1993; Maranto, 1994; Mignery *et al.*, 1990; Ross *et al.*, 1992; Sudhof, 1991; Yamada *et al.*, 1994; Yamamoto *et al.*, 1994; Yoshikawa *et al.*, 1992). To date all of these are derived from five distinct genes, and share an extensive (70-80%) homology in amino acid sequence (Blondel, 1993). They have a differential tissue distribution, summarized in Table 1-1. It appears that, at least at the level of mRNA expression, receptors of types I-IV are all expressed in cerebellum. It is not known, however, whether they coexist within the same cell. There are no functional differences attributed to these isoforms, except slight variations in affinity for IP_3 among isoforms expressed from cDNAs (Newton *et al.*, 1994; Sudhof, 1991). These isoforms however have the most divergent sequences in the

Table 1-1. Summary of Different IP_3 Receptors and Their Tissue Distribution

type	species	tissue source: predominant		secondary		reference
InsP3R-I	mouse rat human *Xenopus laevis*	cerebellum brain kidney		spinal cord adrenal	lungs spleen	Furuichi (1989) Mignery (1990) Yamada (1994) Kume (1993)
InsP3R-II	rat mouse (partial) human	brain lungs placenta	testes	liver kidney	spinal cord cerebellum	Südhof (1991) Ross (1992) Yamamoto-Hino (1994)
InsP3R-III	rat mouse (partial) human	brain lungs thymus spleen	GI testes	liver kidney placenta cerebellum		Blondel (1993) Ross (1992) Yamamoto-Hino (1994)
InsP3R-IV	mouse (partial)	brain cerebellum spinal cord placenta testes		lungs kidney GI liver		Ross (1992)
InsP3R-V	mouse (fibroblast $C_3H10T_{1/2}$ cells)					De Smedt (1994)

long "coupling domain" with which many modulators interact, suggesting that they are subject to different regulation.

In addition to the isoform diversity resulting from the existence of five distinct genes for IP_3 receptor, further complexity is generated by alternative splicing of pre-mRNA from each individual gene. This has been described for type I receptor, which contains two regions, *SI* and *SII* (see Figure 1-2), subject to multiple variant sequence combinations (Mignery, 1990; Nakagawa *et al.*, 1991a; Nakagawa *et al.*, 1991b). The *SII* region is present in most neuronal receptors. Flanked by two consensus sites for PKA phosphorylation within the coupling domain, *SII* was found to influence which site is preferentially phosphorylated (Danoff *et al.*, 1991). The expression of each subtype of the type I receptor varies among brain regions and appears to be subject to tissue-specific and developmental regulation (Nakagawa, 1991a).

Biochemical properties

The abundance of IP_3 receptor in mammalian cerebellum has allowed its first biochemical isolation. As cited, Mikoshiba and coworkers, studying glycoprotein P400, developed a purification scheme well before recognizing that the molecule was the IP_3 receptor. In studies directed specifically to the IP_3 binding component from rat cerebellum, Supattapone *et al.* (1988) reported the first purification of active receptor. In cerebellar membrane solubilized with nonionic detergent, specific IP_3-binding sites were estimated to be at a concentration of 6 pmol/mg total protein. IP_3 bound with K_d ~80 nM. The IP_3 receptor was purified approximately 1,000 fold from the detergent extract by four steps involving ion exchange, concanavalin A- and heparin-agarose affinity chromatography and gel filtration. The final preparation bound [^{3}H]-IP_3 with a specific activity of ~4,000 pmol/mg protein and K_d = 100 nM. The purified protein appeared on denaturing gels as a single polypeptide of 260 kD. This is significantly

smaller than the size predicted by the nucleic acid sequence (313 kD), suggesting anomalous mobility in SDS-polyacrylamide gels or post-translational modifications such as partial proteolysis that reduce the size of the protein.

The measurements of equilibrium binding constants from different receptor preparations have been variable, partly due to the lack of a reliable quantitative assay. A rapid and quantitative ion exchange assay for [^{3}H]-IP$_3$ binding was therefore developed by Hingorani and Agnew (Hingorani & Agnew, 1991). This assay has detected 4-5 fold more receptor binding sites in detergent extracts of cerebellum than the original spun-column gel filtration assay, and first revealed evidence for two classes of binding sites. One class was present at approximately the level described by Supattapone *et al.* (6-8 pmol/mg protein) but bound IP$_3$ with high affinity (K_d=4-6 nM). The second class of sites was more abundant (20-22 pmol/mg protein) but bound ligand with affinity similar to that described by Supattapone *et al.* (K_d=100-150 nM). It was further found that these two classes of sites can be differentiated on the basis of their sensitivity to calcium and temperature, suggesting functional heterogeneity in the cerebellar preparation (Hingorani, 1994).

IP$_3$-activated calcium release

The purified IP$_3$ receptor protein was first demonstrated by Ferris *et al.* to have an intrinsic channel activity by $^{45}Ca^{2+}$-flux assays (Ferris *et al.*, 1989). At the single-receptor level with cerebellar microsomes incorporated into a planar lipid bilayer, Ehrlich and coworkers detected rapid channel activity in response to IP$_3$ (Bezprozvanny *et al.*, 1991; Ehrlich & Watras, 1988). The mean open time was less than 10 ms and there was evidence of four single-channel conductance levels, each of ~20 pS. From these analyses no cooperativity in the effects of IP$_3$ binding was evident (Hill coefficient of 1). Studies by Meyer and coworkers on permeabilized rat basophilic

leukemia cells, however, suggest a highly cooperative process (n_H=3) in IP3-mediated calcium release (Meyer *et al.*, 1988; Meyer *et al.*, 1990). It is not clear whether the discrepancy between these reports reflects an actual difference in the properties of receptors or differences in methodology.

Muallem and coworkers, studying IP3-mediated, hormone-evoked calcium release from intact pancreatic acini, first described a process of "quantal calcium release" (Muallem *et al.*, 1989). They observed that submaximal hormone concentrations released only a fraction of intracellular $^{45}Ca^{2+}$, after which intracellular calcium content remained constant until the application of a higher dose of hormones. This was in contrast to a continuous release process mediated by ionomycin, a calcium ionophore. Increasing concentration of ionomycin resulted in increasing rate of release, and each application resulted in complete emptying of intracellular calcium stores. Similar observations have subsequently been recorded using several different cells, either intact or permeabilized, as well as using purified, reconstituted IP3 receptors (Bootman *et al.*, 1992; Ferris *et al.*, 1992; Missiaen *et al.*, 1992b; Taylor & Potter, 1990). Desensitization of the IP3 receptor did not explain this process, since the cells or reconstituted purified receptors retain full responsiveness to a stimulus following previous exposure to IP3. Other possibilities, such as IP3 metabolism or the rapid attainment of steady state in which release and uptake of calcium are balanced, were also ruled out by the use of a non-metabolizable IP3 thio-analog , Ins(1,4,5,)P3[S]3 in the former (Taylor & Potter, 1990) and the inclusion of vanadate to inhibit Ca^{2+} re-uptake in the latter (Muallem, 1989).

The mechanism underlying quantal calcium release property of the IP3 receptor is still unclear. In their original report, Muallem *et al.* proposed that quantal release resulted from the complete emptying of discrete intracellular stores which varied in their sensitivity to IP3 (all-or-none model). Irvine proposed an alternative model, in which

the quantal response is derived from the rapid attenuation of calcium release from intracellular stores that are homogeneously sensitive to IP_3 (Irvine, 1990). In this scheme, the sensitivity of IP_3 receptor is progressively decreased in response to the reduction of luminal calcium concentration, probably by means of a calcium-sensing protein such as calreticulum, calsequestrin, or the receptor itself.

Cytosolic calcium feedback mechanism

The action of calcium on IP_3 receptor is complex and somewhat confusing, partly due to the tissue-specific variations of different receptor preparations. Calcium inhibits [^{3}H]-IP_3 binding to cerebellar membranes (Worley *et al.*, 1987), enhances binding in liver (Pietri *et al.*, 1990), but has no effect in IP_3 binding to its receptor in vas deferens (Mourey *et al.*, 1990). The inhibitory effect of calcium in cerebellum has been ascribed to an accessory integral membrane protein, not as yet purified, designated calmedin. It was observed by Supattapone *et al.* (1988) that the cerebellar IP_3 receptor binding in the detergent extract was extremely sensitive to low concentrations of free calcium (50% inhibition at 0.3 μM). However, following partial purification, this inhibition was lost. Subsequent studies have indicated that calcium sensitivity requires interaction with calmedin, which is enriched in cerebellum but low in peripheral tissues. Preliminary sizing experiments suggest calmedin a 250-300 kD protein (Danoff *et al.*, 1988). This molecule, however, may not represent a universal mechanism mediating calcium sensitivity on IP_3 receptors. Based on the studies using bovine cerebellar preparations, Mignery has proposed that excess IP_3 is produced due to a calcium-sensitive isoform of PLC. The IP_3 then competes with [^{3}H]-IP_3 binding and results in apparent inhibition (Mignery *et al.*, 1992).

Calmedin is reported to be present only at a low level in liver. There is nevertheless a calcium sensitivity displayed by hepatic type IP_3 receptor. The effect of

calcium, however, appears quite different from that observed in cerebellar receptors. In the liver, micromolar amount of calcium enhances IP_3 binding to the receptor instead of inhibiting it. Calcium has been shown in liver microsomes to act as an allosteric modulator, promoting the interconversion of two affinity states of the receptor (Marshall & Taylor, 1994; Pietri, 1990). The receptor in its low-affinity (K_d=20-60 nM) and activated (A) state can be shifted by micromolar amount of calcium to a high-affinity (K_d=1-3 nM) and inactive (I) state (Mauger *et al.*, 1994).

Finally, the regulatory effect of calcium on IP_3 receptor/channel activity is concentration-dependent. Cytosolic calcium feeds back with dual effects: at the submicromolar range calcium stimulates IP_3-activated calcium release, with the maximal effect occurring sharply around 100-300 nM; beyond 300 nM its effect on the receptor becomes inhibitory. This biphasic profile has been demonstrated in smooth muscle fibers using imaging techniques (Iino & Endo, 1992), by calcium flux in microsomal vesicles resolved by rapid superfusion (Finch *et al.*, 1991), as well as at the single receptor level in a planar lipid bilayer (Bezprozvanny, 1991). The implication is that calcium at a very low concentration actually acts as a co-agonist for the IP_3 receptor so that calcium-induced calcium release is not unique to the ryanodine receptor (although the range of action for these two receptors is different). This positive component of feedback regulation by calcium offers an explanation for the oscillatory activity of calcium release through IP_3 receptors.

Receptor regulation by pH, ATP, sulfhydral reagents, and phosphorylation

In addition to calcium, there are a number of agents capable of modifying receptor function. First, IP_3 binding in solubilized receptors as well as IP_3-stimulated calcium release are favored by alkaline pH within the physiologic range (Joseph *et al.*, 1989; Worley, 1987). The binding capacity is tripled between pH 7.5 and 8.5. Next,

adenine nucleotides allosterically regulate IP_3 receptor in a biphasic manner. Monitoring IP_3-induced calcium flux in purified receptors in reconstituted vesicles, Ferris *et al.* noted that ATP, between 1 and 10 μM, cooperatively enhanced calcium flux, but had a reversed effect between 0.1 and 1 mM concentration. When the reconstituted, purified receptors were studied in a planar lipid bilayer, Mikoshiba and coworkers discovered that both the open probability and the channel conductance were increased by micromolar amount of ATP (Maeda, 1991), although another group reported that only the open probability of the channel was altered (Bezprozvanny & Ehrlich, 1993; Ehrlich & Watras, 1988). The stimulatory effect of ATP may be mediated through direct binding of ATP to the IP_3 receptor. Two putative adenine-nucleotide binding sites (gly-X-gly-X-X-gly) have been identified in the coupling region of the cerebellar IP_3 receptor as illustrated in Figure 1-2 (Furuichi, 1989). The inhibitory effect, on the other hand, was thought to arise from competition between ATP and IP_3 for the IP_3 binding site (Bezprozvanny & Ehrlich, 1993).

Additional evidences for allosteric modulation of the receptor come from work with thimerosal (TMS), a sulfhydral oxidizing agent. In different systems involving permeabilized hepatocytes, liver and cerebellar microsomes, as well as purified and reconstituted cerebellar receptors, TMS was found to elicit increase in IP_3 binding affinity without affecting B_{max}, resulting in augmented calcium flux (Hilly *et al.*, 1993; Kaplin *et al.*, 1994). The high-affinity and active state of the hepatic IP_3 receptor stabilized by thiol reagents is distinguished from its high-affinity but inactive state promoted by high concentration of calcium. The hepatic receptor in these two states displays similar equilibrium constants but has different kinetic parameters, suggesting that the receptor has a rather complex biochemical behaviour (Hilly, 1993).

Finally, purified IP_3 receptors can be phosphorylated by PKA, PKC, CaM kinase II and cGMP-dependent protein kinase, providing another level of functional regulation

as well as a means of "cross-talk" among various second messenger pathways. Phosphorylation is stoichiometric as well as additive with the first three enzymes, suggesting that they act on distinct sites on the receptor (Ferris *et al.*, 1991; Supattapone *et al.*, 1988a). At least in the smooth muscle IP_3 receptor, PKA and PKG appear to act on the same site (Komalavilas & Lincoln, 1994). Phosphorylation of the receptor by both PKA (Nakade *et al.*, 1994) and CaM kinase II (Zhang *et al.*, 1993) has been demonstrated to increase IP_3-induced calcium release.

Clinical correlation

With the IP_3 receptor being a member of a multi-gene family and ubiquitously involved in an important pathway of signal transduction, it will be difficult to believe that it is not affected in certain hereditary disorders. So far, however, there is only circumstantial evidence relating it to pathological states, mostly by affecting intermediary metabolites or enzymes in the polyphosphoinositide cascade rather than the receptor itself.

Of particular interest is the finding of a defective gene in Lowe's oculocerebrorenal syndrome, an X-linked developmental disorder affecting lens, brain, and kidneys (Attree *et al.*, 1992). The gene encodes an enzyme, polyinositol phosphate 5-phosphatase, which directly affects the metabolism of IP_3.

In addition, the inositol phosphate cascade may be linked to manic-depression bipolar disorder. When released, IP_3 is eventually completely dephosphorylated by specific phosphatases and resynthesized into the primary substrate for phospholipase C, PIP_2. The phosphatases (specifically, the inositol monophosphatases) involved in the cycle are especially sensitive to inhibition by lithium, and chronic exposure to lithium consequently reduces phosphatidylinositol pools (Nahorski *et al.*, 1991). It has been

proposed that dampening of this cycle may account for the effectiveness of lithium treatment of manic depressive illness (Kofman & Belmaker, 1993).

A number of mouse neurological mutants are found to have degeneration of Purkinje neurons and disrupted synaptic connectivity associated with a drastically attenuated expression level of the IP3 receptor. These animals suggest corresponding human disorders may exist.

Finally, recent cloning of human genes encoding different IP3 receptor types and their chromosomal maps may facilitate establishing the linkage with any human genetic defects (Yamada, 1994; Yamamoto, 1994).

The present thesis work

This thesis work was begun at the time the biochemical isolation of cerebellar receptor was just made possible and the first IP3 receptor was cloned. I was intrigued by the molecular characteristics of this calcium-signaling molecule in relation to its function and regulation. I was also interested in finding variant receptors for IP3 by molecular cloning techniques. A number of other laboratories were dedicated to the project at the same time, rapidly expanding the repertoire of IP3 receptor isoforms. As the complexity of this receptor class continues to unfold, however, we still have little insight on the functional significance of diversity. By combining molecular biology and gene expression, I could hope to devise a simple preparation of the receptor for detailed biochemical characterization and to examine, specifically, the property of different isoforms. Initially I have limited my attention to two identified splice variants of the type I receptor in attempt to address three questions: (1) Can the cDNA be expressed to form functional receptors when transfected in mammalian cells? (2) What are the biochemical properties of the singly expressed receptor? (3) Do the two receptor splice variants have different functions?

In addressing these questions I have organized the work into three sections. First in Chapter 3, the generation and characterization of molecular markers for the IP_3 receptor are described. The antibodies developed have laid the foundation for studying the receptor expression throughout this research, and have contributed to other work in collaboration. In Chapter 4 an effective expression system is described for the two splice variants of IP_3 receptor. In both transient and stable expression systems a properly glycosylated protein serving as a PKA phosphorylation substrate is capable of assembling into a tetra-oligomeric complex which specifically binds IP_3. Moreover, the transient system is useful for additional structure-function studies which will be described. Finally, a detailed biochemical characterization is carried out for both isoforms using the stable expression system. In Chapter 5, I show that each receptor exhibits a complex binding profile and that the two isoforms differ in their response to the inhibitory feed-back control by calcium. The evidence for their functional difference is provided by binding assays as well as imaging of the IP_3-activated calcium transients.

Chapter 2.

Materials and Methods

Materials

An adult Sprague-Dawley brain λgt10 cDNA library was purchased from Clontech Laboratories (Palo Alto, CA). The expression vectors pCB1 and pCB6 were originally constructed by Drs. D. Russell, M. Roth, and C. Brewer (University of Texas Southwestern Medical Center). The partial cDNA clone for the rat type I IP_3 receptor was constructed by Dr. Gregory Mignery at the University of Texas Southwestern Medical Center (Mignery, 1990) and kindly provided by Dr. Laurie Roman (Yale University). The HEK293 cells were a gift from Dr. Ron Kopito (Stanford University).

The glutathione agarose beads and protein A-Sepharose CL-4B were purchased from Sigma (St. Louis, MO). ^{35}S-methionine (1000 Ci/mmole), α-^{32}P-dCTP, α-^{35}S-dATP and Enhanced Chemiluminescence (ECL) kit were purchased from Amersham (Arlington Heights, IL). ^{125}I-Protein A was from ICN (Costa Mesa, CA), γ-^{32}P-ATP and [^{3}H]-inositol-1,4,5-trisphosphate were from Du Pont New England Nuclear (Boston, MA). The catalytic subunit of cAMP-dependent protein kinase (PKA) was from Promega (Madison, WI). All restriction endonucleases were obtained from New England Biolabs (Beverly, MA) or Boehringer Manheim (Indianapolis, IN).

Horseradish peroxidase (HRP)-, rhodamine-, and fluorescein isothiocyanate (FITC)-conjugated goat anti-rabbit antibodies were from Cappel (Philadelphia, PA). Obtained from BRL (Bethesda, MD) were prestained molecular weight standards, which included myosin (228 kD), phosphorylase b (108), bovine serum albumin (69), ovalbumin (46), carbonic anhydrase (30), β-lactoglobin (18) and lysozyme (14). Dowex

AG 1-X2 resin and all chemical reagents for electrophoresis were from Bio-Rad (Richmond, CA). Geneticin (G-418 sulfate) and Dulbecco's modified Eagle's medium (DMEM) and other special culture media were purchased from GIBCO BRL Life Technologies (Gaithersburg, MD), fetal calf serum was from Hyclone Laboratories (Logan, UT). Sulfo-*m*-maleimidobenzoyl-N-hydroxysuccinimide ester (Sulfo-MBS) was from Pierce (Rockford, IL). Concanavalin A-agarose and wheat germ agglutinin were purchased from EY labs (San Mateo, CA). Fluo-3 was from Molecular Probes (Eugene, OR). Pansorbin, tunicamycin, angiotensin II, and myo-D-inositol 1,4,5-trisphosphate were from Calbiochem (La Jolla, CA). All the other chemicals were purchased from Sigma (St. Louis, MO).

Methods

Mouse mRNA PCR fragments

Total cellular RNA was isolated from adult mouse cerebellum using guanidine isothiocyanate (Chirgwin *et al.*, 1979) followed by cesium chloride density gradient centrifugation as described by Sambrook *et al.* (Sambrook *et al.*, 1989). 10 µg of the total RNA was reverse-transcribed with Moloney murine leukemia virus reverse transcriptase with oligo-dT primers, random hexamers or downstream polymerase chain reaction (PCR) primers. About 1/5 of the resulting cDNA was used as the template for each PCR amplification with Taq DNA polymerase using a Perkin-Elmer/Cetus thermal cycler.

Oligonucleotide primers were prepared for sequences flanking three specific regions within the open reading frame of the mouse receptor for IP_3. As illustrated in Figure 2-1, the first (simply referred to as 5') corresponds to amino acids 419-572, lying well inside the open reading frame near the predicted amino terminus. The second

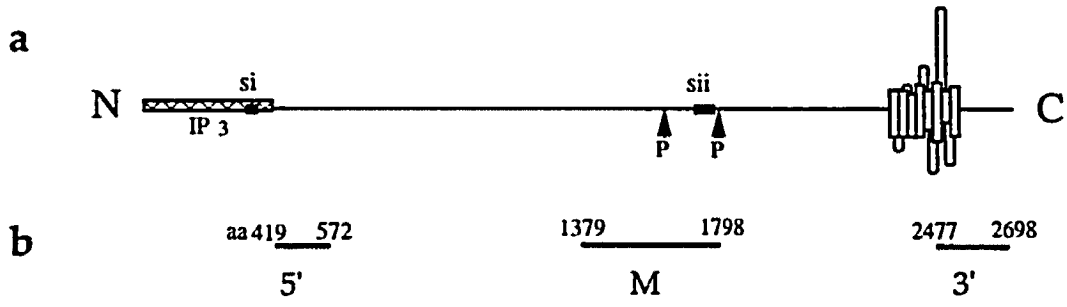

Figure 2-1. cDNA fragments generated by polymerase chain reaction from reverse-transcribed mouse cerebellar mRNA. In (a) is a schematic depiction of the type I IP_3 receptor polypeptide. In (b), the three PCR products are aligned. These fragments have been named after their approximate location in the coding sequence; i.e., 5', M (for middle), and 3'. The corresponding amino acid residues of the IP_3 receptor are provided.

(designated M) corresponds to sequences encoding amino acids 1379-1798, midway between 5' and the predicted membrane spanning region. The last (3') corresponds to amino acids 2477-2698, encompassing the last two membrane spanning segments and extending well towards the carboxyl terminus.

The fragments internal to these primers were amplified by PCR following standard protocol and recommendations (Innis *et al.*, 1990). Typically the reaction involved 30 cycles of 1 minute of denaturation at 95°C, 1 minute of annealing at 50-60°C, followed by 2 minutes of primer extension at 72°C. Cycling was concluded with a final extension at 72°C for 5 minutes. The amplified cDNA fragments were ligated into pBluescript (Promega Biotech) and sequenced from both ends. They were subsequently used for preparing probes for library screening and for the construction of fusion protein antigens as described below.

Screening the rat brain cDNA library

PCR fragments 5', M, and 3' (Figure 2-1) were radiolabeled by primer extension with random primers modified from Keller & Manak (Keller & Manak, 1989) using α-^{32}P-dCTP (specific activity > 3000 Ci/mmole, 10 μCi/μl) and Klenow fragment of *E.coli* DNA polymerase I. The radioactive probes were then used to screen a commercially available rat brain λgt10 cDNA library (Clontech) using methods described by Huynh *et al.* (Huynh *et al.*, 1989).

Initially ten clones were isolated: four from 5', three from M and four from 3'. Reciprocal dot blot hybridization (Sambrook, 1989) was performed to ascertain overlaps, and all clones were end-sequenced for alignment. Four clones were selected (1B, 6, 3mA, and 2A), that encompass nearly the complete open reading frame (together with 5' and 3' untranslated sequences), and their location depicted in Figure 2-2. Two gaps remained, a 216 nucleic acid fragment between bases 3806 and 4022, and a 643

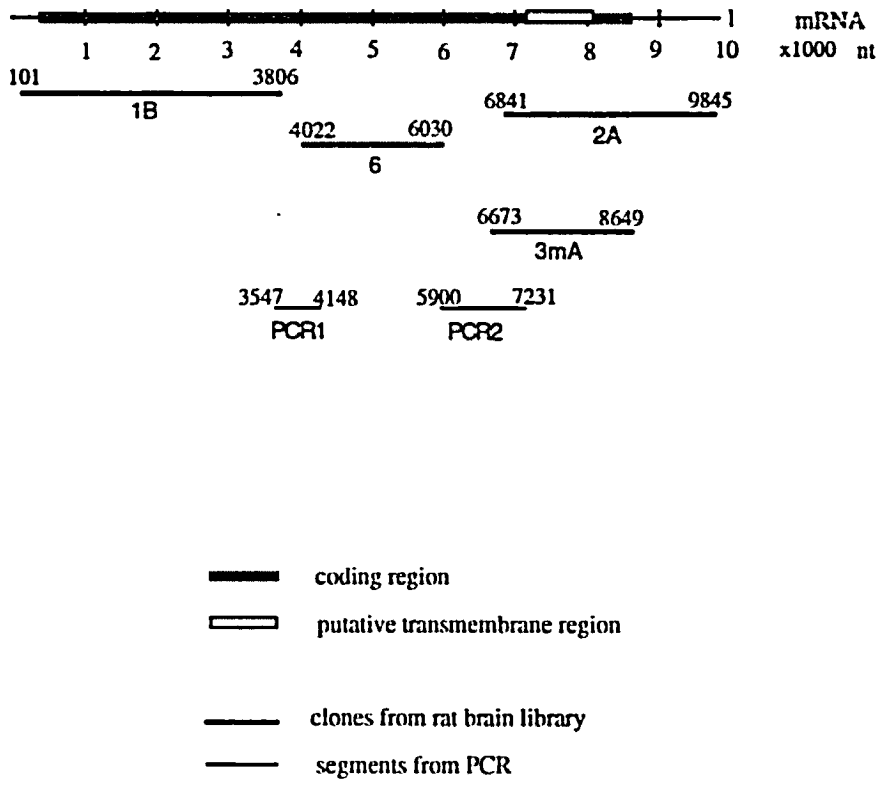

Figure 2-2. Summary of cDNA fragments obtained from screening a rat brain library and from polymerase chain reaction of reverse transcribed rat cerebellar mRNA. On top is a schematic map of the receptor mRNA (containing 5' and 3' untranslated regions as well as the coding region). Below, each fragment is aligned and its nucleotide number indicated on both ends. Only the longest, non-overlapping clones isolated from the library are shown. nt = nucleotide

base gap between bases 6030 and 6673. PCR fragments with built-in restriction sites were then generated to fill these two gaps (Figure 2-2).

Construction of recombinant cDNA for IP_3 receptor

The full-length cDNA for rat cerebellar IP_3 receptor was constructed by splicing the fragment 1B described above with a partial clone obtained from Mignery (Mignery, 1990) at Kpn I site. This full-length clone was found to contain the *SII* region, as expected in neuronal form of the receptor, but lacked the *SI* sequence. *SI* region with additional sequences flanked by native Bgl I and Kpn I sites was therefore obtained by PCR using two primers (nt 1137-1158 and complimentary nt 1581-1602). The PCR product was purified and spliced with the full-length clone, and was sequenced to confirm its authenticity. Both cDNA clones were modified at the 5' end by Afl III restriction enzyme cleavage to rid most of the 5' untranslated sequences. This end was further modified with a Bam HI linker and the 8.3-kb fragment (between Afl III and Xba I) was ligated into the expression vector, pCB6 at Bgl II and Xba I sites. The Bgl II site was subsequently lost because of the ligation with the compatible but dissimilar ends of Bam HI sequences. The full-length construct lacking *SI* region was named IP_3R-F or simply F, and the construct containing *SI* was named IP_3R-G or G.

Construction of truncated receptor cDNAs

Nf or Ng represent the N-terminal portion of full-length rat type 1 IP_3R isoforms, F or G, respectively, up to the Bst BI site just before the start of the transmembrane region (refer to Figure 4-1b). Each cDNA fragment was spliced into the expression vector, pCB1. The expressed protein had a calculated MW of 238 kD.

Construct "C" is a truncated version of the IP_3R that starts at the transmembrane region and ends at the C-terminus (nt 7002-end, aa 2225-2859; see

Figure 4-1b). It was constructed by ligating the Bst BI-Xba I fragment with a synthetic adapter at the 5' end containing a new built-in restriction site of Bam HI and an optimal initiation leader sequence (Kozak, 1986). The adapter was made by annealing two oligonucleotides with sequences (5'→3') GATCCCAGCCATG and CATGGCTGG. The fragment was then spliced directionally into pCB6 vector at Bgl II/Xba I sites. This yielded an expressed protein of 70 kD computed MW.

Construction of fusion protein antigens

The bacterial expression vectors, pGEX (Smith & Johnson, 1988) were used for subcloning the various cDNA segments of the mouse cerebellar IP_3 receptor, and for generating fusion polypeptides with the C-terminus of the *Schistosoma japonicum* glutathione S-transferase.

Four fusion protein antigens were prepared, each named by its approximate location in the receptor primary sequence with a prefix "fp", denoting fusion protein. Fp-5' (nucleotides 1586-2045) was constructed by splicing a 460 bp RsaI fragment of the receptor cDNA into pGEX-3X at Sma I site; fp-m (4466-5723), Sac I-Taq I fragment in pGEX-2T at Sma I site; fp-3'α (7761-8027), Pvu II-Hph I fragment into pGEX-I at Sma I; and fp-3'β (8140-8421), Bgl II-Sma I fragment directionally into Bam HI and Sma I sites. Each recombinant was sequenced up to the first 200 base pairs to confirm the correct reading frame.

Procedures for preparing fusion proteins were adopted from that of Smith & Johnson (1988). Overnight cultures of recombinant-transformed *E.coli* bacterial strain XL1-Blue were diluted 10 fold (to ~0.1-0.2 O.D. at 600 nm) into 400-500 ml of fresh Luria-Bertani (LB) broth and incubated at 37°C with vigorous aeration for one hour or until the O.D. reached 0.4-0.5. IPTG was then added to 0.1 nM, and the incubation continued for additional 3-4 hours. The cells were pelleted, resuspended in a solution of

1% Triton X-100 in PBS (TPBS), lysed on ice with brief bursts of sonication for a total duration of 1 minute. The lysate was centrifuged at 10,000 rpm for 5 minutes at 4°C.

In the case the fusion product was soluble (e.g., fp-3'α), the supernatant was collected and mixed with 1 ml of a 50% (w/v) slurry of glutathione agarose beads (Sigma), incubated for 5 minutes at 4°C. The beads were collected following a brief centrifugation on a table top clinical centrifuge, washed 3 times in TPBS, and the fusion protein was eluted with 1 ml of 50 mM Tris HCl, pH 7.2 containing 5 mM of reduced glutathione (Sigma). Aliquots were prepared for SDS-PAGE analysis. The beads were recycled by washing with 3 M NaCl and stored at 4°C in PBS at 50% (w/v). In case the fusion polypeptides were insoluble (e.g., fp-5', m, and 3'β), SDS-polyacrylamide gel purification followed by electroelution was performed as described by Hunkapiller (Hunkapiller *et al.*, 1983).

All of the isolated fusion proteins were confirmed to contain the core protein of glutathione S-transferase by Western immunoblot using a polyclonal antibody (anti-DRK1) developed in the laboratory (Trimmer, 1991) against a potassium channel segment spliced with the transferase. These fusion protein antigens were then sent to the Pocono Rabbit Farm & Labs for raising polyclonal antibodies in rabbits.

Design of type I receptor-specific synthetic peptide antigens

The amino acid sequences of type I (Mignery, 1990) and type II (Sudhof, 1991) rat IP3 receptors were compared, and two segments were chosen for chemical synthesis of the peptide antigens. Sp-2A is a 16-amino acid piece (amino acids 1745-60 of rat type I receptor) within the region encompassed by fp-m. It includes one of the two consensus sites for PKA phosphorylation. Sp-3A (amino acids 2485-2501 of type I), a 17-amino acid piece within fp-3'α, has unique sequences not found in the similar region

of ryanodine receptor (Furuichi, 1989) and significantly different from the sequences in the published type II-IV receptors (Blondel, 1993; De Smedt, 1994; Ross, 1992).

The peptides were synthesized by Multiple Peptide Systems (San Diego, CA) with an additional cysteine residue at the carboxyl termini. Each was coupled to Keyhole Limpet Hemocyanin (see below), and sent to the Pocono Rabbit Farm & Labs for polyclonal antibody production.

Coupling of synthetic peptides to Keyhole Limpet Hemocyanin (KLH)

G-50 Sephadex (Pharmacia) was first swollen in distilled water overnight at room temperature, then equilibrated in 50 mM NaPi, pH 6.0. A column was prepared by packing the beads in a disposable glass Pasteur pipette plugged by a small amount of glass wool.

The coupling of synthetic peptides to KLH via a sulfo-MBS linkage was performed as described by Lerner *et al.* (Lerner *et al.*, 1981). 5 mg (~ 1 ml) of KLH was first dialyzed through four changes of 50 mM NaH_2PO_4 at 4°C, then mixed with 0.8 mg of sulfo-MBS and incubated at room temperature for 30 minutes. This mixture was passed through the G-50 Sephadex column and the flow-through collected. 5 mg of lyophilized synthetic peptide was dissolved in 2 ml of buffer containing 50 mM NaPi, pH 7.2 and 1 mM EDTA, and was allowed to react with the MBS-KLH complex at room temperature overnight with gentle rotation.

Strip-purification of antibodies

A preparatory gel with 1-1.5 mg of fusion protein antigen was run and transferred to nitrocellulose paper. The antigen band on nitrocellulose was visualized by staining with 0.5% Ponceau S reversible stain for 5 minutes, sliced out, and destained in water as described (Ukomadu, 1993).

The nitrocellulose strip was first blocked in 2% hemoglobin (Hb) in PBS at room temperature for 3 hours. Subsequently 2 ml of antisera per 0.5 mg of antigen was added to 3 ml of Hb-PBS to cover the strip in a capped tube. Absorption was allowed to take place at room temperature or 4°C overnight. The strip was subsequently washed six times, 5 minutes each, with alternating washes of 0.1 x PBS (15 mM NaCl, 10 mM NaPi, pH 7.2) and 5 x PBS (750 mM NaCl, 10 mM NaPi, pH 7.2).

Finally the antibodies were eluted with 2 ml of 1 M proprionic acid (pH 2.2) containing 100 µg/ml BSA, and the eluate neutralized with 1.6 ml of 2 M Tris base containing 1 mg/ml BSA (to pH 7.4-7.5). The resulting solution of specific antibodies was dialyzed against four changes of PBS containing 0.02% sodium azide.

Isolation of antibodies through Protein A column

A column was prepared from 1.5 g of Protein A-Sepharose beads pre-swollen in 50 ml PBS, pH 7.4 at 4°C. Affinity purification procedures were performed as described by Harlow & Lane (Harlow & Lane, 1988). The crude antibody was first adjusted to pH 8.0 by addition of 1/10 volume of 1 M Tris, pH 8.0 before passing through the Protein A column. The column was washed sequentially with 10 x volume of 0.1 M Tris, followed by 0.01 M Tris, pH 8.0. Finally the antibodies were eluted with 100 mM glycine, pH 3.0 stepwise in 500-µl fractions, each collected in an Eppendorf tube containing 50 µl of 1 M Tris, pH 8.0 to neutralize the eluate. The fractions containing the antibodies were identified by spectrophotometric reading of O.D. at 280 nm.

Microsomal membrane preparation from rat cerebellum

Isolation of membranes was modified from that described by Anderson *et al.* (Anderson, 1989). Rat cerebella were dissected and placed in ice-cold buffer (~40 ml

per 1 g of tissue) of 320 mM sucrose, 5 mM NaPi, pH 7.4 and 1 mM EDTA, supplemented with protease inhibitors (a combination of 0.5 µg/ml leupeptin, 0.7 µg/ml pepstatin A, and 0.2 mM PMSF). The cerebella were homogenized on ice using a Potter-Elvejhem homogenizer, and the homogenate collected by centrifugation at 2,500 rpm at 4°C for 10 minutes. The supernatant was collected and centrifuged again at 10,500 rpm, 4°C for 60 minutes. The final pellet containing microsomes was recovered by homogenization in the same buffer in a volume that is 2.5 x the original tissue weight.

Western immunoblot

A 5-15 or 4-10% linear gradient of SDS-polyacrylamide gel based on the Maizel system (Maizel, 1971) was run and then the protein samples were electro-transferred onto a piece a nitrocellulose membrane. Each strip of the blot was first incubated in BLOTTO (Carnation dry milk 3.5% in PBS) at room temperature for one hour, then allowed to react with 1:200 dilution of various crude antisera with or without preabsorption with the fusion protein or synthetic peptide antigens. The blots were washed three times for 10-15 minutes each with BLOTTO, and then incubated in ^{125}I-Protein A diluted in BLOTTO to 0.5 µCi/ml, room temperature, 45 minutes. Finally, the blots were washed three times in BLOTTO, followed by two brief rinses with PBS, blotted dry, placed on a piece of paper covered with Saran wrap, exposed to Kodak X-Omat RP film (Rochester, NY) with one intensifying screen overnight.

In some cases, HRP-conjugated secondary antibody (1:1000 dilution) was used instead of ^{125}I-Protein A. The washing procedures remained the same except that BLOTTO was made as 7.5% Carnation dry milk in PBS with 0.1% Tween 20. The blots were then incubated in ECL solutions for 1 minute and processed for autoradiography with exposure time 20-60 seconds.

Metabolic labeling and pulse-chase

Cells were plated in 35-mm dishes and labeled with [^{35}S]-methionine as they just reached confluence (usually 3-4 days after plating). The labeling procedure was that described by Ukomadu (Ukomadu, 1993). First they were preincubated in methionine-free DMEM for 30 minutes, then changed into the same medium plus 150 µCi/ml [^{35}S]-methionine, 37^{0}C for 1 hour. After the label was thoroughly washed away with warm phosphate-buffered saline (PBS) or medium, cell incubation was continued in regular DMEM containing unlabeled methionine. At different time points of chase, cells were harvested by first washing with PBS supplemented with 1 mM of Ca^{2+} and Mg^{2+}. They were then lysed in buffer (50 mM Tris HCl, pH 7.4, 150 mM NaCl, 5 mM EDTA, 1 mg/ml bovine serum albumin, and 1% Triton X-100) and followed by immunoprecipitation procedures.

Immunoprecipitation

The procedures of cell lysis and immunoprecipitation were modified from that of Ukomadu (Ukomadu, 1993). Rat cerebellar microsomal membranes or cultured cells were solubilized with lysis buffer (150 mM NaCl, 50 mM Tris-HCl, pH 7.4, 5 mM EDTA, 1% Triton X-100) supplemented with protease inhibitors. The lysate was precleared with prewashed Protein A-Sepharose CL-4B, and the supernatant was aliquoted into tubes for immunoreaction with 5-10 µl of various crude antisera, with a final volume brought up to 1 ml in lysis buffer. The mixture was incubated on a rotator at 4^{0}C for one to three hours. Then 20 µl of prewashed Protein A beads were added to each sample and incubation continued for another hour. Finally, each sample was washed three times with wash buffer (500 mM NaCl, 50 mM Tris-HCl, pH 7.5, 5 mM EDTA, 1% Triton X-100, and 0.2-0.5% SDS). The resulting pellet was either added with

resolving sample buffer for SDS-PAGE, or followed first by *in vitro* phosphorylation and then SDS-PAGE.

In vitro phosphorylation by PKA

The immunoprecipitated protein samples were washed twice with the kinase buffer (20 mM Tris-HCl, pH 7.4, 200 mM NaCl, 5 mM $MgCl_2$, 1 mM EDTA). The final pellet was resuspended in 20 µl of the kinase buffer plus 2 µCi of $Na_2[\gamma\text{-}^{32}P]$-ATP and 0.05 µg of the catalytic subunit of PKA. The mixture was incubated at 30°C for 10 minutes as described by Emerick (Emerick, 1991). Reactions were terminated by adding an equal volume of 2x resolving sample buffer and heating at 70°C for 5 min. Samples were then electrophoresed through a 4-15% gradient gel and processed for autoradiography.

Preparation of rat tissue for immunohistochemistry

The procedure is adopted from that of Fryer *et al.* (Fryer *et al.*, 1992). An adult rat was anesthetized and a midline incision in the thorax and along the diaphragm was made to expose the heart. Incisions were made in the right atrium and the apex of the left ventricle, through the latter a cannula was inserted near the root of aorta and PBS, followed by 4% paraformaldehyde infused. The tissues were dissected out and placed in a Falcon tube with 4% paraformaldehyde in phosphate buffer, pH 7.4, and allowed to fix at 4°C with gentle rocking for at least 3 hours. Prior to sectioning, the tissue was placed in 30% sucrose in phosphate buffer at 4°C, overnight.

Immunohistochemical staining

Cryosections of 40-µm thickness were obtained from fixed adult rat brain as described (Fryer, 1992). Sections were incubated with affinity-purified antibodies

diluted in DMEM with 5% FCS and 2% Triton X-100 with gentle shaking at room temperature overnight. After three washes with 0.1 M phosphate buffer (pH 7.4), HRP-conjugated goat anti-rabbit secondary immunoglobulins diluted to 1:250 in the same medium was added for another 2-hour incubation at room temperature. Sections were then washed and stained by chromogenic reaction using 3',3'-diaminobenzadine (Sigma).

Cell culture and transfection

The calcium phosphate precipitation method (Graham & van der Eb, 1973) was employed for the transfection of cells. HEK293 cells (Graham *et al.*, 1977) were plated on 10-cm culture dishes containing 10 ml of Dulbecco's modified Eagle's medium (DMEM) supplemented with L-glutamine, penicillin/streptomycin, and 10% fetal calf serum. Cells were incubated at 37°C with 5% CO_2 and transfected when reaching 50-80% of confluence.

To make the transfection mixture, into one sterile Eppendorf tube 0.5 ml of 2x HEPES buffer was aliquoted, and into another tube 61 µl of 2 M $CaCl_2$, 8 µg of DNA and water to a final volume of 0.5 ml were combined. The content of the second tube was added dropwise to the first with concomitant mixing. The resulting calcium phosphate-DNA mixture was then slowly layered onto a plate of cells. The quantity of various components was scaled according to the size of culture plates and the amount of medium used. For example, into a 35-mm dish which usually held 2 ml of medium, 200 µl of the transfection mixture was added; 0.4 ml of mixture was used for a 60-mm dish containing 4 ml medium; 1 ml was used for a 10-cm dish with 10 ml medium.

At 16-20 hours after transfection, the medium was removed, and fresh medium added. The incubation was continued under the same conditions until experiments were performed.

Selection of stably transfected cell lines

HEK293 cells were plated at a low cell density and grown to about 20% confluent, and then transfected using calcium phosphate method as described above with IP_3R cDNA clones in the expression vector, pCB6. At 48 hours post-transfection, the selection medium (DMEM + 10% FCS with G418 at 0.6 μg/ml) was applied to eliminate most of the cells that had not stably incorporated the DNA into the genome. As illustrated in Figure 2-3, the selection process was continued until the surviving cells formed visible foci of growth. The colonies were individually picked by sterile cotton swabs and inoculated into fresh selection medium in cell wells for further expansion. Each colony was screened for expression of IP_3R by both Western immunoblots and immunocytochemistry. The stable cell lines were thereafter maintained in 0.6 μg/ml G418.

Total membrane preparation from cultured cells

Initial [^{3}H]-IP_3 binding assay on fractionated membranes from the cells indicated significant binding capacity in the nuclear fraction in addition to the microsomal membranes. In order to include all receptors in the preparation, total membranes were isolated by sequential high speed centrifugation as described (Hingorani, 1994).

First, cells were harvested in PBS, pelleted by centrifugation at 1,500 rpm for 10 minutes. The pellet was then resuspended in ice-cold hypotonic buffer (10 mM Tris HCl, pH 7.4, 0.5 mM EDTA, 0.5 mM EGTA) supplemented with leupeptin (0.5 μg/ml), pepstatin A (0.7 μg/ml), and PMSF (0.2 mM) using a Potter-Elvejhem homogenizer. The homogenate was subject to centrifugation at 100,000 x g at 4°C for 40 minutes. The resulting pellet was resuspended in the same buffer followed by repeated homogenization and centrifugation procedure.

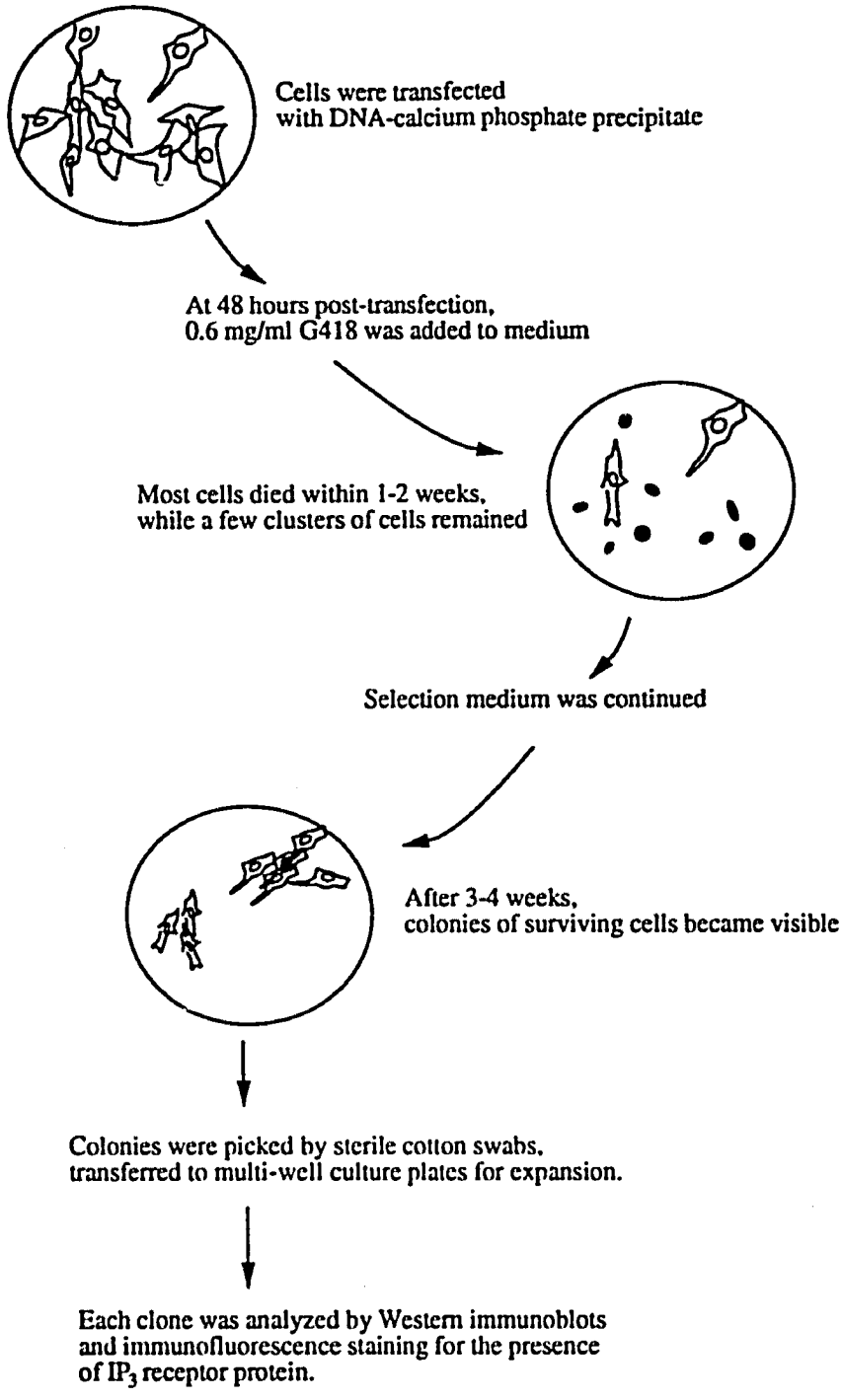

Figure 2-3. Schematic illustration of stable cell line selection.

For experiments involving the addition of calcium, the membrane pellet was subject to additional homogenization and sedimentation in a similar buffer except with 1 mM HEDTA substituting EDTA and EGTA.

Solubilization of membrane proteins

Freshly prepared total membranes were suspended in ice-cold binding buffer (20 mM Tris-HCl, pH 8.0, 100 mM KCl, 20 mM NaCl, 1 mM EDTA, or HEDTA in calcium studies) plus 1% Triton X-100. The homogenate was sedimented at 80,000 x g at 4°C for 40 minutes. The supernatant contained the soluble membrane extract, typically at a concentration of 2-3 mg/ml of the total membrane protein, and was stored on ice until assayed.

[^{3}H]-IP$_3$ binding assay

Unless specified, all [^{3}H]-IP$_3$ binding assays were performed on detergent (Triton X-100)-solubilized membranes incubated at 0-4°C using the ion-exchange assay method described by Hingorani (Hingorani & Agnew, 1991).

First, a label mix was prepared by diluting the commercial stock of [^{3}H]-IP$_3$ (17-20 µCi/mmol, Du Pont-NEN) with high-purity unlabeled IP$_3$ (Boehringer-Mannheim) to 1.8 Ci/mmol in binding buffer (as formulated above). Reaction components were mixed in a microcentrifuge tube or microtiter plate incubated in ice-water in the following order: binding buffer, ± 12-15 µM unlabeled IP$_3$ (Sigma), ± calcium, and label mix containing [^{3}H]-IP$_3$ with specific activity diluted as described. Finally, membrane solution was added and mixed thoroughly, and the reaction mixture was allowed to equilibrate in the same bath for 5-6 minutes before aliquoted for syringe assay. The actual application of reaction mixture to the side-wall of the syringe and manipulation of the plunger to force

the mixture through Dowex AG 1-X2 resin (Hingorani & Agnew, 1991) was performed either in a cold room (4°C) or at room temperature.

Protein assay

The amount of protein was determined by a modified Lowry method (Lowry *et al.*, 1951) using the D_C protein assay kit (Bio-Rad Laboratories). Typically 50 µl of the membrane extracts was diluted 3 fold with water, and the samples were assayed in 50-µl aliquots in duplicates. An equal amount of water plus assay reagent was used as the blank. 1 mg/ml of BSA was diluted serially to generate a standard curve with protein concentrations ranging from 0 to 50 µg in 50 µl. The colorimetric reaction was allowed to take place at room temperature for 15 minutes to 1 hour before measurements of O.D. at 750 nm were made.

Studies of N-linked glycosylation

Cells were incubated at 37°C in a medium containing 2.5 µg/ml tunicamycin for 2 hours prior to and throughout the period of metabolic labeling (described above). The labeled proteins were then immunoprecipitated from the cell lysate and electrophoresed through SDS-polyacrylamide gels. For binding with lectin gels or heparin-agarose, unlabeled cells were first treated with tunicamycin and subsequently lysed in a modified buffer containing 20 mM Tris HCl, pH 7.4, 120 mM NaCl, 0.5 mM EDTA, 1% Triton X-100. The soluble extract was then diluted into similar buffer to reduce the detergent concentration to less than or equal to 0.1% before the addition of lectin- or heparin-agarose gels. 1 mM of Ca^{2+} and Mg^{2+} was added to the binding solution in the case of precipitation with concanavalin A. The precipitation procedure was similar to routine immunoprecipitation except for the use of lysis buffer formulated above for the

washings. The final precipitate was then added with sample buffer for SDS-PAGE followed by Western detection.

Analytical sucrose gradient sedimentation

Sucrose gradient centrifugation procedure was modified from that by Nelson *et al.* (Nelson & Hammerton, 1989). Whole-cell lysate (from each 10-cm dish) or membranes were solubilized in 200 µl of binding buffer containing 1% Triton X-100, sedimented at 48,000 x g for 5 minutes. The supernatant was then layered onto a sucrose-buffer solution in an SW 50.1 polyallomer tube. Each tube contained 0.4 ml of 60% sucrose cushion, carefully layered with 4.4 ml of linear 5-20% (w/w) gradient of sucrose solution prepared in the binding buffer plus 0.1% Triton X-100. The samples were sedimented at 189,378 x g at 4°C for 3 and 1/2 hours using an SW 50.1 rotor. 250-µl fractions were collected from each tube for the assay of [^{3}H]-IP_3 binding.

A mixture of protein standards was used in the sedimentation, including apoferritin (17.2 S), catalase (11.35 S), aldolase (7.35 S), BSA (4.6 S) and cytochrome C (1.7 S).

Calcium imaging

All calcium imaging experiments were performed with instruments and reagents kindly provided by Dr. Ann Cornell-Bell (Yale University) following procedures as described (Cornell-Bell *et al.*, 1990).

Cells were plated onto 22-mm^2 glass cover slips. The slips were transferred from culture medium to a 35-mm dish containing 5 µM of fluo-3 in the acetomethoxyester form (fluo-3AM, Molecular Probes) diluted in 1.5 ml normal saline (137 mM NaCl, 5.3 mM KCl, 1 mM $MgCl_2$, 25 mM sorbitol, 10 mM HEPES, 3 mM $CaCl_2$) and incubated at

37°C for 45 minutes. At the end of incubation, the cover slip was mounted on a superfusion chamber seated on the stage of a confocal microscope.

A typical experimental protocol involved saline wash at room temperature for 100 recording frames (with an elapse time of 1.8 sec/frame), agonist (100 nM angiotensin II in saline) for 200 frames, followed by another 100 frames of saline wash. Changes in intracellular calcium evoked by angiotensin II were examined by confocal scanning laser microscopy at 488 nm using the fluorescein isothiocyanate (FITC) excitation filter set on a Bio-Rad MRC 600 CSLM, a silicon-intensifier target tube (SIT) camera (Hamamatsu C-2400), a digital image processor (Imaging Technology), and an optical memory disk video recorder (Panasonic TQ-2026F). Time-lapse video imaging was accomplished using software XSOM that was written for Bio-Rad by Dr. Stephen J. Smith (Stanford University).

Images were displayed on a Sony Trinitron high resolution monitor at 54x real time (displaying 30 frames/sec, each frame represents 1.8 seconds in real time).

Imaging data analysis

Images and calibration data were recovered from optical disk for quantitative analysis with a frame grabber (Imaging Technology PFGplus-640). Digitization of the fluorescence signal in individual cells was conducted by averaging over an area of 5 by 5 pixels using the IMAGEPRO computer program. These data were then converted into calcium transient traces by plotting $\Delta F/F$ (relative fluorescence change) versus real time in seconds, using the Igor Pro (WaveMetrics Inc., Oswego, OR) analysis program. With the same program the data were transformed by Fourier function, and finally presented in the form of power spectra.

All statistical analyses were performed with StatView (Abacus Concepts, Inc., Berkeley, CA).

Chapter 3.

Characterization of IP_3 Receptor Distribution & Functional Effects of the Antibodies

Introduction

Antibodies provide an indispensable tool for studying the distribution, expression, functional regulation and diversity of protein molecules. A number of monoclonal (Otsu *et al.*, 1990) and polyclonal (Mignery *et al.*, 1989; Satoh *et al.*, 1990) antibodies raised against rodent brain IP_3 receptor proteins or peptides have been described. From these work much knowledge has been gained about the receptors present in the central nervous system and in peripheral tissues.

Early reports on the subcellular immunolocalization of the receptor within Purkinje neurons have been partially conflicting. These discrepancies may be due to the variable sensitivity and specificity of each antibody, or due to the different fixation methods employed by various groups. The receptors were consistently seen concentrated in subcompartments throughout the endoplasmic reticulum (ER). More careful examinations using immunogold labeling and electron microscopy (Otsu, 1990; Satoh, 1990) demonstrated the localization on the smooth ER, scantily on the rough ER and the outer nuclear membrane, as well as some smooth membrane structures either in multiple stacks or in doublets, singlets beneath the plasma membrane. These membrane elements (referred to as cisternal stacks) are likely the continuous extensions of the ER, or may represent a specialized, elaborate organelle such as the so-called "calciosome" present in some cells (Rossier & Putney, 1991; Terasaki *et al.*, 1994). Studies by Takei *et al.* (Takei *et al.*, 1994) suggest, however, that these stacks of cisternae are not permanent

structures. The stack formation is an adaptive response of ER to hypoxic conditions, but is nevertheless due to the presence of a high concentration of IP_3 receptor in these membranes (Takei, 1994).

Although IP_3 receptors are found exclusively on the intracellular membrane of Purkinje neurons, they have also been detected on the plasma membrane of lymphocytes (Khan *et al.*, 1992a; Khan *et al.*, 1992b), olfactory cilia (Cunningham *et al.*, 1993), endothelium, smooth muscle cells and keratinocytes (Fujimoto *et al.*, 1992). These may represent variant receptors for IP_3.

In order to study the cerebellar IP_3 receptor, I have used its cDNA sequence to develop several polyclonal antibody markers that are directed to topographically distinct segments of the receptor. The task of making such an array of antibodies was undertaken with the understanding that each antibody may have different properties and, thus, different utility. Furthermore, it was hoped that these region-specific antibodies may be used to probe the topology of the receptor molecule in addition to its gross distribution. In this chapter I intend to provide an account of the generation of various antigens and the basic characterization of the derived antibodies.

Four antibodies raised against fusion proteins of the receptor segments demonstrated immunological reactivity with both detergent-solubilized cerebellar membranes and partially purified receptors. These antibodies, although directed to the type I receptor sequence, may be reactive with other receptor types because of the extensive sequence homology among the various receptor gene products. The properties of each antibody were tested in Western immunoblots, immunohistochemistry, immunoprecipitation, as well as functional modulation. Two additional polyclonal antibodies were raised against short stretches of peptides of the rat type I receptor. These peptide segments were chosen since their amino acid sequences were distinct from those in other known receptor gene products designated as types II, III, and IV (Blondel,

1993; Ross, 1992; Sudhof, 1991). The two type I-specific antibodies were then used to assess the composition of IP_3-binding sites in cerebellum. The implication of the results as well as the use of these antibodies in other collaborative efforts was discussed.

Results

Sequence-specific antigens and antibodies

The four fusion protein antigens were prepared as described in Chapter 2. Their locations are depicted in Figure 3-1. On the SDS-polyacrylamide gel, all but 3'α have molecular weights which conform with the values computed from the length of cDNA segment. Fp-3'α (aa 2477-2566) has an apparent MW on the gel that is larger than calculated value, possibly due to erroneous transcription and translation of extra sequences encoded in the expression vector, or due to aberrant migration pattern caused by an unusual conformation assumed by this polypeptide, which does contain a hydrophobic stretch predicted to traverse the membrane. Fp-5' (aa 419-572) was prepared from sequences near the N-terminus, just bypassing the alternative splice site, *SI*, and the putative IP_3 binding domain (Sudhof, 1991). It has been found to be toxic to the bacteria under the growth conditions employed; the bacterial culture did not increase density as did the other cultures with prolonged incubation after IPTG induction. Fp-m (aa 1379-1798) encompasses a long stretch of sequence near the mid-region of the cytoplasmic domain, including the two consensus PKA phosphorylation sites flanking the *SII* region. Fp-3'α resides in sequences preceding the last putative membrane-spanning segment, whereas fp-3'β (aa 2604-2698) follows the segment immediately. All four fusion peptides were isolated and demonstrated to contain the core peptide, glutathione S-transferase, which was recognized by DRK1 polyclonal antibody (Trimmer, 1991).

Figure 3-1. Topographic location of antigenic segments of IP_3 receptor. The schematic depiction of an IP_3 receptor subunit is shown on top of the facing page, and its transmembrane region is enlarged below. The four segments of heavy lines labeled fp-5', m, 3'α, 3'β represent the receptor fragments made as fusion protein antigens. The two hatched circles (sp-2A & 3A) mark the location of the receptor sequence used for peptide antigen synthesis. The amino acid residue numbers are provided in parentheses for each segment. *fp* denotes fusion protein (with glutathione S-transferase from *Schistosoma japonicum*); *sp* denotes synthetic peptide.

The enlarged transmembrane region is illustrated as an alternative topology of the channel domain, containing 6 instead of 8 membrane-spanning segments. The evidence for this version is presented by Michikawa (Michikawa *et al.*, 1994).

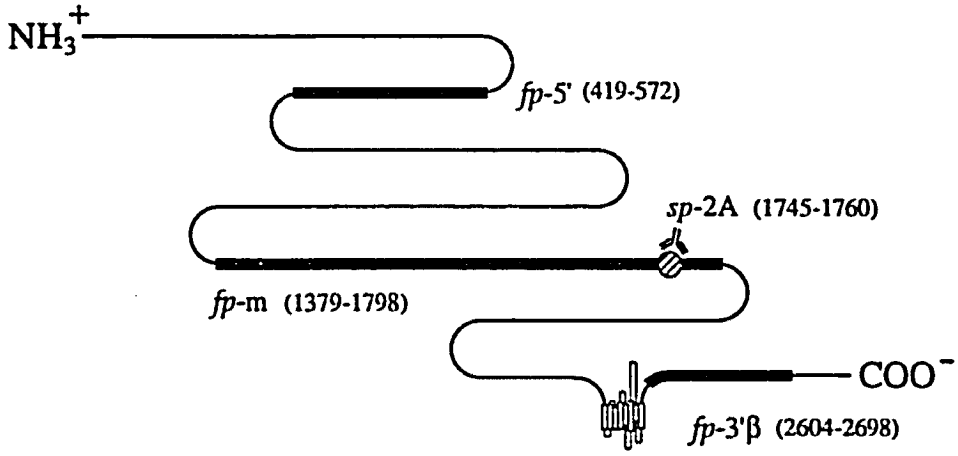

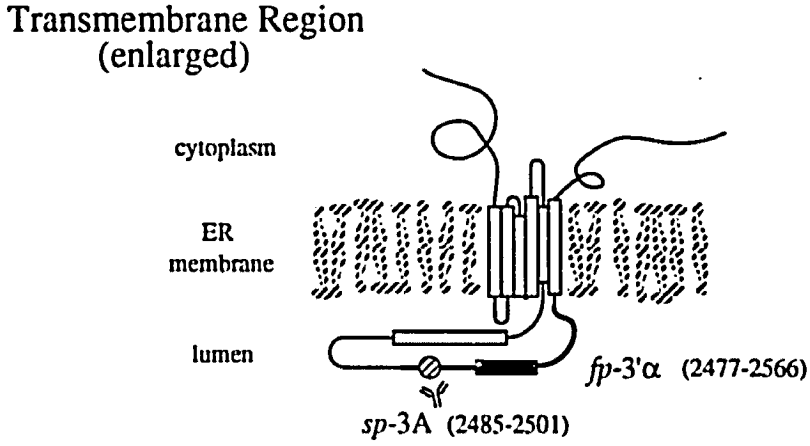

Recent molecular cloning revealed the existence of multiple receptor types encoded by different genes. Each had a different tissue distribution but shared, with the type I receptor predominantly found in cerebellum, similar functional domain motifs as well as an extensive sequence homology at the amino acid level. Using the published amino acid sequences (Ross, 1992; Sudhof, 1991), two stretches of peptides unique to the type I receptor sequence were identified and synthesized for antibody preparation. These sequences chosen were identical in rat and mouse. The location of these two segments were also depicted in Figure 3-1. Solely based on the known primary amino acid sequence, sp-2A is expected to distinguish type I receptor from type II, whereas sp-3A should further distinguish the type I receptor from type III and IV receptors.

Rabbit polyclonal antisera were prepared from each of these sequence-specific antigens and were demonstrated to react with the original antigens on Western immunoblot for the fp-antibodies (Figure 3-2) or dot blot for the sp-antibodies. On the Western additional bands were labeled above the identified fp-m and fp-3'α polypeptides. These are likely protein aggregates, due perhaps to the interaction of the hydrophobic segments present in each of the two antigen polypeptides.

Each of these polyclonal antibodies were characterized by various immunochemical procedures as described in the following sections. The immunoreactivity profile of each antibody is summarized in Table 3-1.

Immunoreactivity with the IP_3 receptor partially purified from rat cerebellum

A simplified receptor purification scheme with a WGA column has been devised in our laboratory (Hingorani & Agnew, 1992) and used to isolate IP_3 receptor from detergent extracts of rat cerebellar membranes. Figure 3-3 illustrates that each of the antisera reacted strongly with the purified receptor on Western immunoblots. Reactions

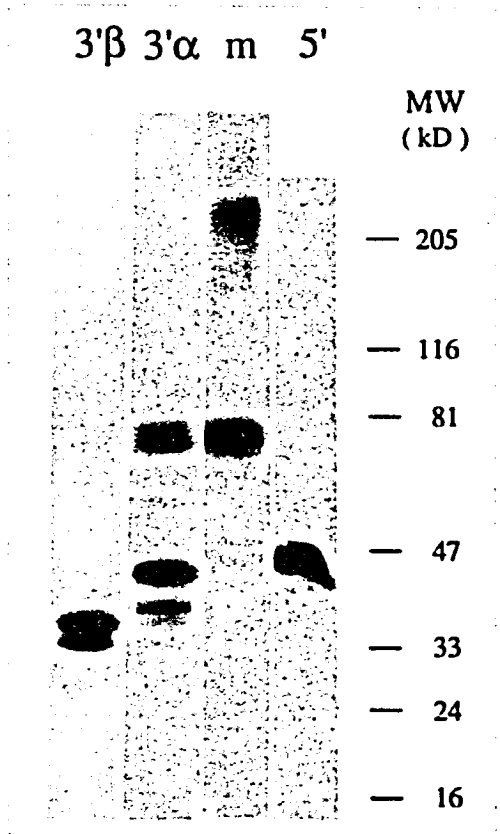

Antigen	Size (kD)
fp-5'	42
fp-m	70
fp-3'α	36 (apparent 42)
fp-3'β	37

Figure 3-2. Western immunoblot demonstrating staining of the four fusion polypeptides by their respective antibodies. The fusion proteins (about 0.5 µg each) were electrophoresed through a 5-15% SDS-polyacrylamide gel and transferred to nitrocellulose membrane. The membrane was cut into strips, each of which was allowed to react with its corresponding antibody. Crude primary antibodies were diluted to 1:200, and ^{125}I-protein A was used at 0.5 µCi/ml. The molecular weight standards (MW) are shown on the right side of the Western blot. A table summarizing each fusion polypeptide and its molecular weight is provided.

Table 3-1. Characteristics of polyclonal antibodies generated against the IP_3 receptor.

Antibody	Western blot	Immuno-precipitation	Immuno-histochemsitry
5′	+++ [a]	+	++
M	++	+++	+++
3′α	+	o	+++
3′β	++	++	+
sp-2A	+++	+++	+++
sp-3A	+++	+++	+++

[a] The relative effectiveness of each antibody in various immunochemical assays was rated as follows: +++, strong reaction; ++, moderate reaction; +, weak reaction; o, no detectable immunoreaction.

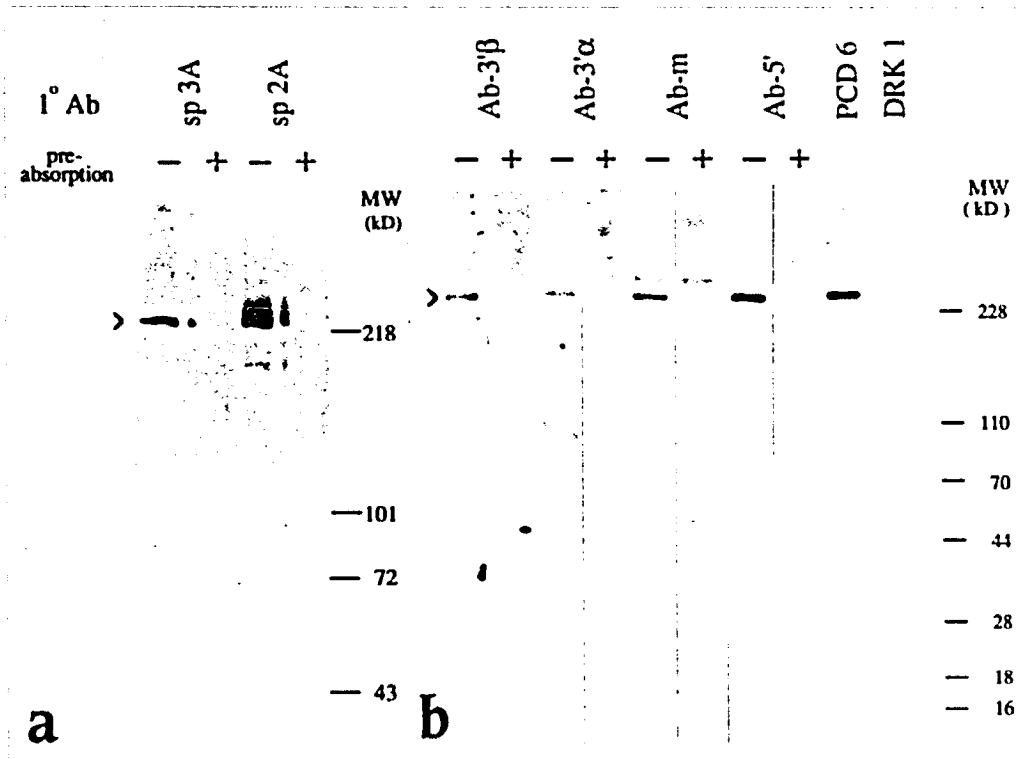

Figure 3-3. Western blot showing the immunoreactivity of the fp- and sp-antibodies against partially purified IP_3 receptor. 0.5 µg of the IP_3 receptor partially purified from rat cerebellum was loaded per lane. Specific immunoreaction of the four antibodies raised against the fusion proteins is shown on the right panel (b). The crude antisera were used at 1:200 dilution preabsorbed with GST ‡ (- lanes) or with the respective GST-IP_3R fusion antigen (+ lanes). ‡GST--glutathione S-transferase

PCD6 (gift of Dr. P. De Camilli) is a polyclonal antibody raised against a synthetic peptide of aa 2658-76 of the mouse receptor sequence. DRK1, a polyclonal antibody against the delayed rectifier potassium channel, serves as a negative control.

The left panel (a) demonstrates the immunoreactivity of the two antibodies directed against synthetic peptides. Each antibody was diluted to 1:250, without (- lanes) or with (+ lanes) preabsorption by 20 µg of the respective synthetic peptide.

were specifically blocked by pre-absorption with the original corresponding antigen (i.e., fusion protein or synthetic peptide).

Immunoreactivity with crude receptor

Western immunoblot of unpurified receptors in the microsomal fraction of rat cerebellum was also tested with each antiserum, and the result is illustrated in Figure 3-4a. In each case, a single band of MW ~260 kD was identified. Ab-3'α , however, revealed a reactivity on Westerns that was weaker than the other antibodies. In the affinity-purified preparation, it also faintly labeled one to two bands of higher molecular weight (Figure 3-4b). Although these bands may well be the aggregated receptor molecules, the possibility remains that Ab-3'α may be cross-reactive with other proteins.

Immunoprecipitation ability monitored by PKA phosphorylation

The ability of the antibodies to react with the native, unpurified receptor was tested by immunoprecipitation experiments performed on microsomal membranes solubilized in 1% Triton X-100. Figure 3-5 demonstrates a single band detected by enzymatic phosphorylation. Among the antibodies directed to various fusion proteins, those against fp-m were most effective in immunoprecipitation, fp-3'β were less effective, followed by fp-5', while antibodies against 3'α were virtually ineffective. The two synthetic peptide antibodies, on the other hand, proved to be superior in their immunoprecipitating ability. The lower intensity of receptor precipitated by sp-2A antibodies may result from the antibodies' interference with *in vitro* PKA phosphorylation rather than a weaker ability to precipitate.

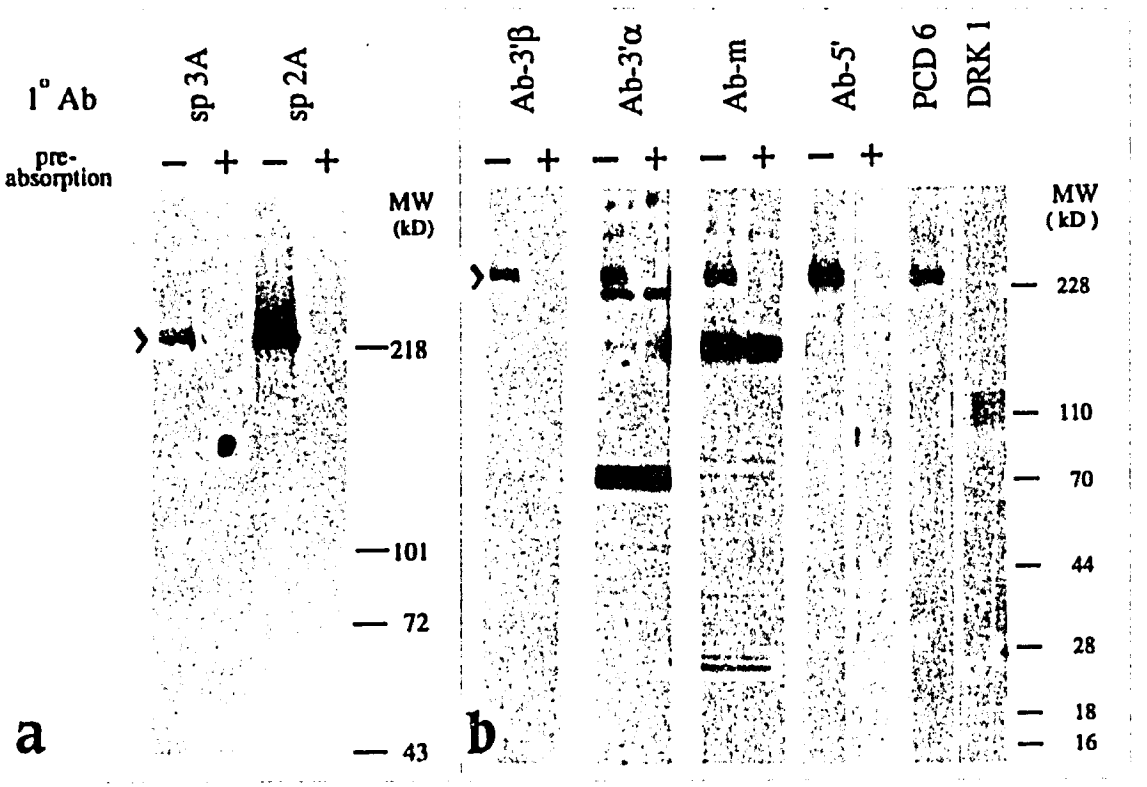

Figure 3-4 (a). **Western analysis of unpurified receptors in rat cerebellar membranes.** 100 μg of cerebellar microsomal proteins were loaded per lane and transferred to nitrocellulose membrane. Membrane strips were allowed to react with 1:200 dilution of respective antisera with (+ lanes) or without (- lanes) preabsorption. Arrowheads point to the IP_3 receptor bands.

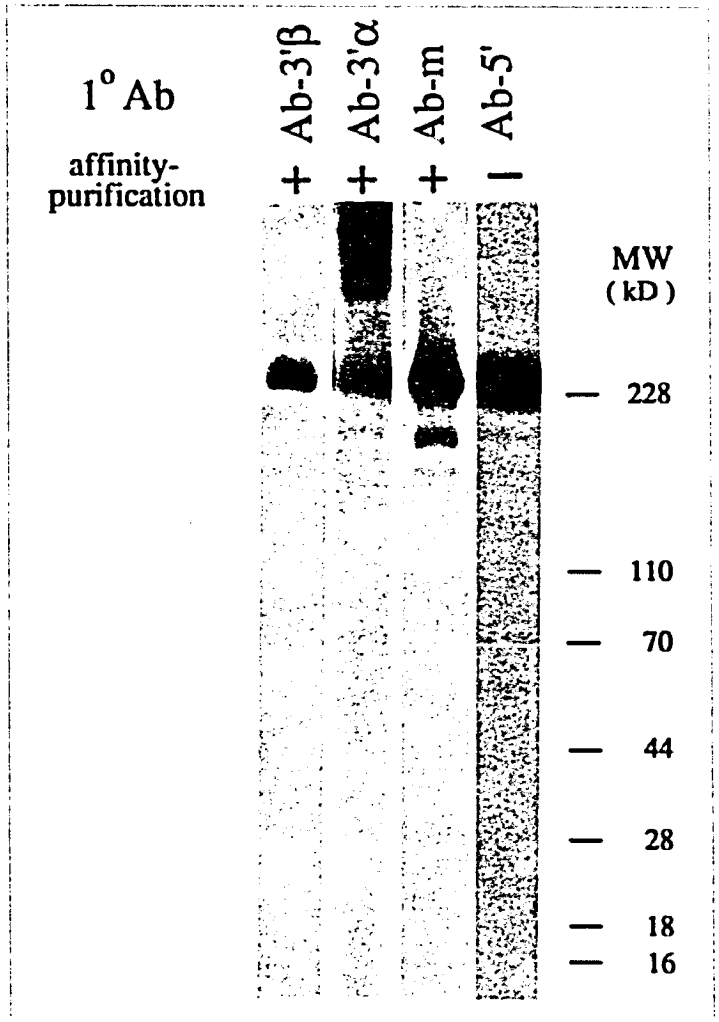

Figure 3-4 (b). Western immunoblot of IP_3 receptors in rat cerebellar microsomes identified by affinity-purified fp-antibodies. Each purified antibody (by strip-purification procedure outlined in Chapter 2) was used in Western analysis at 1:50 dilution, followed by reaction with ^{125}I-protein A at 0.5 μCi/ml. Ab-5′ was not purified due to unavailability of its original fusion protein antigen. The crude antisera of Ab-5′ (1:200), nevertheless, provided a sensitive and specific marker for the IP_3 receptor.

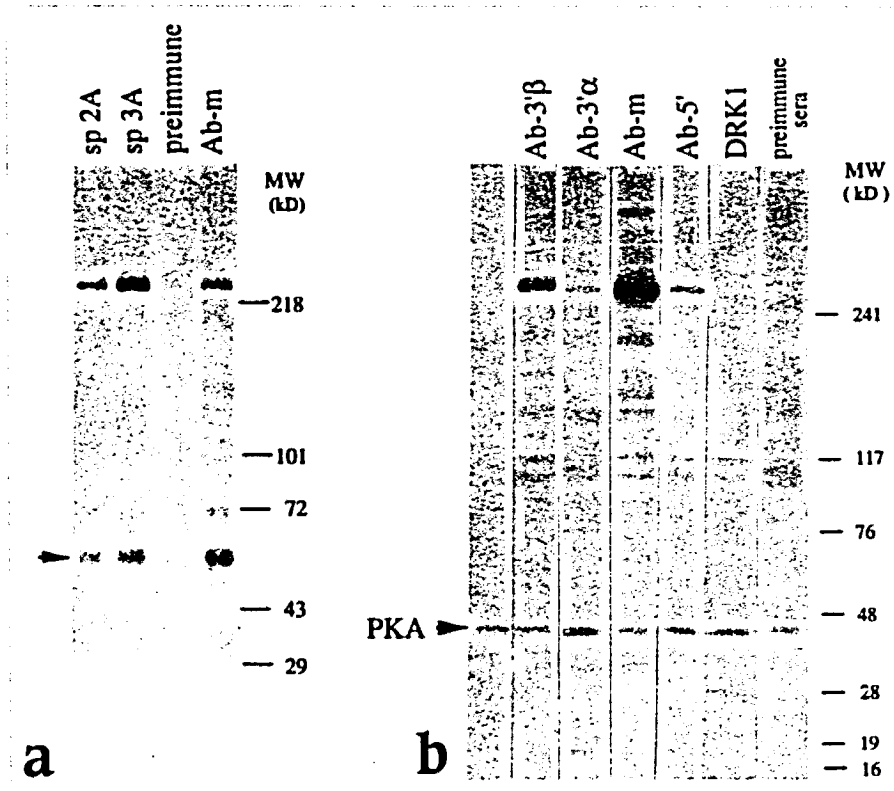

Figure 3-5. Immunoprecipitation and phosphorylation of native receptor from detergent-solubilized membranes. Solubilized cerebellar microsomes were processed for immunoprecipitation and *in vitro* phosphorylation by the catalytic subunit of PKA as described in Chapter 2. The labeled proteins were detected by autoradiography following electrophoresis through a 4-15% gradient gel.

Right panel (b): immunoprecipitation with fp-antibodies. Note the major labeled protein bands at MW ~260 kD. The unlabeled left lane included an aliquot of the reaction mixture without any substrate in order to reveal PKA. Left panel (a): immunoprecipitation with sp-antibodies. Ab-m was also included in the procedure for comparison of immunoprecipitation efficiency. Arrowheads point to the autophosphorylated PKA subunit.

Quantitative immunoprecipitation of type I receptors from solubilized rat cerebellar membranes with sp-2A and sp-3A antibodies

The type I IP_3 receptor has been identified as the cerebellar type because of its extraordinary abundance in this tissue source. From molecular cloning, however, it is shown that there are other receptor types expressed in cerebellum as well (De Smedt, 1994; Ross, 1992). I was curious about the relative abundance of each isoform and wondered to what extent the receptor heterogeneity may contribute to the complex biochemical properties of the receptor. To test this, both sp-2A and sp-3A antibodies designed to react specifically with type I receptor were used to deplete IP_3-binding sites selectively from detergent solution of total cerebellar membranes. Antibodies of increasing amount from pre-immune serum or sp-antiserum were first adsorbed to protein A-Sepharose beads. A small sample of detergent-solubilized membrane extract was then aliquoted into each tube containing antibody-protein A beads, followed by assay of the supernatant for [^{3}H]-IP_3 binding and by Western detection. As illustrated in Figure 3-6, both binding assay and Western revealed a similar profile of nearly complete and specific depletion of receptors, whereas minimal depletion was observed in the preimmune control. This suggests that type I receptor is the predominant type in cerebellum, likely to occupy at least 80-90% of the IP_3-binding population.

Immunohistological staining

To test the utility of the antibodies as immunocytochemical markers, experiments were performed on tissue sections from various regions of rat or cat brain.

Both fp-5′ and fp-m antisera gave strong and clean immunohistochemical signals, as anticipated from their cytoplasmic localization within the receptor. Antibody against fp-3′α, while being weaker on Western and completely ineffective in immunoprecipitating the native receptor from solution, was found to our surprise to be a

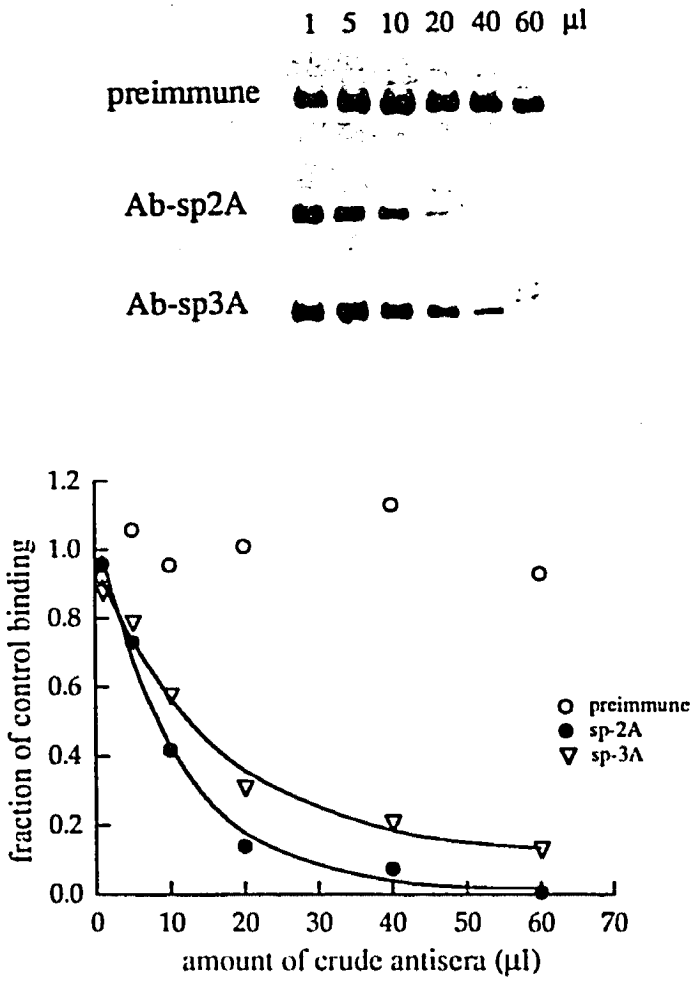

Figure 3-6. **Quantitative immunoprecipitation.** Solubilized cerebellar microsomes were processed for immunoprecipitation as described in Chapter 2. The top panel is a Western blot identifying the IP3 receptors after preadsorption with 1-60 µl of preimmune or type I receptor-specific antibodies (sp2A & sp3A). The bottom panel demonstrates the depletion of [^{3}H]-IP3 binding activity in the same fractions. The experiment was replicated twice with the same results. This demonstrates that both sp2A and sp3A (specifically directed to the type I receptor) were able to precipitate the majority of the IP3 receptors in cerebellum.

superior marker on tissue staining. This antibody, however, seemed to stain some regions unrecognized by fp-5' or fp-m antibodies, including the olfactory tubercles in the CNS and skeletal muscles (communication with Fergusson). The difference in staining pattern may be due to its sensitivity, or more likely due to its cross-reactivity with other proteins, with other IP_3 receptor types as well as ryanodine receptors being probable candidates. Such suspicion would be consistent with the finding that fp-3'α covered a stretch of hydrophobic sequence closely homologous among a number of ligand-gated membrane protein channels (Furuichi, 1989), although a detailed epitope-mapping may yield more information.

As expected from previous studies, immunoreactivity in cerebellum illustrated in Figure 3-7 is most prominent in Purkinje neurons, with a strong staining detected throughout the somata, dendrites, and axons. We have also observed that Lugaro cells, a rare cell type found in cerebellum, were labeled. This staining pattern was consistent for all fp- and sp- antibodies with one exception. Ab-3'β appeared to label not only the molecular and Purkinje cell layers, but also the granule cell layer to a lesser degree. This was observed most clearly in a low-magnification field, but at higher magnification the stain failed to give a clear definition of the cell body and its arbors as did all the other antibodies.

Additional sites of immunoreactivity were observed clearly in the pyramidal cells of the cerebral cortex, confined to distinct layers (III and V), as well as the hippocampal neurons in the CA1 through CA3 regions. The cell body, dendrites, and axon of the cortical pyramidal neuron were labeled, whereas in the hippocampal neuron only the cell body and dendrites were clearly visible.

Figure 3-7. **Immunohistochemical staining of various brain sections from adult rats.** Cryosections were processed for immunoreaction with strip-purified Ab-M or Ab-3'α at 1:50 dilution. In each case a peroxidase reaction was employed with 3',3'-diaminobenzadine as the chromogen. For some sections (c-f) 2% nickel sulfate was also included in order to intensify the signal.

Specific immunoreaction is detected in (a) cerebellum. Note the distinct labeling of the Purkinje cell body (in the Purkinje cell body layer) and dendrites (in the molecular layer). The Purkinje neuron axon is also labeled but not evident in this micrograph. In contrast, granule cells (in the granule layer) are devoid of any immuno-staining. Magnification at x200. MOL--molecular layer, PCL --Purkinje cell body layer, GrL--granule layer. (b) Purkinje neurons in cerebellum, x400. The labeling is perinuclear in the cell body and is distributed throughout the dendrites. (c) cerebral cortex, with labeling of the pyramidal neurons (with cell bodies organized in layers III & V) and their processes, x100. (d) the pyramidal neurons in cerebral cortex, x200. (e) hippocampus. P marks the labeled pyramidal neurons in the CA1 region. x100. (f) the pyramidal neurons in the hippocampal region, x200. Both the cell body and the processes are labeled.

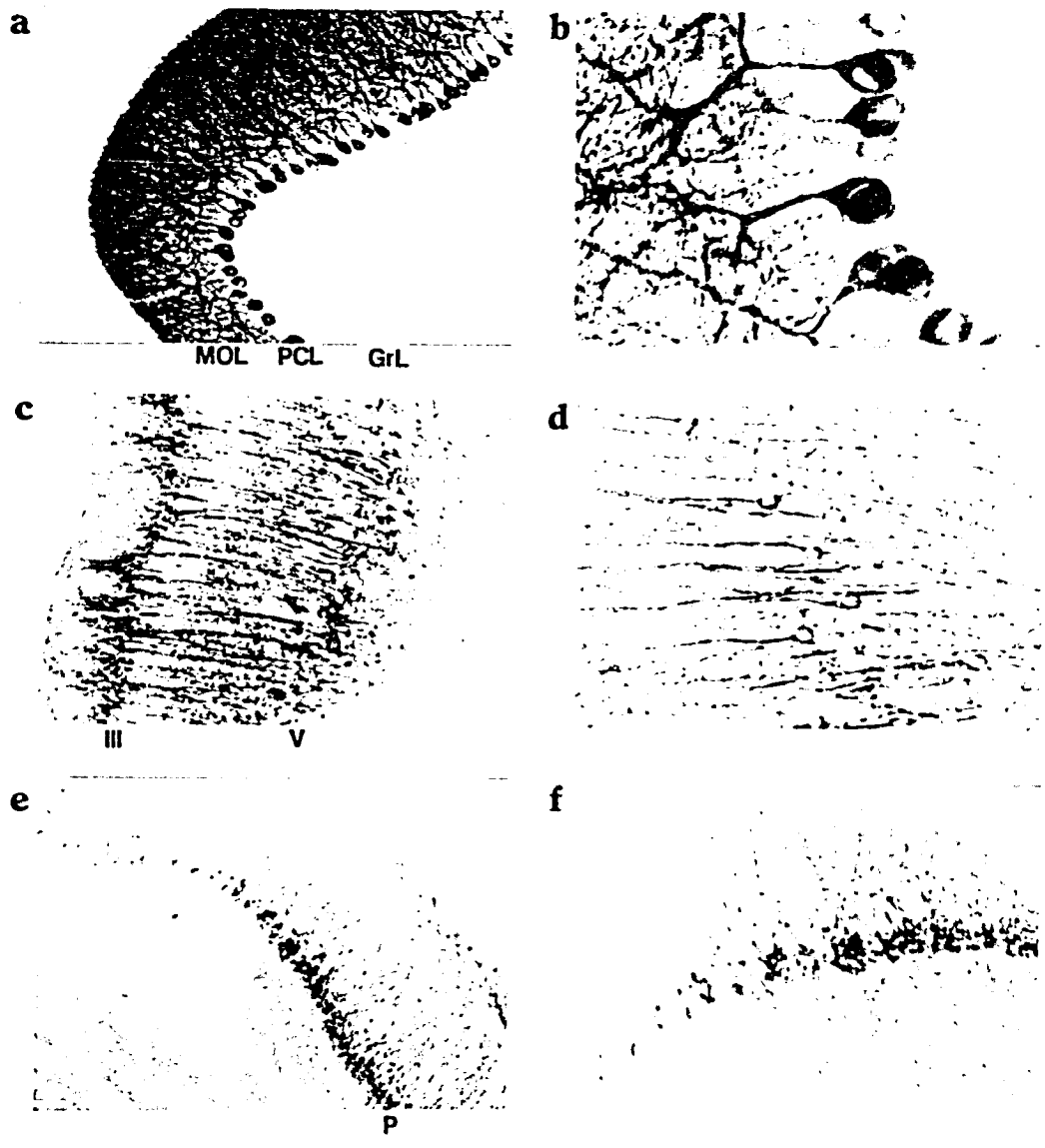

The effect of antibodies on IP_3 binding

Finally, I was interested in examining whether any of the polyclonal antibodies would affect IP_3 receptor function. Each antibody was allowed to react with membrane extracts from rat cerebellum, and the mixture was tested for binding with [^{3}H]-IP_3. Figure 3-8 shows that none of these antibodies interfered with ligand-binding. This negative outcome was somewhat anticipated from the regions of the receptor with which most of these antibodies interact except for Ab-5'. Ab-5' was raised against a region near the IP_3-binding site. It was however confirmed to exert no functional effect in similar binding assays covering a wide range of antibody concentrations.

Summary & Discussion

Technical aspects of antigen preparation

When the design and production of an antigen is coupled with the knowledge of a cloned DNA sequence, the preparation of the antigen and its antibodies has been made extremely efficient and specific. It is efficient because a large quantity of the antigen can be made by genetic engineering and recombinant techniques, bypassing the difficulty of protein isolation from often limited native tissue source; specific, because the exact region with which the antibodies interact is known.

Here two methods of antigen preparation were employed: bacterial expression of fusion proteins and peptide synthesis. Both have proven to be effective, although there were unanticipated outcomes. The pGEX expression vectors have been used precisely because of the ease of over-producing fusion protein antigens that are supposedly soluble. Each antigen peptide is linked to the C-terminus of the soluble core protein, glutathione S-transferase, making affinity-purification feasible. In reality, however, three of the four fusion protein constructs were trapped in the insoluble pellet.

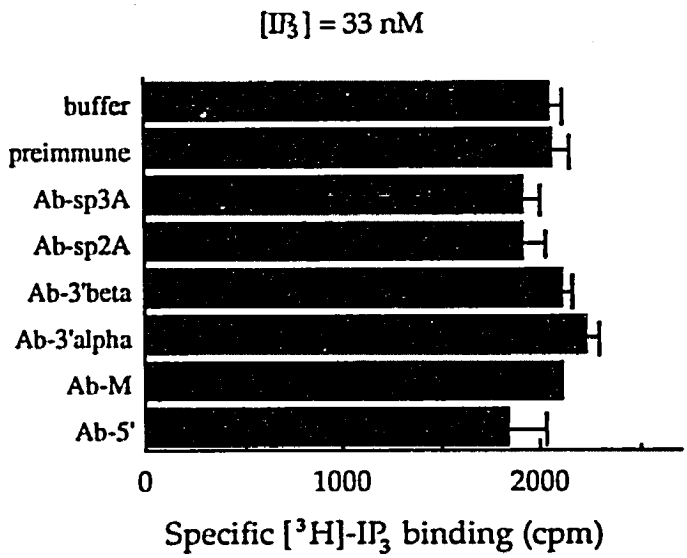

Figure 3-8. **Effect of antibodies on IP3-binding of receptors.** Rat cerebellar microsomes were solubilized with 1% Triton in binding buffer, from which 200 µg of total protein was incubated with 20 µl (~ 10 mg/ml of IgG) of various crude antibody at 4°C for 30 minutes. The mixture was then tested for binding with [^{3}H]-IP3 using the syringe assay. Binding assay was performed in duplicates plus one point of competition with excess unlabeled IP3. The error bar was not shown where the error was too small to visualize. The experiment was duplicated with similar results.

There appeared no correlation with the nature of the antigen peptide; i.e., the predominance of hydrophilic versus hydrophobic residues or the total length of the fusion peptide. Conceivably some of these polypeptides were mis-folded or mis-targeted by the bacteria because of their foreign, mammalian sequences; they may be synthesized by the polyribosomes attached to the bacterial inner (cytoplasmic) membrane, rendering these peptides either specifically or non-specifically associated with the insoluble membrane fraction. It is also interesting that the various polyclonal antibodies made against these fusion protein antigens had different utility in a number of immunochemical assays. These differences have been summarized in Table 3-1.

Although more expensive, synthetic peptides provide an alternative to bacterial protein expression and are perhaps the fastest way of preparing pure antigens with specific sequences in a more confined region. This feature has not only been explored for proteins that are highly conserved, but is also particularly useful, as in this study, for identifying a protein among its homologues by a narrow but unique sequence region. There is one major disadvantage: because of the narrower range of epitope displayed by the synthetic peptide, the anti-peptide antibodies often do not recognize the native antigen, making their utility somewhat limited (Harlow & Lane, 1988). It is therefore a pleasant surprise that the two antibodies raised against synthetic peptides in this study show uniformly superior reaction in wide range of assays including immunoprecipitation and immunohistochemistry, which often require recognition of the native antigens. This again demonstrates that each step in the preparation of immunogen and antibody represents an unknown variable, and that the property of each resulting antibody has to be empirically determined.

Receptor distribution and function

By using the antibodies generated here, the IP_3 receptors have been studied in a number of tissues including the *Xenopus* oocyte, rat liver and pancreas, and cultured astrocytes from various rat brain regions. These represent collaborative efforts, and the results will be briefly mentioned without formal presentation of the data.

The antibodies-M and 3'α specifically labeled sub-populations of cultured astrocytes, most intensely along the nuclear membrane. On Western blot the identified band migrates around 200 kD (Figure 3-9). This may represent the nuclear version of the IP_3 receptor (Malviya *et al.*, 1990), and may explain the observed nuclear origin of calcium wave generation upon agonist stimulation. In a pilot study both antibodies have also localized the receptor (most likely the type III receptor) to the apical aspects of hepatocytes and pancreatic acinar cells, again corresponding to the origin of calcium waves in these cells.

Although the *Xenopus* oocyte represents a quite different species and tissue source, its IP_3 receptor shares a 90% identity in amino acid sequence with that from mouse cerebellum (Kume, 1993). All four fusion protein antibodies specifically identify the *Xenopus* oocyte IP_3 receptor as a 250 kD protein on Western blots. In addition, Ab-M which reacts with an epitope encompassing part of the receptor-coupling domain and Ab-3'β which resides in the cytoplasmic C-terminal tail (refer to Figure 3-1) are discovered to block receptor activation. Both antibodies specifically inhibit IP_3-stimulated calcium release in membrane extracts monitored by fura-2 fluorescence, as well as nuclear vesicle fusion detected by phase contrast microscopy. These results directly implicate the IP_3 receptor's role in mediating calcium mobilization which is required for nuclear vesicle fusion after each mitotic event in *Xenopus* oocytes and eggs (Sullivan *et al.*, 1995).

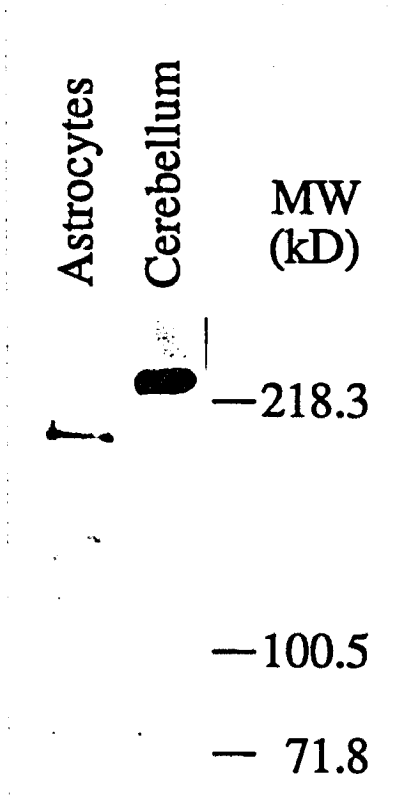

Figure 3-9. Identification of IP3 receptors in astrocytes by Western blot. Immunoreactivity of Ab-5' is demonstrated with a protein band ~ 200 kD in the cell lysate from cultured hypothalamic astrocytes. The identified protein appeared smaller than the cerebellar IP3 receptor.

Both in rat cerebellar (Figure 3-8) and *Xenopus* oocyte (Sullivan, 1995) membrane extracts it has been demonstrated that none of the fusion protein antibodies affect IP_3 binding to the receptor. The functional modulation by Ab-M and 3'β, therefore, is probably mediated at the level of channel activation. For Ab-M this is consistent with the notion that the long stretch of "coupling region" represents a flexible arm which transduces the signal of ligand-binding at the receptor N-terminus to the transmembrane channel domain near the C-terminus. This coupling region is also the site for multiple modulators of the receptor such as ATP, phosphorylation by PKA, PKC, and CaM kinase II (Ferris & Snyder, 1992). The involvement of the cytoplasmic C-terminal tail in channel activity, on the other hand, is also not unexpected. This tail contains cysteine residues that may interact with sulfhydral reagents (Kaplin, 1994). A monoclonal antibody which recognizes an epitope that is distinct from but close to the region encompassed by 3'β polypeptide has been found to inhibit IP_3 receptor activation (Miyazaki *et al.*, 1992; Nakade *et al.*, 1991). It will be quite informative to study the effect of these antibodies on purified, reconstituted IP_3 receptors in a controlled, isolated system such as a planar lipid bilayer. Do these antibodies form an occlusional barrier near the channel opening, or do they alter channel gating by stabilizing certain inactivated or deactivated state? Do they affect other modulators that are involved in receptor regulation?

Apart from these studies, this thesis work has focused more on the central nervous system. The immunohistochemical studies have confirmed findings from other laboratories. The IP_3 receptors have a wide distribution, including Purkinje cells in the cerebellum, pyramidal neurons in cerebral cortex and hippocampal formation, olfactory tubercles, and cells in the entorhinal region. Many of these regions overlap with the expression pattern of the subtype(s) of metabotropic glutamate receptors that are coupled to the phosphoinositide second messenger pathway (Masu *et al.*, 1991;

Nakanishi, 1994). These glutamate receptors are involved in long-term depression (LTD), a form of neuronal plasticity. At least in cerebellum, LTD requires membrane depolarization and the activation of both AMPA-sensitive glutamate receptors (an ionotropic subtype) and metabotropic receptors (Linden & Connor, 1993). PKC has been implicated as the necessary and sufficient down-stream cellular mediator of LTD in cultured Purkinje neurons in response to cytoplasmic free calcium rise (Linden & Connor, 1991). It is not known, however, whether the IP3 receptor is directly involved in the process. Presumably IP3 receptor can contribute to cytoplasmic calcium by a release from the intracellular source.

The immunohistochemical staining in cerebellar Purkinje cells is strikingly intense, corresponding to the high receptor density in this tissue. It has been estimated from autoradiography of [^{3}H]-IP3 binding that in cerebellum the IP3-binding sites are 1,000 fold more abundant than in peripheral tissues (Worley *et al.*, 1989). In Purkinje cells the immunohistochemical reactivity was observed throughout the somata, the dendritic shafts and spines, as well as the axons. The receptors' axonal localization is somewhat surprising, albeit unambiguously demonstrated by several different antibodies. It was also confirmed at high-resolution EM level, where receptors were detected along cisternae beneath the axonal plasmalemna which were probably continuous with the endoplasmic reticulum in the cell body (Mignery, 1989).

The existence of IP3 receptors in the synaptic terminals implicates its function of modulating the efficacy of neurotransmission (Mignery, 1989; Peng *et al.*, 1991). The role of axonally located IP3 receptors, on the other hand, is curious. Typically an axon, whether myelinated or unmyelinated, is considered a specialized neuronal process studded with ion channels which transmit electrical impulses. Although not impossible, it is quite novel to envision G protein-coupled surface receptors also exist along the axonal membrane and activate phospholipase C to locally produce IP3. An alternative

to this scheme would be that IP_3 molecules are generated in the cell body and then diffuse into the axon. The distance traveled by IP_3 via diffusion has been estimated to be ~24 μm (Allbritton *et al.*, 1992), which would allow signal propagation through the cell body of a typical Purkinje neuron (20-40 μm in diameter), but unlikely through the entire length of its axon. Therefore, a signal relying solely on passive diffusion of IP_3 produced in the cell body would be short-ranged, unless some other mechanism for IP_3 receptor activation exists. For example, a submicromolar amount of free calcium acts as a coagonist and may activate the receptor at a given IP_3 concentration (Bezprozvanny, 1991; Finch, 1991). One plausible source of calcium along the axon is the voltage-gated calcium channels. The presence of IP_3 receptor in axons also provokes another question: might the IP_3 receptors expressed in the axon be different from those in the soma and dendrites? Their properties may be different because of various receptor isoforms, or because of differential regulations. Many of these possibilities can not be sorted out until there is an understanding of how each receptor molecule behaves and how many different receptor isoforms are present in the same cell.

Receptor heterogeneity

An appreciable number of IP_3 receptor isoforms have been identified by molecular cloning techniques. These isoforms may be derived from different genes, or from alternative splicing of the pre-mRNA of the same gene. Two or more isoforms could co-exist in one single cell. It is intriguing whether these various receptors are pre-sorted into different subcellular compartments within the same cell, and whether they display different properties.

The use of two synthetic peptide antibodies that were raised specifically against the type I receptor serves as the first attempt to assess the receptor heterogeneity in cerebellum at the protein level. In the literature there has been a wide range of binding

affinity reported for similar biochemical preparations of receptors, and it has been suggested that the difference may be due to various receptor subtypes. We have observed, however, that both synthetic peptide (sp)-antibodies precipitate quantitatively nearly all [^{3}H]-IP$_3$ binding sites from membrane solutions, and such depletion is corroborated with Western detection of the same supernatant fractions. This result suggests that type I receptor makes up the majority of the receptor population in rat cerebellum. The biochemical complexity observed in native receptors prepared from cerebellum, however, could still be due to the heterogeneity generated by alternatively spliced variants of the same receptor type. My studies did not address the relative abundance of these splice variants since none of the antibodies generated would distinguish the type I receptor specifically at the *SI* or *SII* region. Yet another explanation for the observed biochemical complexity is that the same receptor type may be modulated by different regulatory factors, resulting in functional diversity. On the other hand, there is evidence that each receptor molecule is capable of exhibiting complex properties. This question will be explored further in Chapter 5.

Chapter 4.

Expression of Rat Type I IP_3 Receptors in Transfected HEK293 Cells

Introduction

Although found in all tissues, the IP_3 receptor is present at a very high density in cerebellar Purkinje neurons (Worley, 1989), in which it is localized to the endoplasmic reticulum. Its abundance in cerebellum facilitated its first biochemical isolation and characterization as well as molecular cloning and sequencing (Maeda *et al.*, 1989; Mignery, 1989; Supattapone, 1988b). This cerebellar receptor, also designated the type I receptor, is the major but not the exclusive IP_3 receptor type in cerebellum (De Smedt, 1994). It has also become a model for the structure and function of the other receptor types found in the peripheral tissue.

The receptor purified from rat cerebellum migrates in the SDS-polyacrylamide gel as a 260-kD protein band. Four of these 260-kD polypeptides non-covalently assemble to form the functional receptor/channel unit, providing its four-fold symmetry and quatrefoil appearance on EM (Chadwick *et al.*, 1990; Maeda, 1991). Each subunit is a phosphoprotein subject to modification by a number of kinases. There is also unique glycosylation on the receptor that allows interactions with Concanavalin A (Con A) and wheat germ agglutinin (WGA). This property has been utilized effectively for affinity purification of the receptor (Ferris, 1989; Hingorani & Agnew, 1992).

Heparin competitively inhibits IP_3 binding to the receptor, with an estimated EC_{50} of 10 μg/ml. The mechanism of inhibition is thought to be an electrostatic

interaction of heparin with the receptor near the ligand binding site. No other specific antagonists have been identified.

The purified protein functions as an IP_3-activated calcium release channel. Upon reconstituting the receptor into liposomes, Ferris and coworkers were able to demonstrate flux of Ca^{2+} ions in response to IP_3 (Ferris, 1989). This activity is modulated by various factors, including calcium, pH, ATP, redox agents, and phosphorylation. Purified cerebellar receptors also display the unique property of quantal calcium release.

Exactly why the receptors exist in the Purkinje cells in such an extraordinary abundance remains elusive. The significance of its structural diversity—a result of multiple genes as well as alternative splicing of a single gene product—and possible functional diversity is also an enigma. Attempts to dissect out functional differences in the various receptor types have been hampered by the heterogeneity of receptor forms found in tissue extracts. Thus, we believe it critical to reduce the complexity of the preparation so that each individual receptor type may be examined in a greater detail. In particular, a system is sought that can produce the receptor protein in a quantity amenable to biochemical isolation and characterization. For these reasons we have cloned the type I receptor from rat brain and expressed it in a mammalian cell line.

A few groups have expressed the receptor in this way. Mikoshiba's group, by transfecting a fibroblast L cell line (Miyawaki *et al.*, 1990) and NG108-15 cells (mouse neuroblastoma-glioma hybrids) (Furuichi, 1989), demonstrated that the expressed receptor binds to IP_3 with a high affinity and thus can be activated to release calcium from membrane vesicles. In another study, Mignery *et al.* have used COS cells for transient expression of full-length, as well as various truncated mutant clones for structure-function studies (Mignery, 1990). From a number of mutagenesis experiments the IP_3 binding site was localized to the first 788 residues of the N-terminus of each

subunit. In these expression systems, however, it appears that a significant amount of endogenous receptor activity exists, and the receptor protein purified from these cells was not sufficient for detailed biochemical assays.

We have chosen a human embryonic kidney cell line (HEK293) as a vehicle to express the receptor under the control of a potent cytomegalovirus (CMV) promoter. Here we show that this simple system provides a highly efficient and reliable means of producing the full-length and truncated receptor proteins in a transient expression system. Furthermore, stable cell lines can be established under a selection medium. These stable lines offer a simplified preparation in which one single isoform is abundantly expressed as a defined, homo-oligomeric receptor suitable for structural and functional studies. The background activity is negligible in [^{3}H]-IP$_3$ binding. In this chapter I provided an account of the expression system while exploring the following questions: (1) Is the receptor capable of binding IP$_3$? Does it assemble to form a higher order (e.g., tetrameric) ensemble? Is it glycosylated and phosphorylated as in the native tissue? What is its subcellular location? (2) Would truncated forms, without membrane-spanning segments, be expressed that are capable of binding [^{3}H]-IP$_3$? Would these assemble to form multi-subunit complexes? Would they associate with complementary constructs encompassing the membrane spanning domains? Finally, the implications of these results were discussed and additional questions posed.

Results

IP$_3$ receptor-specific antibodies

The expression of IP$_3$ receptors in the transfected cells was characterized by a number of sequence-specific polyclonal antibodies, which have been fully described in Chapters 2 and 3. Typically Ab-5' was used for Western immunoblots, Ab-M and 3'α

for immunocytochemistry, and Ab-M for immunoprecipitation. These antibodies were directed to fusion proteins corresponding to topographically distinct segments of the cerebellar receptor. In addition, sp-2A and sp-3A, antibodies generated from synthetic peptides specific to the type I receptor, were used in various immunochemical procedures.

Transient expression of full-length and truncated IP_3R in transfected cells

Construction of cDNA clones

The full-length cDNAs of two alternatively spliced isoforms of the type-I IP_3 receptor were selected for expression using the vector pCB6 as depicted in Figure 4-1a. The only structural difference between the two clones lies in the 45-nucleotide segment, which makes up the 15-amino acid *SI* region near the N-terminus. IP_3R-F denotes the construct without insert and, IP_3R-G with *SI* insert. We have also constructed a number of truncated versions of the receptor. The detailed account of which is provided in Chapter 2. All these constructs are summarized in Figure 4-1b.

Immunological detection of IP_3 receptor in cells

A single band of molecular weight ~260 kD from each transfected cell lysate (Figure 4-2a) was identified on Western blot by Ab-5', which also recognized the native receptor of a comparable molecular mass from rat cerebellar microsomes. Cells transfected with the vector pCB6 (mock), however, showed minimal background immunoreactivity.

The receptor expression was further characterized by metabolic labeling of cellular proteins with [^{35}S]-methionine at 40-48 hours post-transfection followed by immunoprecipitation from the detergent-solubilized cells. Figure 4-2b shows that a single intense band (estimated MW 280 kD) is obtained from cells transfected with each

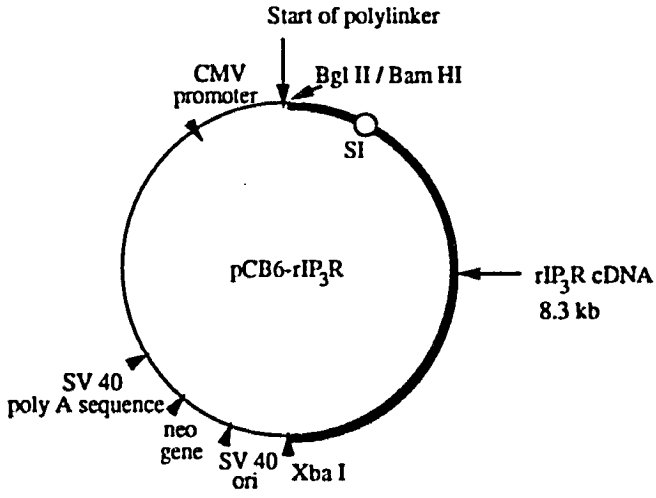

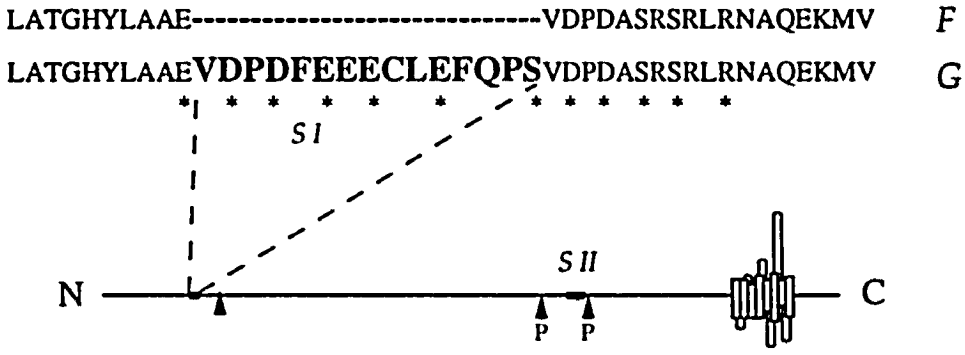

Figure 4-1. (a) **pCB6 expression vector with cloned IP3R-F and IP3R-G cDNA.** On top is a schematic drawing of pCB6, with the rat type I IP3 receptor cDNA cloned into the Bgl II and Xba I sites. Below depicts the 15-amino acid sequence (*SI* region) that is different between the two splice variants, F and G.

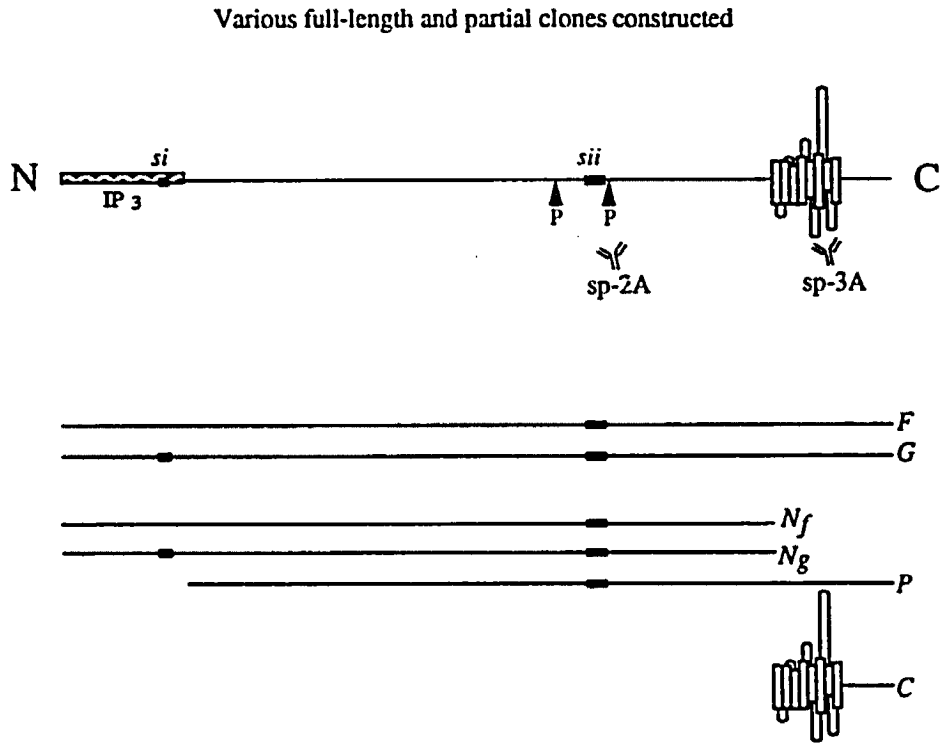

Figure 4-1. (b) **Summary of full-length and truncated clones.** On top is a schematic representation of various functional domains of the IP3 receptor. The antigenic sites with which the two antibodies, sp2A and sp3A interact are also shown. Below, several constructs are aligned. First, F and G represent the two full-length splice variants. Nf and Ng were both truncated at Bst BI site (of cDNA), just before the start of the membrane-spanning sequences. P is a mutant protein that lacks the amino-terminal 418 residues, which form part of the ligand-binding domain. Finally, C was constructed with a synthetic initiation leader sequence plus the receptor cDNA sequence starting from Bst BI site and ending at Xba I site (at the end of the coding region).

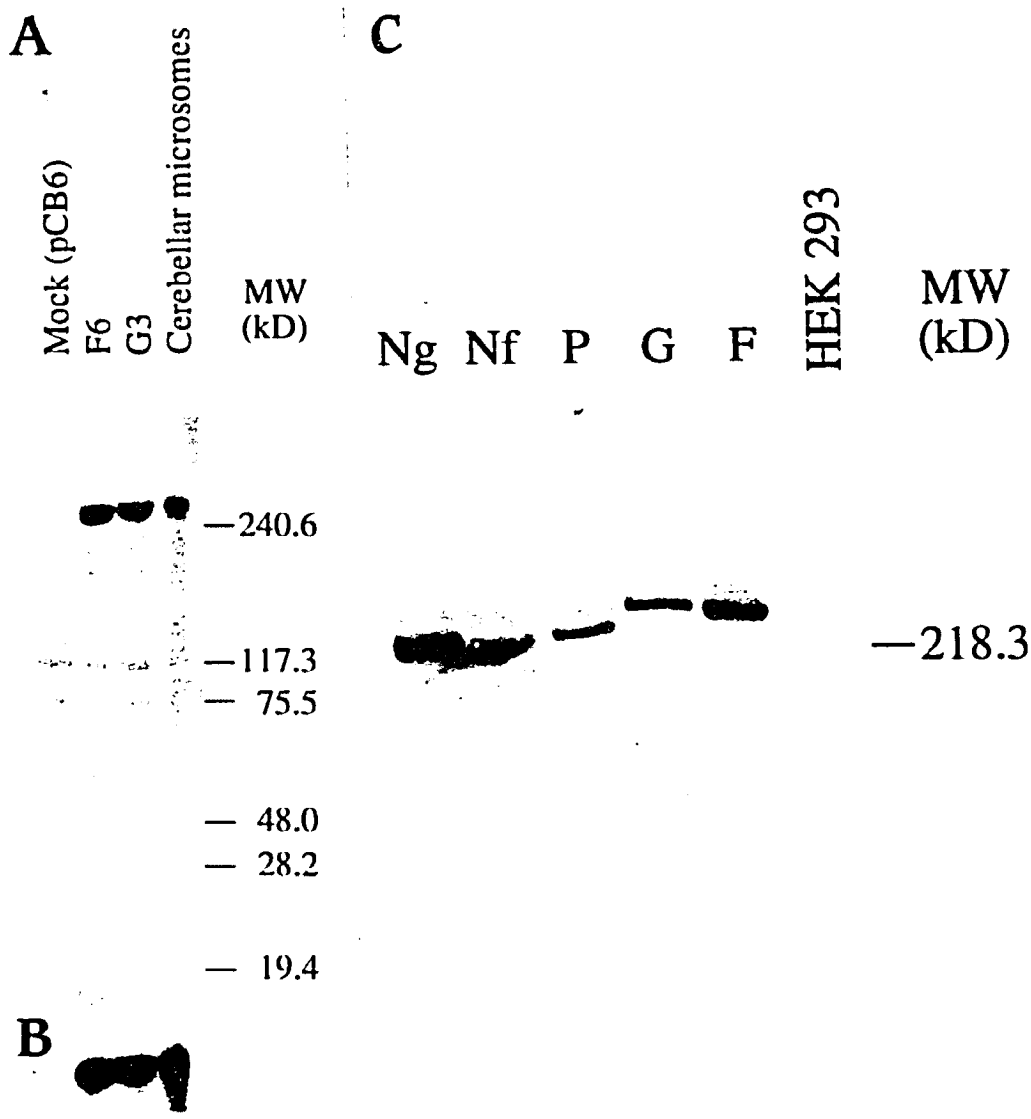

Figure 4-2. (a) **Western detection of full-length (A) and truncated (C) IP3 receptor proteins expressed in HEK293 cells.** The bottom left panel (B) represents an over-exposure of the full-length IP3 receptor protein bands for assessment of the endogenous level. In each case, the mock (pCB6)-transfected HEK293 cells expressed an endogenous receptor that is less than 1/10 of the level in the transient expression system.

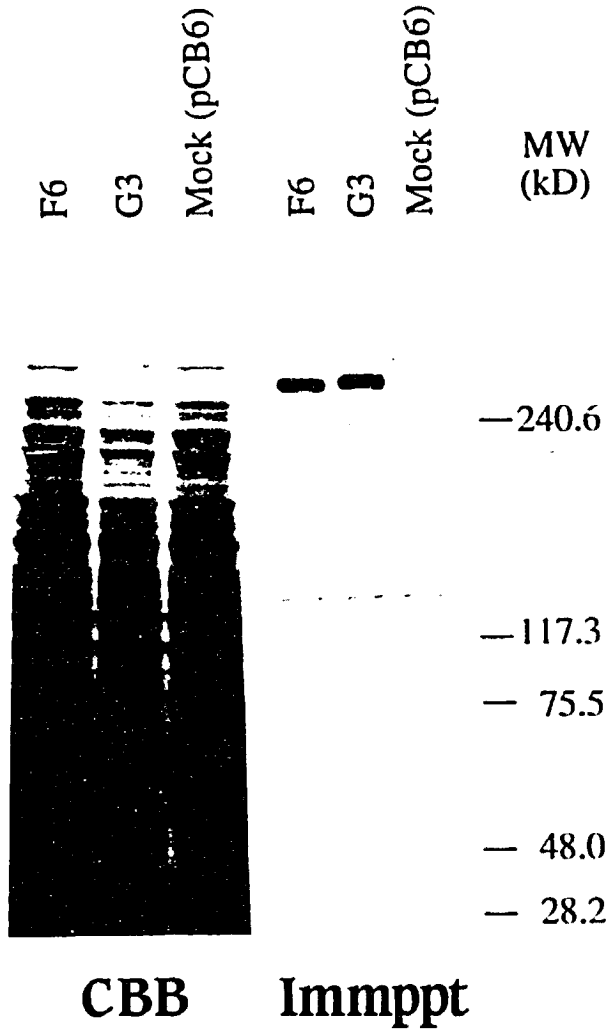

Figure 4-2. (b) **Metabolic labeling and immunoprecipitation of full-length receptors.** Cells were transfected and labeled in 150 μCi/ml of [^{35}S]-methionine at 37°C for 1 hour. They were then lysed, immunoprecipitated with Ab-M, and visualized by autoradiography following electrophoresis (right panel). Note major band of immunoreactivity at 280 kD for both F & G. The left panel shows proteins from the corresponding total cell lysate electrophoresed and stained by Coomassie Brilliant Blue (CBB). The lack of a defined band in the CBB-stained gel indicates that the IP_3 receptor is not a major protein in the transfected cells.

construct but not from mock-transfected cells. The protein expressed from the IP3R-G construct appeared slightly larger (by about 1 kD) than its counterpart, IP3R-F. Although the expression level seemed high, the protein was not readily apparent above endogenous bands on Coomassie-stained gel.

The various truncated clones of the receptor were also expressed and characterized by similar methods (Figure 4-2c). On Western blots the N_f and N_g polypeptides migrated at ~218 kD, somewhat smaller than 238 kD predicted from the encoding cDNA sequence. While failing to appear on Western blot with various antibodies directed against the transmembrane region, polypeptide C was detected at a relatively low expression level with metabolic labeling followed by immunoprecipitation with Ab-sp3A (Figure 4-6b). It appeared as multiple bands around 51-61 kD (again, slightly smaller than the calculated value of 70 kD). We suspect that these multiple bands may be proteolytic fragments of this artifactual construct which could be unstable while *in vivo*, or alternatively, various intermediates of core peptides and glycosylated products, or a combination of these possibilities. The appearance of construct C in transfected HEK293 cells is confirmed by immunofluorescence labeling with appropriate antibodies (Ab-3'α or sp-3A). These micrographs are not shown, for the positive cells have a perinuclear and reticular staining pattern similar to that in cells expressing full-length receptors.

Immunolocalization and transfection efficiency

While at times the endogenous receptor protein in the kidney cells was detected on Western blots and estimated by metabolic labeling to be as high as one fifth of the expressed protein level, immunofluorescence labeling of mock-transfected cells revealed minimal background (Figure 4-3 b). Transfected cells, on the other hand, showed intense fluorescence (Figure 4-3 d & e) in a lattice-like pattern typically seen with labeling of the

Figure 4-3. **Immunofluorescence of HEK293 cells** transfected with (a-b) pCB6 (mock), x700 or (c-d) pCB6-IP3R-G, x700, each detected by Ab-3'α. Note the reticular pattern seen with the full-length constructs. The phase contrast micrographs (a, c) indicate that the transfection efficiency is ~10%. Panels (e) & (f) compare the staining patterns observed for cells expressing the full-length construct, G in (e), and those transfected with Ng construct which express a truncated, soluble form of the receptor in (f). Magnification in (e) & (f) is at x480.

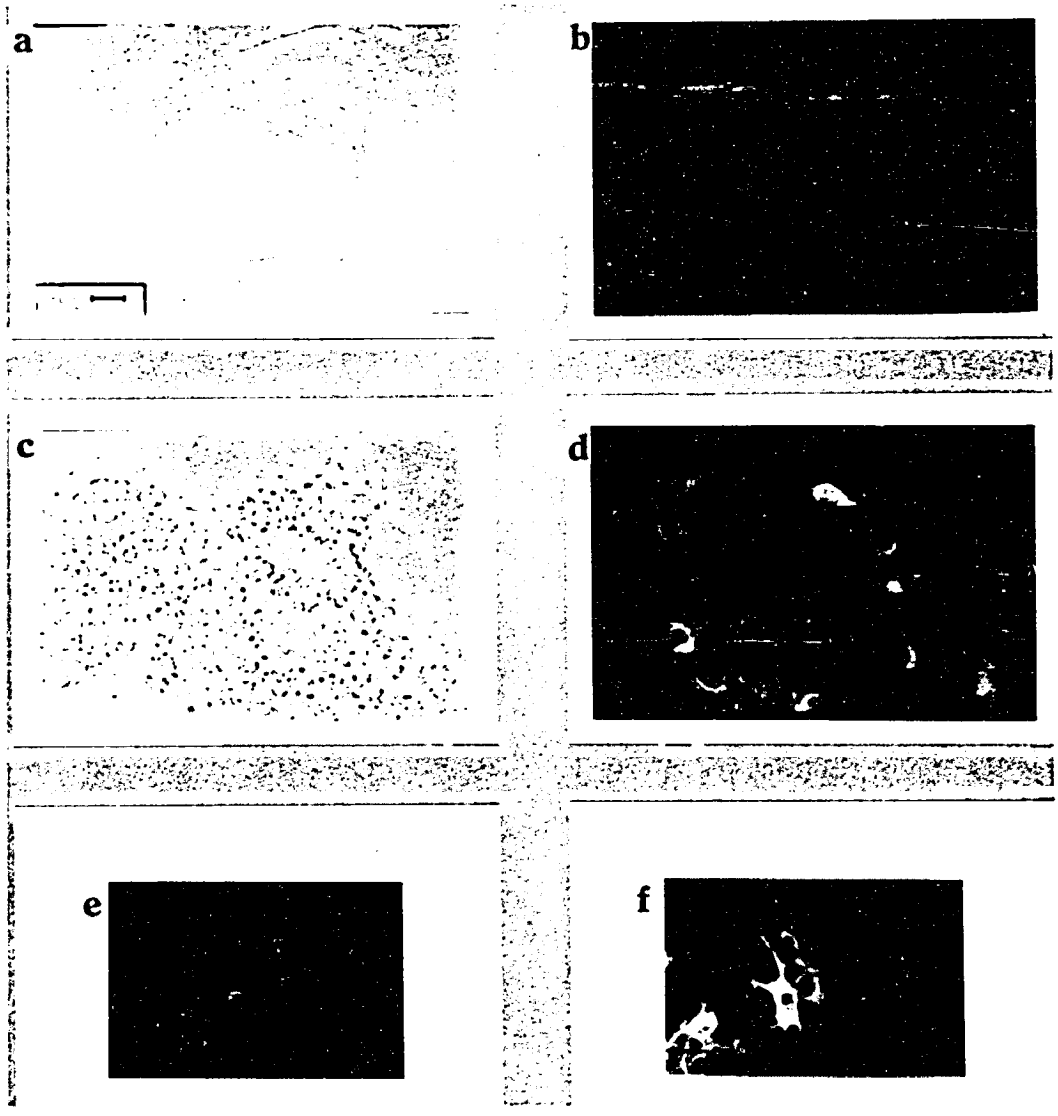

endoplasmic reticulum (Terasaki, 1994). N_f and N_g, soluble proteins due to their lack of the transmembrane domain, had a distinctively different labeling profile as illustrated in Figure 4-3 f. Immunofluorescence carried out on cells transfected with these constructs localized these proteins to the cytosol.

By counting the number of fluorescent cells within a cluster of cells identified by phase contrast micrography, the typical efficiency of transfection was estimated to be 20% under the conditions used. The efficiency was found to be quite variable, ranging from 10 to 50%, often depending on the age of the cells.

The synthesized receptor is relatively stable

The synthesized IP_3 receptor protein could be detected as early as 10 hours post-transfection and reached a maximum level around 40-48 hours. Biochemical assays were therefore performed at 40-48 hours post-transfection.

To gain a sense of the metabolic stability of full-length receptors, I conducted pulse-chase experiments as described in Chapter 2. Two independent trials were performed for each construct, and the $t_{1/2}$ was found to be ~7 hours for IP_3R-F and 5 hours for IP_3R-G (Figure 4-4).

The receptor is a substrate for PKA

I next tested whether the expressed protein could be phosphorylated as in its native form. Both full-length isoforms contain the *SII* region (believed to be present in the receptor isoform expressed in neuronal tissues), which is flanked by two consensus PKA phosphorylation sites (see Figure 1-2). The transfected cells were briefly treated with a PKA or PKC activator (forskolin and phorbol 12-myristate 13-acetate or PMA, respectively), lysed, and the IP_3 receptor immunoprecipitated with antibodies and phosphorylated *in vitro* using the catalytic subunit of protein kinase A. As illustrated in

Figure 4-4. **Pulse-chase and measurement of the metabolic stability of receptors in the transient expression system.** Cells were transfected with the full-length construct, F/G or the parent vector, pCB6. The synthesized proteins were labeled by incubating the cells in DMEM (methionine-free) containing 150 μCi/ml of ^{35}S-methionine. After 30 minutes, cells were washed, reincubated at 37°C and harvested at the indicated time points. The IP3 receptor proteins were precipitated with Ab-M and detected by autoradiography following SDS-PAGE (top panel). The plot of ln (I/I_0) was generated by scanning the intensity of the IP3 receptor bands using the BioImage gel scanner (bottom panel). For the estimate of the degradation rate (k), a first-order rate of decay of the form $\frac{dN}{dt} = -kN$ was assumed, where N denotes the number of protein molecules and is directly proportional to the densitometric measurement of the labeled protein intensity.

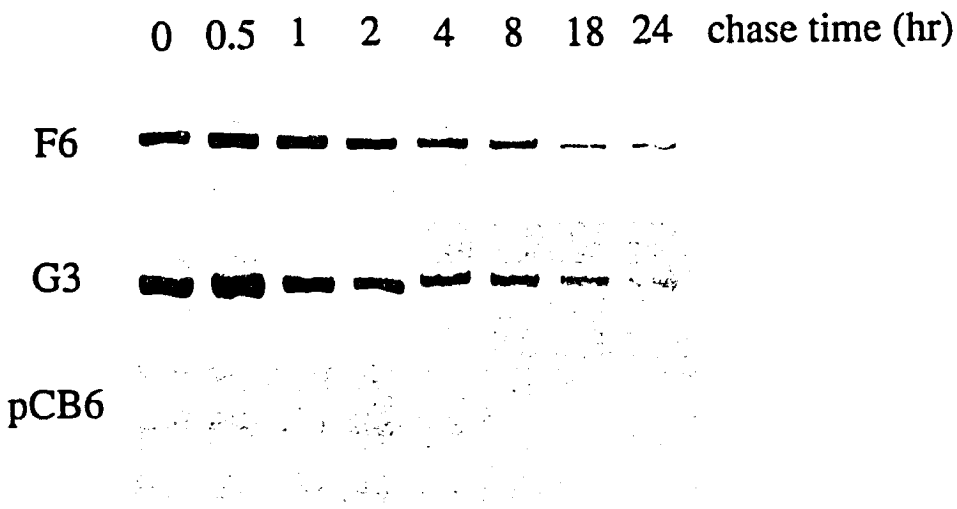

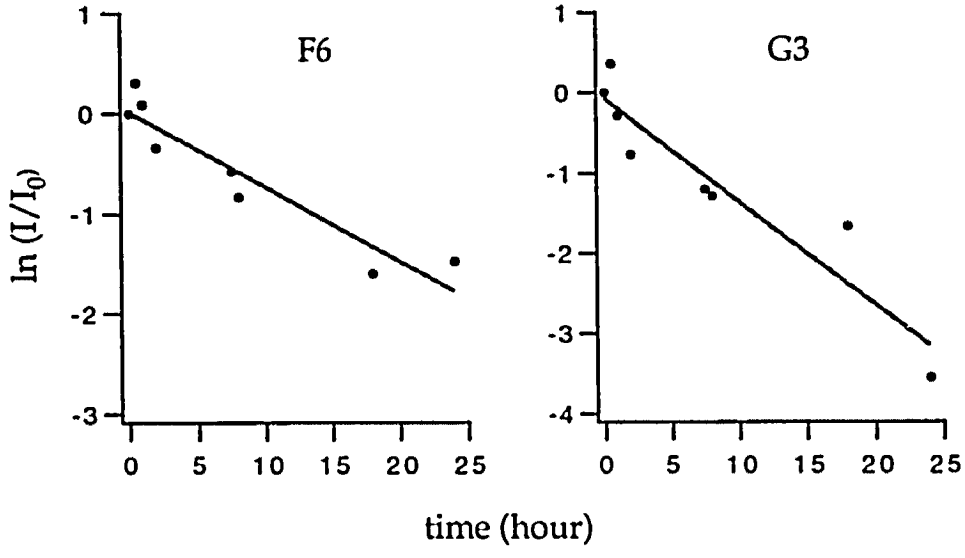

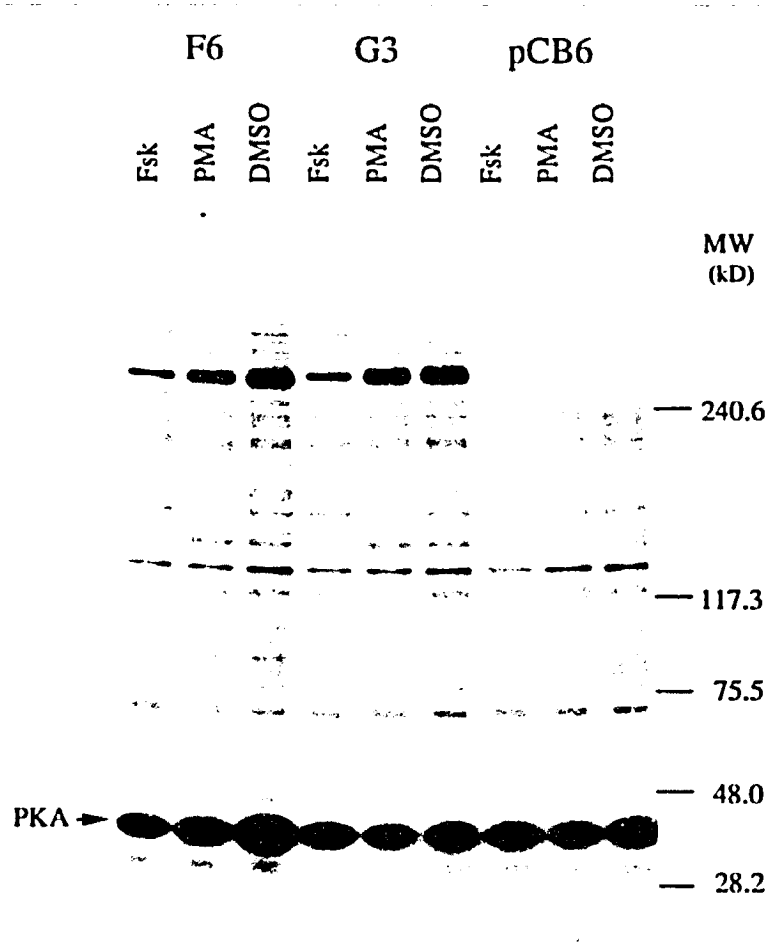

Figure 4-5. ***In vitro*** **phosphorylation by PKA.** Within each set of cells transfected with pCB6, IP3R-G, or IP3R-F, there were three subsets undergoing different treatment for 15 minutes prior to harvest: DMSO (solvent, as a control), PMA (a PKC activator), and Fsk (a PKA activator). The cells were subsequently lysed, and the IP3 receptors immunoprecipitated, followed by phosphorylation with the catalytic subunit of PKA *in vitro*. Note the phosphorylated receptor bands at MW~260 kD. The amount of back-phosphorylation of the receptor accomplished by PKA appeared diminished in both F- and G- transfected cells that had undergone forskolin (Fsk) treatment.

Figure 4-5, forskolin pretreatment diminished the receptors' potential for further phosphorylation by 2-3 fold as compared to their basal state (control cells treated with solvent DMSO alone). In addition to the residues phosphorylated by PKA, the IP_3 receptor has been demonstrated by others to be a target for PKC. Such sites were not revealed, however, or ineffectively revealed by back phosphorylation with PKA following PKC activation with PMA. Although my experiment performed for the IP_3 receptor revealed no change in PKA back-phosphorylation, this does not mean that the receptor is not subject to phosphorylation by PKC. The result does suggest, however, that either PKC site is already phosphorylated endogenously in unstimulated cells, or the site has a peptide sequence unrecognized by PKA.

The protein is glycosylated

To test whether the expressed receptor is glycosylated, we examined its synthesis in the presence or absence of tunicamycin, an inhibitor of N-linked glycosylation. On SDS-polyacrylamide gels we failed to detect any molecular weight difference between proteins isolated from tunicamycin-treated cells and those from the control cells (Figure 4-6a). Besides the possibility of O-linked glycosylation, another possibility is that the molecular mass of attached sugar comprises only a small fraction of the total receptor mass. Since the limit of the resolution power of polyacrylamide gels for a large protein was a concern, I next examined the truncated fragments of the receptor. Figure 4-6b demonstrates the result with metabolically labeled polypeptides N_f, N_g and C, with or without tunicamycin treatment in a transient expression system. Only the truncated receptor fragment C appeared to be glycosylated. As mentioned previously, construct C had a lower expression level than the others, and it appeared on the polyacrylamide gel as multiple bands. Among these multiple bands, some were shifted to locations of higher MW under conditions that allowed glycosylation (from 45-

Figure 4-6. **Studies of N-linked glycosylation.** (a) Cells were transfected and the synthesized proteins were labeled with ^{35}S-methionine at 37°C for one hour in the presence or absence of tunicamycin. Following immunoprecipitation and SDS-PAGE (5%), the receptors were visualized by autoradiography as shown here. Note the major labeled protein bands at ~260 kD in both F and G. The molecular weight of these full-length receptors appears unaltered with tunicamycin treatment, even on a low-percentage gel.

(b) Cells were transfected with each truncated construct and metabolically labeled as in (a). The synthesized proteins were precipitated from each cell lysate with Ab-sp2A (for N-constructs) or sp3A (for C-construct). Note that a difference in molecular weight is detected only in the partial clone "C" after tunicamycin treatment. The lanes labeled +/- denote a combination of proteins with or without tunicamycin treatment; they were run together for a close examination of molecular weight shift.

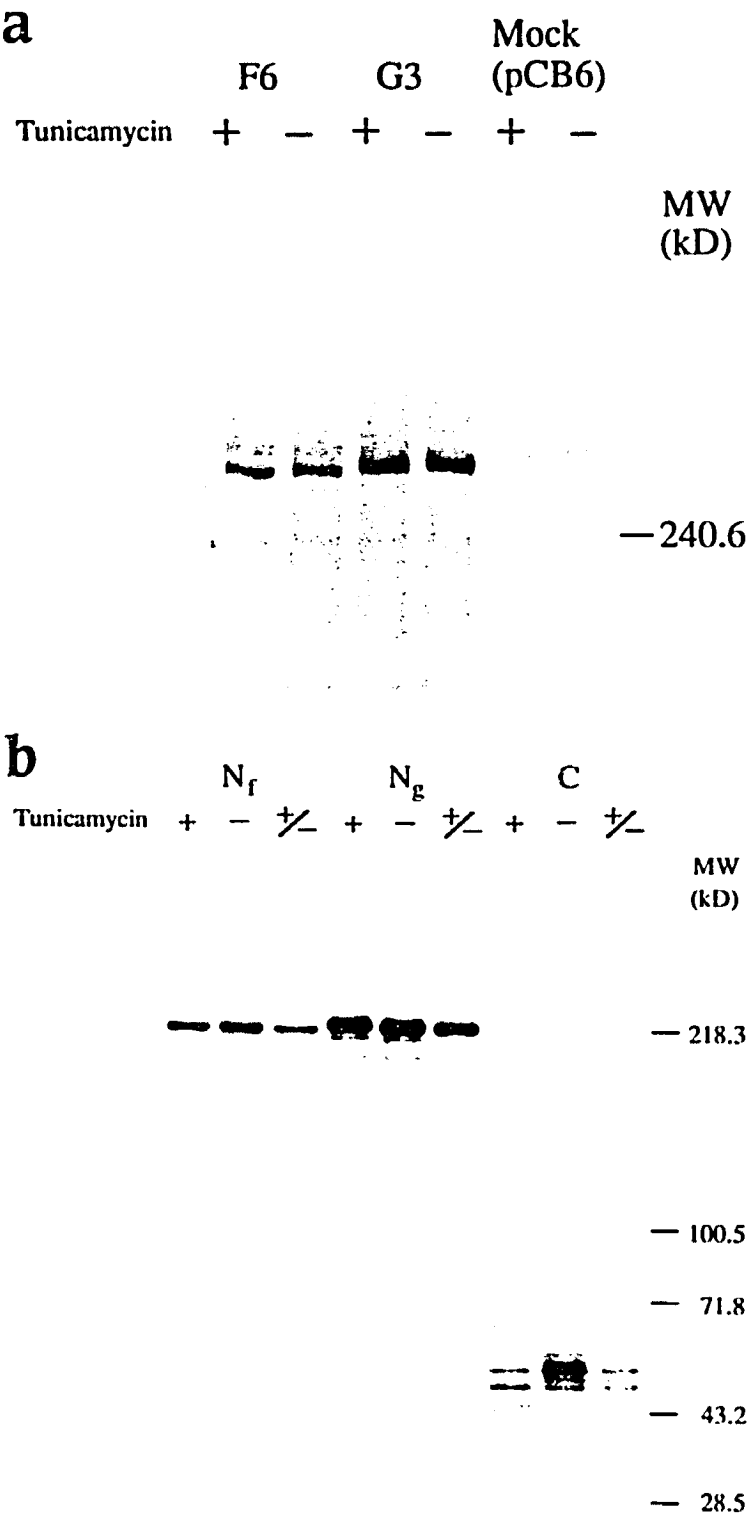

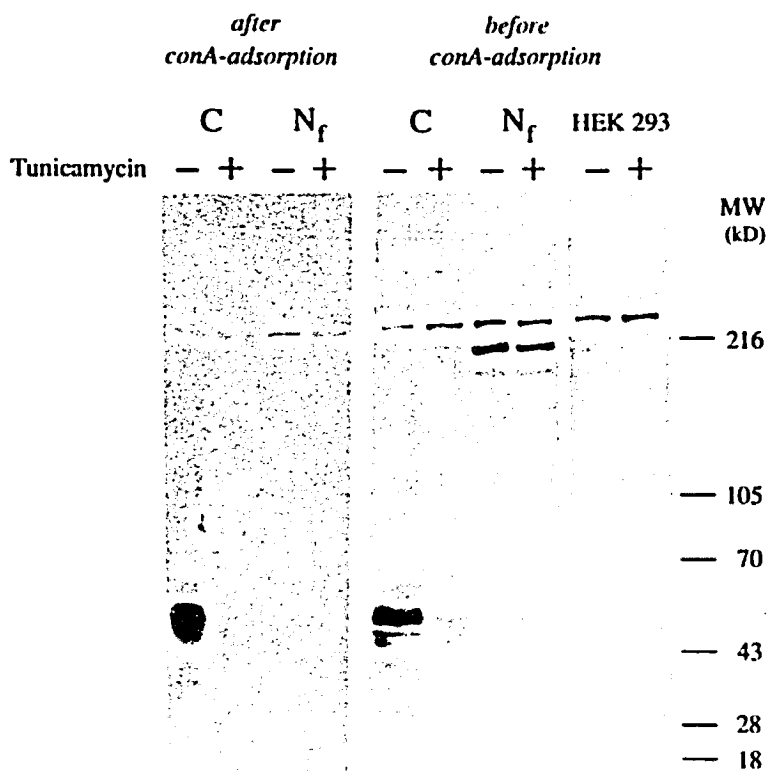

Figure 4-6. (c) **Studies of N-linked glycosylation using lectin gels.** The HEK293 cells were transfected with either Nf or C construct, treated ± tunicamycin, lysed, and subject to adsorption with Con A‡-agarose. The precipitated proteins were eluted, electrophoresed through a 4-15% SDS-polyacrylamide gel, and electro-blotted onto nitrocellulose membrane. A mixture of antibodies (Ab-5', sp2A & sp3A) were used for Western detection of the truncated receptor fragments. The upper band ~240 kD across all lanes represents the endogenously expressed IP_3 receptor. This study demonstrates that only the "C" fragment of the receptor contained N-linked sugars recognized by Con A. ‡Con A, *Concanavalia ensiformis* agglutinin

56 kD in the presence of tunicamycin to 51-61 kD in its absence), although there were some overlapping bands. This shift was not observed with N_f and N_g. To clarify the nature of this shift in molecular weight, yet another approach was taken with N_f and C. Instead of immunoprecipitation of labeled receptor proteins, Con A-agarose gel was used to precipitate glycosylated proteins from the cell lysate, and the IP_3 receptor proteins or fragments were then identified by Western immunoblot with mixed antibodies directing to both N- and C-terminal regions. In Figure 4-6c it is apparent that fragment N_f, whether with or without tunicamycin inhibition, did not contain a glycosylated residue capable of binding Con A. In contrast, fragment C was precipitated by Con A (and consolidated into a single broad, fuzzy band). Treatment with tunicamycin abolished its precipitability.

Stable expression of two alternatively spliced isoforms

Establishment of stable cell lines

Stable cell lines were established from HEK293 cells transfected with each of the two full-length constructs, IP_3R-F and IP_3R-G (Chapter 2). Figure 4-7 illustrates a subset of stably expressing clones. Those with names beginning with F express the receptor protein from the IP_3R-F isoform construct. Likewise, those beginning with G are derived from IP_3R-G. The subscript letter denotes individual clones. Fd, Fe, Gb and Gg express full-length receptor protein. Note, however, that Fa had abundant receptor expression as detected by Ab-5', but its molecular mass (220 kD) was lower than that expected of a full-length protein (280 kD on the same blot). Subsequent immunocytochemical studies using several antibodies directed to various segments of the receptor suggested that Fa expressed a truncated version which lacked at least part of the transmembrane region and the C-terminal tail. When the cells were lysed to yield soluble proteins and the insoluble membrane fraction, 50% of the total [^{3}H]-IP_3 binding

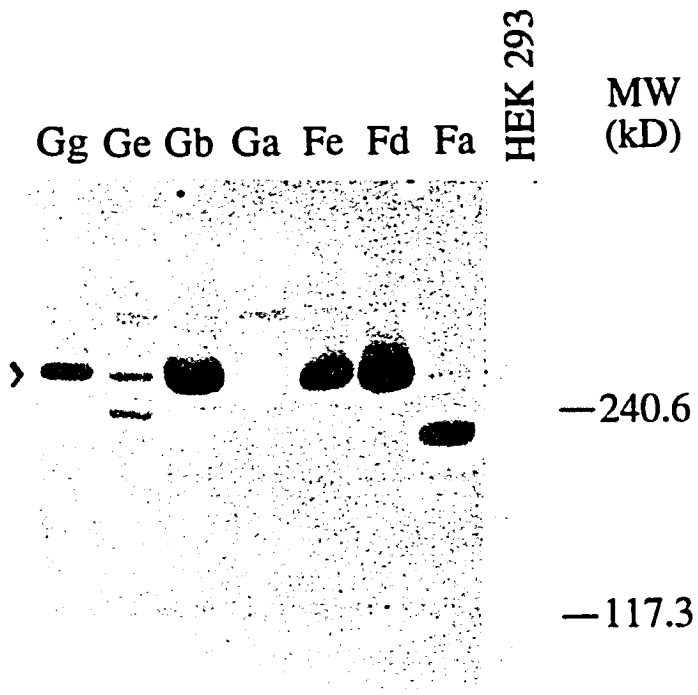

Figure 4-7. Screening for stable clones that express IP3R by Western immunoblot. Cells from clonal expansion were grown in duplicates using 24-well plates. One set of the clonal cells were harvested, lysed, and prepared for Western immunoblots. Ab-5' was used as the primary antibody at 1:200 to detect positive expressions. The arrow points to the full-length IP3 receptor band (~260 kD).

Figure 4-8. **Confirmation of F & G identity.** Total cellular RNA was isolated from each stable cell line, reverse-transcribed, and the cDNA amplified near the *SI* region using a pair of PCR primers (see Chapter 2). This is illustrated below. The first line represents a schematic map of the rat type I IP3 receptor cDNA (with coding sequence of 8,247 bp in length; bp=base pair, nt=nucleotide). The amplified region is internal to the two PCR primers designated P1 and P2. This region is enlarged in the second and third line, depicting the difference between F and G constructs. Because of the presence of *SI* in the G construct, an Acc I restriction site is introduced. The various restriction sites are marked by arrowheads and the length of fragments is indicated.

F & G receptor constructs could be distinguished at the amplified region by two ways after being resolved on 4% agarose gels (3% NuSieve/1% SeaKem agarose, FMC Corporation). On the facing page the top panel demonstrates the 45-base pair difference between F & G constructs due to *SI*. The bottom panel demonstrates that the presence of *SI* in G constructs provided an Acc I restriction enzyme site, resulting in 320- and 145-bp fragments after cleavage (also refer to the schematic illustration). The F constructs were unaltered by Acc I digestion.

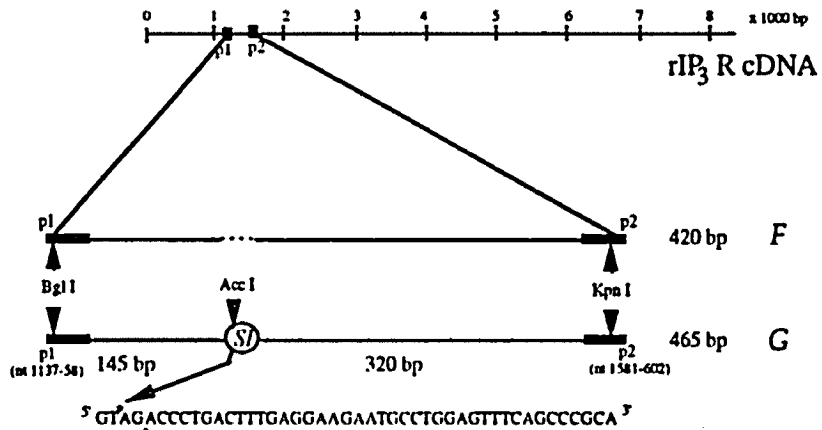

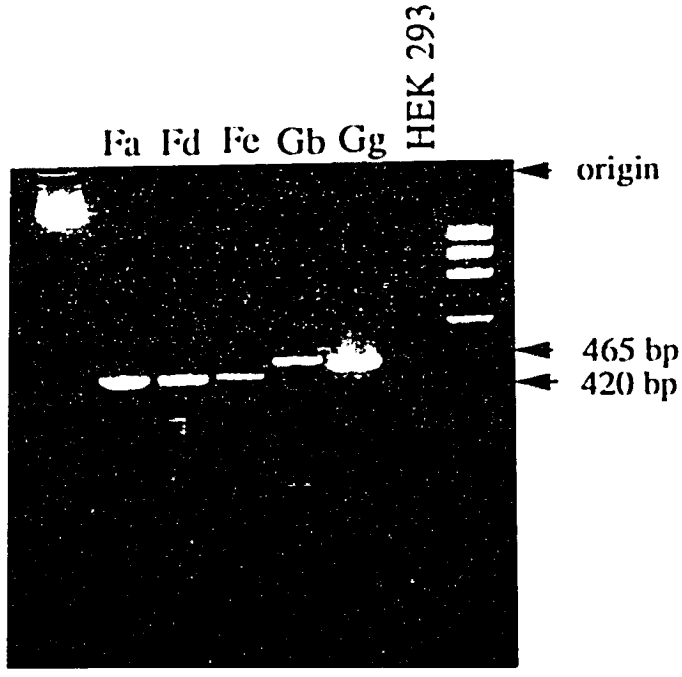

after AccI digestion

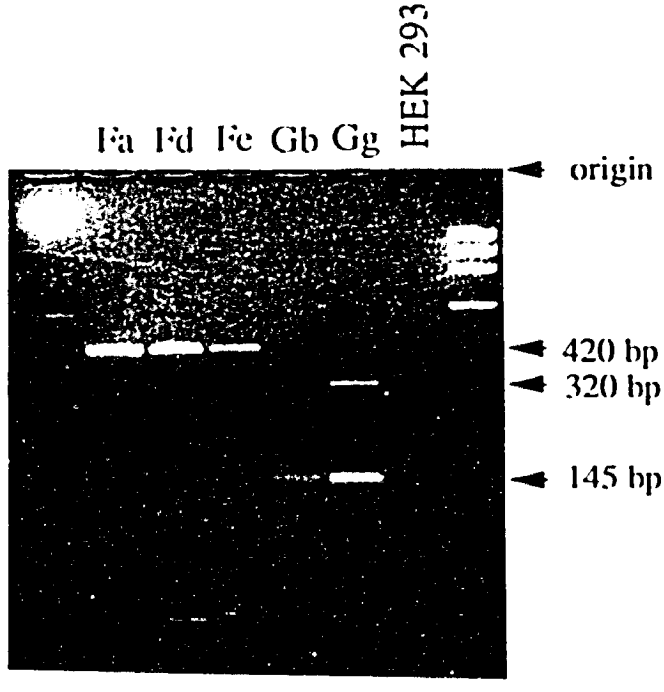

was detected in the soluble fraction, suggesting that Fa was indeed a soluble variant of the receptor probably produced incidentally by recombination during genomic insertion. Ge appeared to comprise a mixture of full-length and truncated receptors, and Ga did not reveal a protein band at the anticipated molecular weight. These two clones, therefore, were not further characterized.

To confirm that each stable cell line indeed expressed a receptor isoform of the correct origin, reverse transcription followed by PCR was performed on the cellular RNA isolated from each line. Figure 4-8 shows that each G-cell line could be distinguished from the F-cell line by the presence of 45-base pair *SI* sequences in the amplified cDNA.

Basic characterization of stably expressed proteins

A total of four clones– Fd, Fe, Gb and Gg–were selected for further characterization. Each clone produced a band of MW~280 kD on Western blots, equivalent in size to the IP_3 receptor from cerebellar microsomal membranes. Data presented in Figure 4-9 also indicated that the expression level of each clone (from about 10^5 cells) was comparable to the amount of receptor in 100-150 μg of total protein from rat cerebellar microsomes.

Pulse-chase experiments were performed to study the metabolic stability of newly synthesized receptor in the stable cell lines (Figure 4-10). From two independent trials for each of the four clones, the average half-life was 14 hours (Fd: 12, Fe: 14, Gb: 11, and Gg: 18). This was about 2-2.5 fold longer than the receptor half-life in the context of transient expression. Other parameters are summarized in Table 4-1.

As in the transient expression system, glycosylation was not revealed by a shift in apparent molecular weight due to tunicamycin treatment. Approximately the same amount of the receptors, however, could be precipitated by antibody sp-2A, heparin- and Con A-agarose, indicating that they were indeed glycosylated (Figure 4-11).

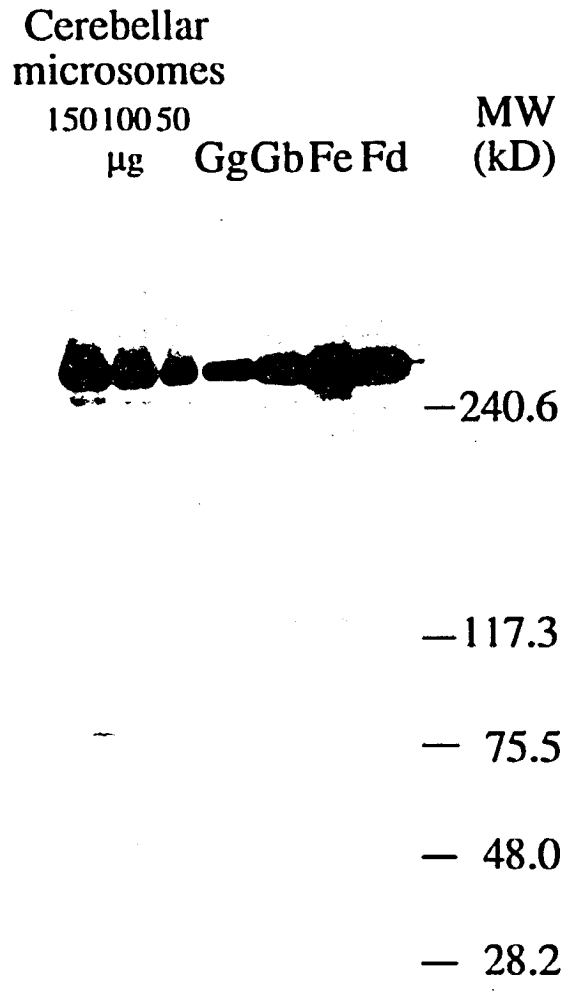

Figure 4-9. **Semi-quantitative estimate of receptor expression.** An equal proportion of cell lysate from a 35-mm dish (containing about 10^5 cells) was loaded per lane for each stable cell line. A known amount (of total protein) of cerebellar microsomes was loaded in parallel for comparison. A Western blot was prepared from these samples, and the receptors were detected using Ab-5′ at 1:250 dilution and ^{125}I-Protein A at 0.5 µCi/ml.

Figure 4-10. **Metabolic stability of receptors expressed in stably transfected cell lines.** Stable cell lines were plated and grown to near confluence. Each was labeled in DMEM (methionine-free) with 150 μCi/ml of ^{35}S-methionine for 30 minutes at 37°C. Cells were then washed, reincubated in regular DMEM until finally harvested at the indicated time. The IP3 receptor proteins were immunoprecipitated and detected by autoradiography. The plots for estimating the receptor half-life were generated by digitizing the intensity of each IP3 receptor band with a gel scanner. The rate constant for degradation, k was estimated from the slope of each plot, and the receptor half-life, $t_{1/2}$ was calculated according to the relationship $t_{1/2} = 0.692/k$.

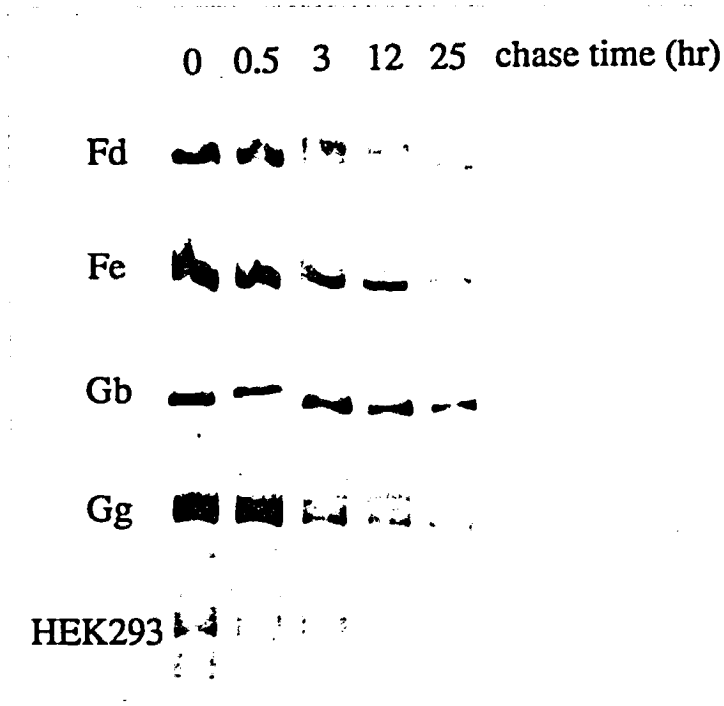

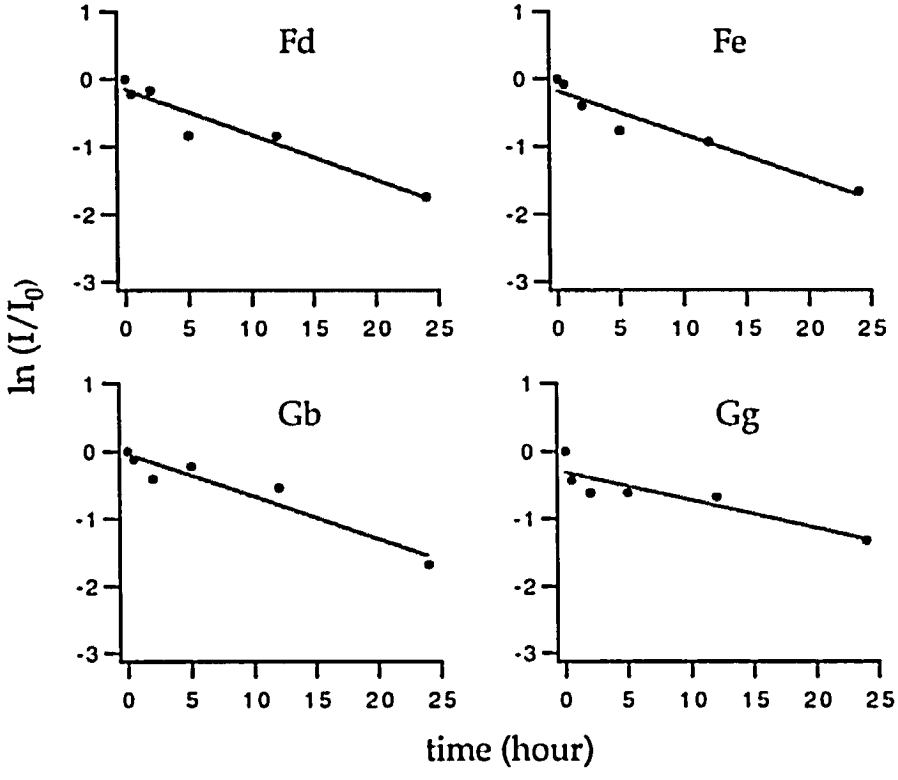

Table 4-1. **Parameters calculated from biosynthetic studies on stable cell lines.**

	Fd	Fe	Gb	Gg
$t_{1/2}$ (hours)	12	14	11	18
B_{max} (pmol/mg)	29	29	22	12
τ (hours)	17	20	16	26
k_1, degradation rate (hr^{-1})	0.058	0.05	0.063	0.039
k_0, synthesis rate ($\frac{pmol}{mg} \cdot hr^{-1}$)	1.682	1.45	1.386	0.462

The equation for protein biosynthesis used here assumes a zero-order rate for synthesis (i.e., a constant rate of synthesis, k_0) and a first-order rate for degradation (refer to Appendix for equations). From pulse-chase experiments, k_1 (rate of degradation) was estimated from the plot of $\ln(N_t/N_0)$ or $\ln(I/I_0)$ versus chase time, where *N* denotes the number of protein molecules at time t or time 0, and *I* denotes intensity of protein band measured by densitometry. The time constant, τ is inversely proportional to k_1. The half-life, $t_{1/2}$ is calculated from the relationship, $t_{1/2} = \ln 2/k_1$. The values of maximum binding, B_{max} were estimated from a number of [^{3}H]-IP$_3$ binding isotherms on receptors prepared from the various stable cell lines (see Table 5-1). Finally, k_0 (rate of synthesis) is related to k_1 by the equation: $B_{max}=k_0/k_1$.

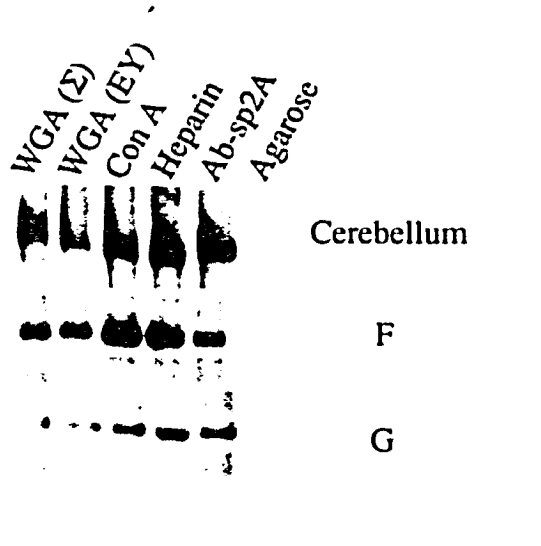

Figure 4-11. **Precipitation of expressed IP3 receptors in the stable cell lines with lectin gels.** Detergent-solubilized cerebellar microsomes, F- and G-cell lysates were aliquoted into 6 equivalent fractions for precipitation with various reagents including two different preparations of WGA[†]-agarose, Con A-agarose, heparin-agarose, as well as Ab-sp2A (as a positive control) and unconjugated agarose (as a negative control). The precipitates were electrophoresed and transferred to a Western blot, and the IP3 receptor band was detected by Ab-5'. The IP3 receptors synthesized in the stable cell lines, F & G, were recognized by lectin gels including Con A and WGA. WGA appeared to have a lower specific activity than Con A in each case. About an equivalent amount of receptor proteins could be precipitated by Ab-sp2A (followed by Protein A-agarose), heparin-agarose (perhaps interacting with the IP3 receptor near the ligand-binding site), and Con A-agarose. Agarose gel alone had no effect.

[†] WGA, wheat germ agglutinin

Immunocytochemistry and morphology

Immunofluorescence microscopy with Ab-M showed the labeling of all cells in the field (Figure 4-12), indicating the homogeneity of each stable cell line. The amount of fluorescence per cell appeared somewhat less than that observed in the positive cells in the transient expression system. Nevertheless, the fluorescence intensity well surpassed the background level in the parent HEK293 cells.

It was also noted that both Gb and Gg underwent a morphological change. This was especially prominent in Gg, but was consistently observed in both lines after cells were allowed to settle in culture for approximately three days after plating. The cells assumed a smaller, round cell body shape, with development of multiple slender cell processes extending to adjacent cell processes. Moreover, in contrast to the parent HEK293 line, G cells maintained significant cell-to-cell distance and never grew to complete confluence.

Functional properties

The expressed receptors bind IP_3

The full-length receptors, as well as the N_f, N_g truncated forms specifically bound [^{3}H]-IP_3. The binding was sensitive to both heparin and 1 mM of free calcium (Figure 4-13b). Binding activities of the full-length receptors were detectable only from detergent-solubilized membrane fractions. The truncated forms, lacking the transmembrane domain, could be isolated from the cytosol of the transfected cells. However, roughly 50% of the total binding activity remained in the membrane fraction (Figure 4-13a).

Because of their consistence in expression and the ease of preparation, only the receptors isolated from stably transfected cells were characterized by full binding isotherms. Figure 4-14 illustrates an example of the isotherm of [^{3}H]-IP_3 binding in each

Figure 4-12. **Immunofluorescence of stable cell lines using Ab-3'α or Ab-M.** (a, a') untransfected HEK293 cells, (b, b') Fe, (c, c') Gg, (d, d') Gb, (e, e') Fa, and (f, f') Fd, each at magnification x360 . Note the prominent morphological transformation of Gg cells (c'). A similar but less dramatic phenotype is expressed by Gb cells (d'), but it usually requires at least three days of culture after each plating. Fa cells (e') express a truncated, soluble version of the IP_3 receptor that is labeled by Ab-M but not Ab-3'α or 3'β, indicating that this receptor lacks at least part of the membrane-spanning domain and the C-terminal tail. Each immunofluorescence micrograph is accompanied by a corresponding phase-contrast micrograph on the left.

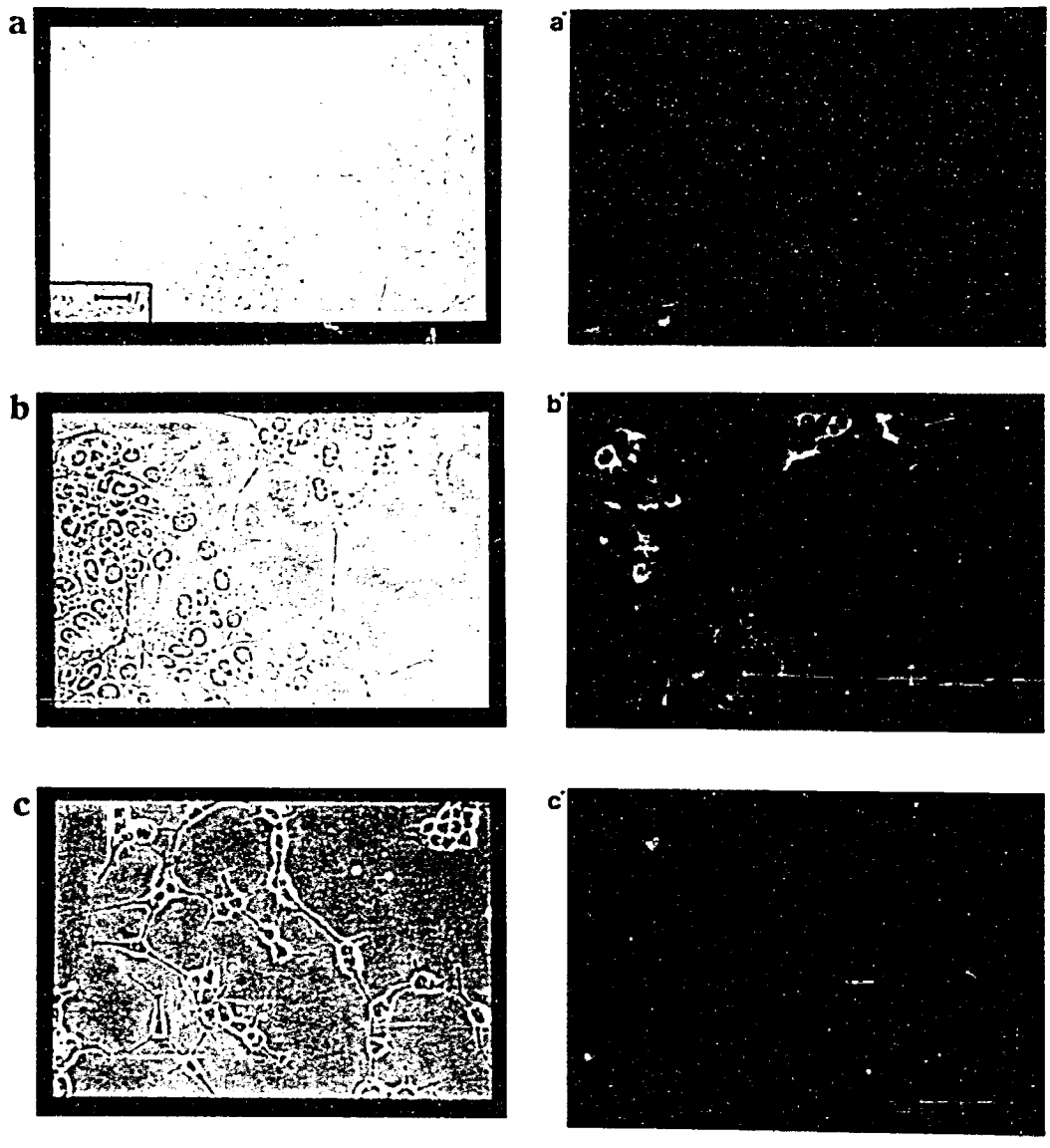

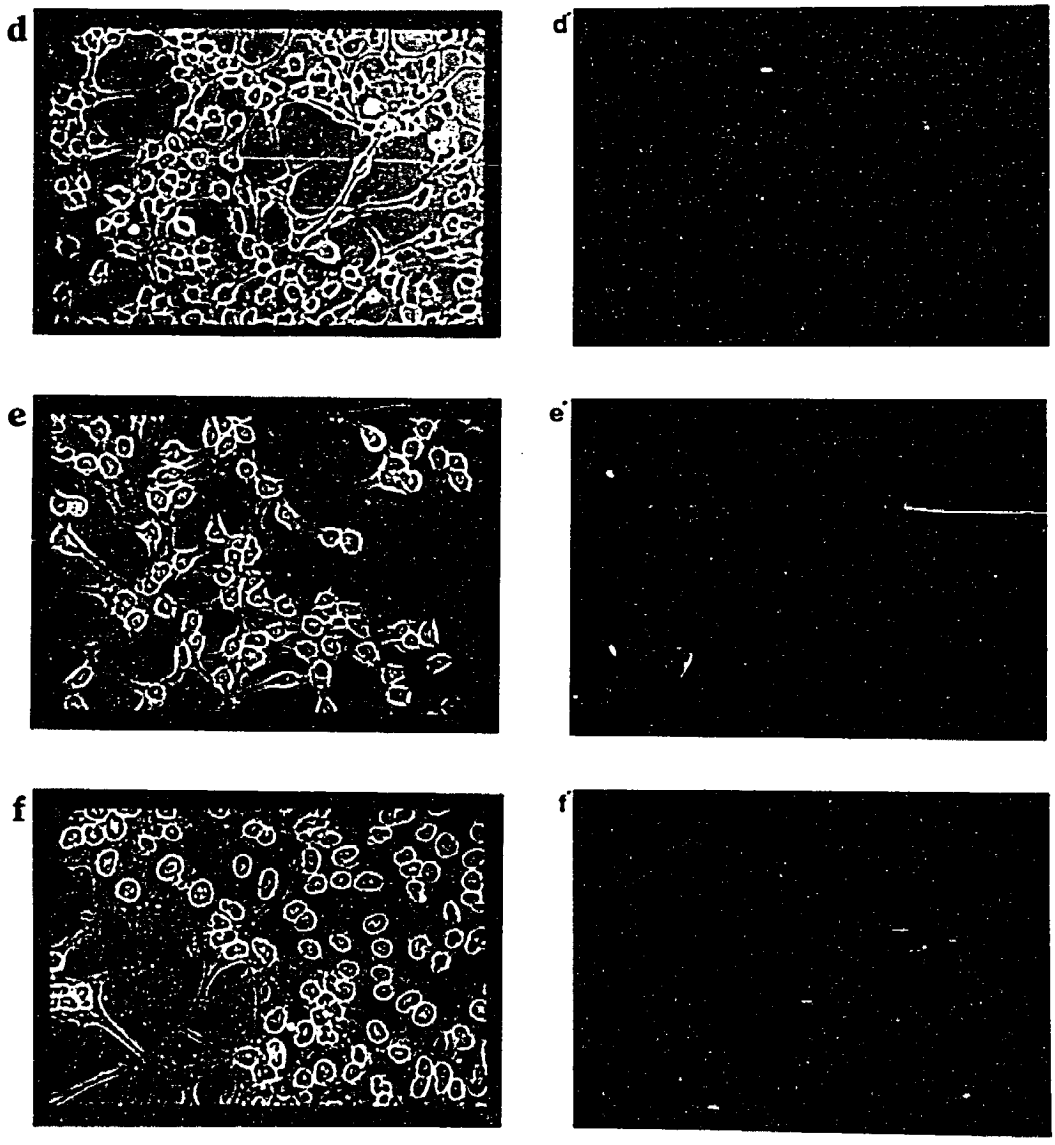

Figure 4-13. **[^{3}H]-IP$_3$ binding of expressed IP$_3$ receptor proteins.** (a) Stable cell lines or transfected cells were harvested in PBS-EDTA, pelleted, and then lysed in hypotonic buffer with a homogenizer to release proteins in the "soluble fraction". The pellet contained the "insoluble membrane fraction", from which the membrane proteins were extracted by homogenization in a buffer containing 1% Triton X-100. Binding activity of the full-length receptors was detected only in the detergent-solubilized membrane fraction, whereas that of the truncated receptors lacking the membrane-spanning segments was detected in both the soluble (cytosolic) fraction and the membrane fraction. The experiment was repeated at least twice for each construct with similar results.

(b) IP$_3$-binding was inhibited by heparin and Ca^{2+} in all of these receptor constructs. Represented here are cells transfected with the full-length (F8) or the truncated (Nf) construct. The same results were obtained from the G- or Ng-transfected cells, as well as from the stable cell lines including Fd, Gb (full-length) and Fa (truncated). The expressed full-length proteins were liberated by cell lysis in a buffer containing 1% Triton. The truncated proteins were harvested from both the cytosolic and the membrane fractions as described above. These truncated proteins from both fractions demonstrated the same sensitivity to heparin and calcium.

a. different location of expressed receptor proteins

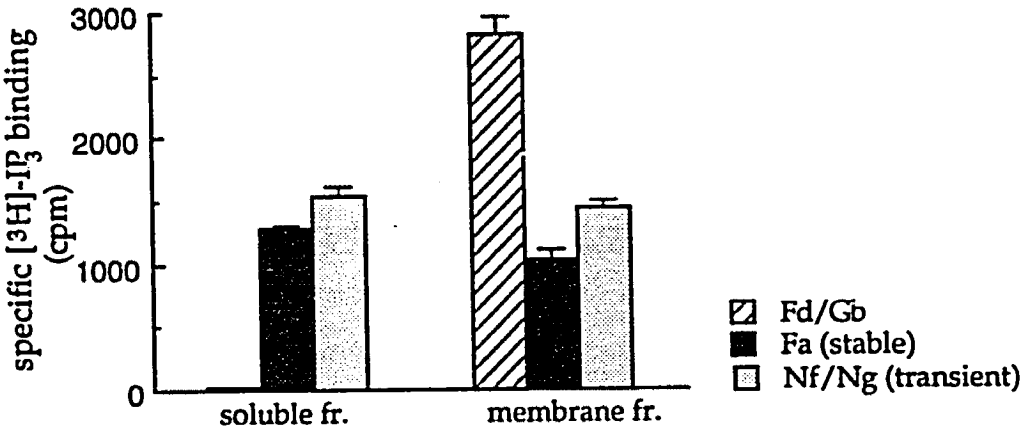

b. sensitivity to calcium and heparin

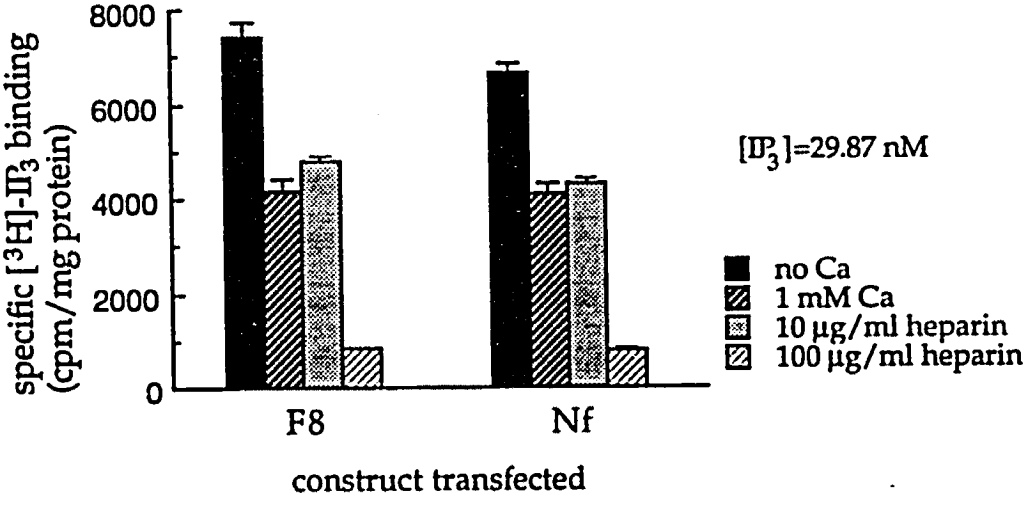

Figure 4-14. **Langmuir binding isotherms.** [^{3}H]-IP$_3$ binding was measured in solubilized membranes prepared from untransfected HEK293 cells, and stably transfected F and G cells. Each filled circle represents the mean of duplicate measurement of total IP$_3$-binding, whereas the hollow circle represents single competition assay with excess unlabeled ligand. The error bar indicates the range of scatter from duplicate binding measurement.

Each isotherm was fitted for estimation of K_d & B_{max}, assuming a single class of non-interactive binding sites. Shown here are the typical isotherms representative of each cell type. Five to six trials of assay have been performed from different receptor preparations for the measurements of binding parameters.

Also displayed here is the binding isotherm for Fa, which expresses a soluble version of the IP$_3$ receptor in F cells. Indirect immunofluorescence with several sequence-specific antibodies has indicated that this truncated receptor lacks at least part of the transmembrane region and the C-terminal tail.

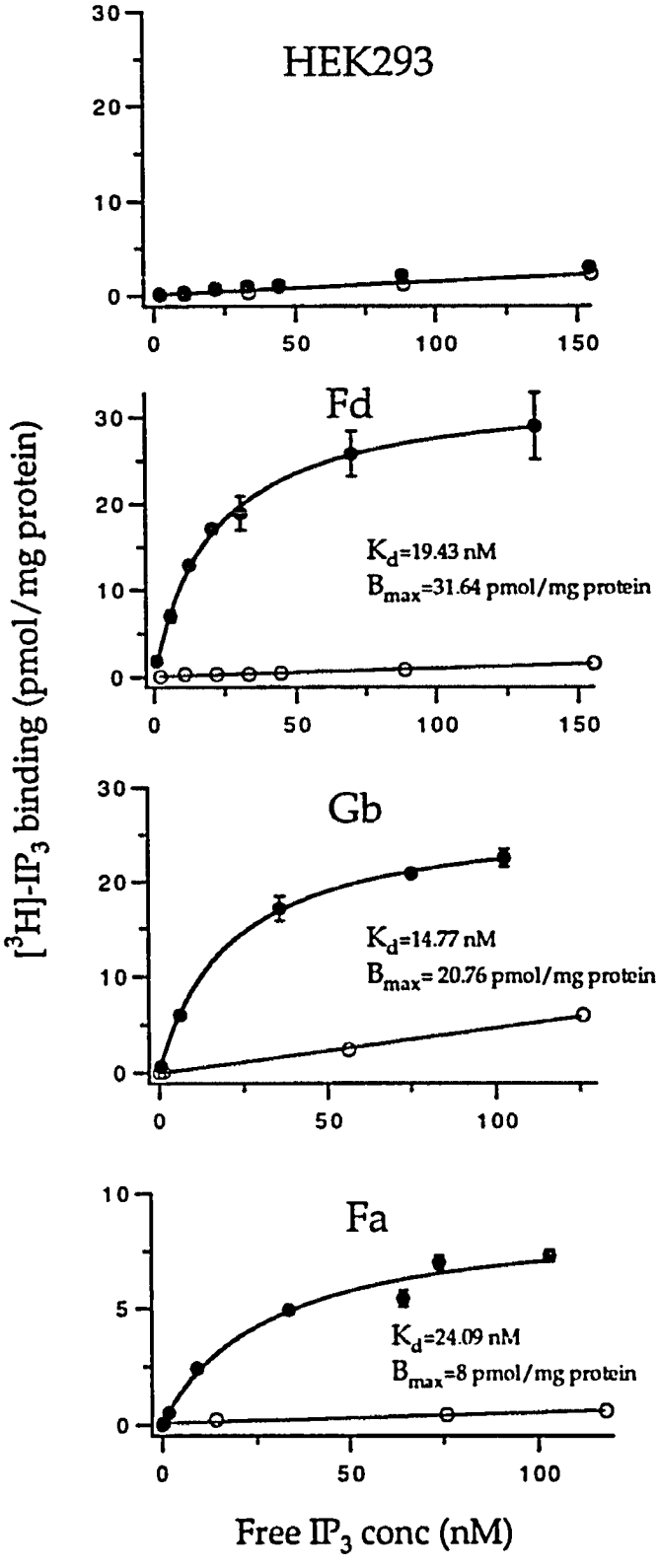

representative cell line. The parent HEK293 cells, although containing endogenous IP_3 receptors detectable by sensitive immunological means, revealed virtually no binding above the non-specific background. Both F and G isoforms had a high affinity for IP_3, with a K_d ~ 20 nM. Binding isotherms were also performed on receptors isolated from the stable cell line, Fa, which expressed a truncated version of the F-type receptor (*SI-*). The K_d for Fa receptors was found to be slightly higher (25 nM).

Equilibrium ligand-binding properties of the expressed receptor are not influenced by temperature in the absence of calcium

The native IP_3 receptors isolated from rat and bovine cerebellum displayed sensitivity to temperature, which produced a shift of apparent binding affinity (or rather, the proportion of receptors exhibiting high versus low binding affinity in the same preparation). The receptors isolated from the stably transfected cell lines, however, displayed a relative stability of ligand-binding over a range of temperatures at 0 Ca^{2+} as shown in Figure 4-15.

In native cerebellar membrane extracts, 1 mM Ca^{2+} completely inhibits IP_3-binding at room temperature, a process thought to involve a calcium-requiring phosphatase which metabolizes IP_3 (Hingorani, 1994). This is in contrast to an incomplete inhibition in the expressed receptor preparation. Note, however, that the inhibitory effect of calcium on IP_3-binding of these expressed receptors appeared accentuated with increasing temperature from 0°C to 30°C. This suggests that there may be a slight calcium-dependent enzymatic activity in the expression system. Alternatively, high temperatures may favor a more rapid dissociation of IP_3 from its receptor promoted by calcium, thus exaggerating the apparent inhibitory effect. The latter possibility could be tested by kinetic studies measuring the rate of dissociation at different temperatures.

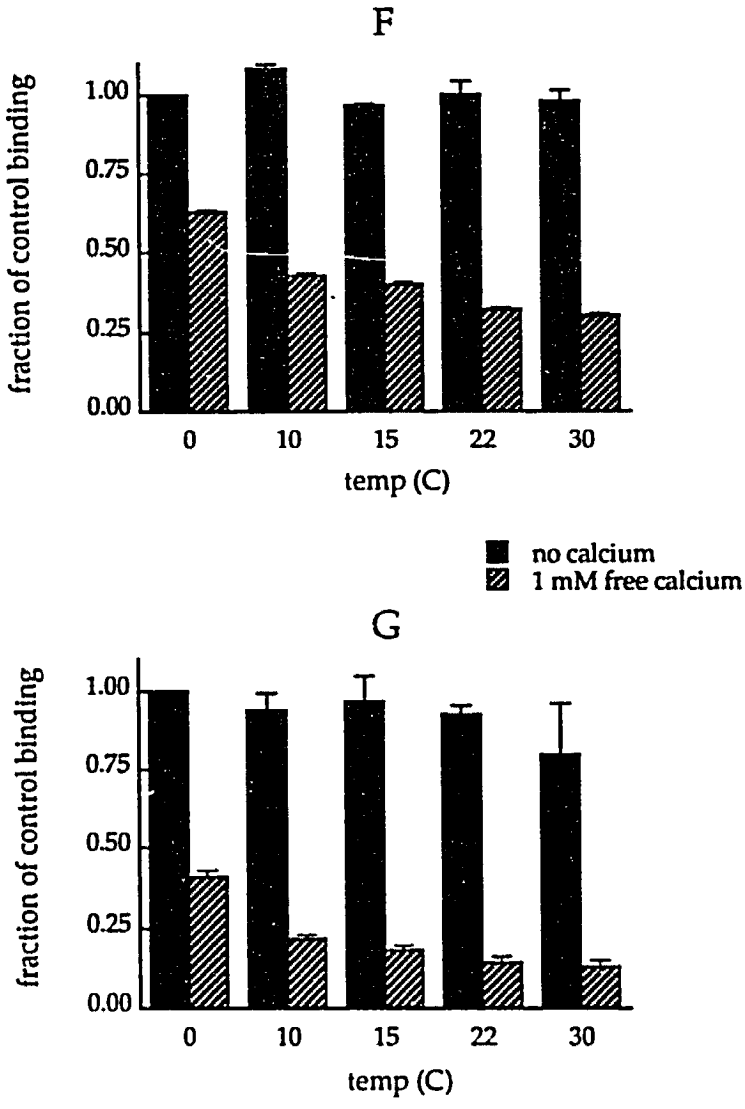

Figure 4-15. **Effect of temperature on [^{3}H]-IP$_3$ binding at 0 and 1 mM [Ca^{2+}]$_{free}$.** Detergent-solubilized membranes from F or G cells were incubated with 89.3 nM of IP$_3$ at indicated temperatures for five minutes, and then assayed for bound [^{3}H]-IP$_3$. The binding activity of each point is displayed as a fraction of control binding, which was performed at 0°C in the absence of added calcium. Each value represents the mean of normalized data from two independent trials.

The hydrophobic membrane-spanning domain is necessary for oligomerization

The full-length receptors were confirmed to be in a higher molecular weight ensemble by sucrose gradient sedimentation, whereas the truncated receptors (Nf or Ng in the transient expression, Fa in the stable system) remained monomeric (Figure 4-16). The estimated sedimentation constants ($S_{20,w}$) were 24 S for the full-length, assembled receptors and 11 S for the truncated receptors.

By mixing and matching these full-length and truncated receptor cDNA constructs, I attempted to approximate the receptor regions required for subunit assembly. Initially HEK293 cells were transfected with different combination of constructs---F & Nf, F & C, or C & Nf---lysed and immunoprecipitated under mild conditions with segment-specific antibodies. The precipitated proteins were subsequently detected by mixed antibodies encompassing all receptor regions tested. Figure 4-17a illustrates the result of this study. No co-precipitation was detected in any of these combinations, suggesting that neither the N-terminal 4/5 of the receptor (soluble fragment) nor the remaining C-terminus (including the membrane-spanning portion) provided the sufficient region for interaction with its full-length counterpart.

Next, I took a different approach to study whether a longer construct, P, which lacks only the N-terminal 418 amino acids, could co-assemble with the full-length receptor subunits. The stable cell line Fd was transfected with Nf, P, or C cDNAs. At 48 hours post-transfection, the cells were harvested, lysed, and the detergent extracts sedimented through a 5-20% sucrose gradient. As demonstrated previously, Fd migrated under this condition as a multimeric protein complex with a peak IP_3-binding activity near fractions 12-13. Both [^{3}H]-IP_3-binding and Western immunoblot identified F peak at fraction 12 in Nf- and C-transfected Fd cells. The distribution of F proteins in P-transfected Fd cells, however, was shifted to a lower molecular weight range (Figure 4-17b). This suggested that construct P had formed oligomeric complexes with the F

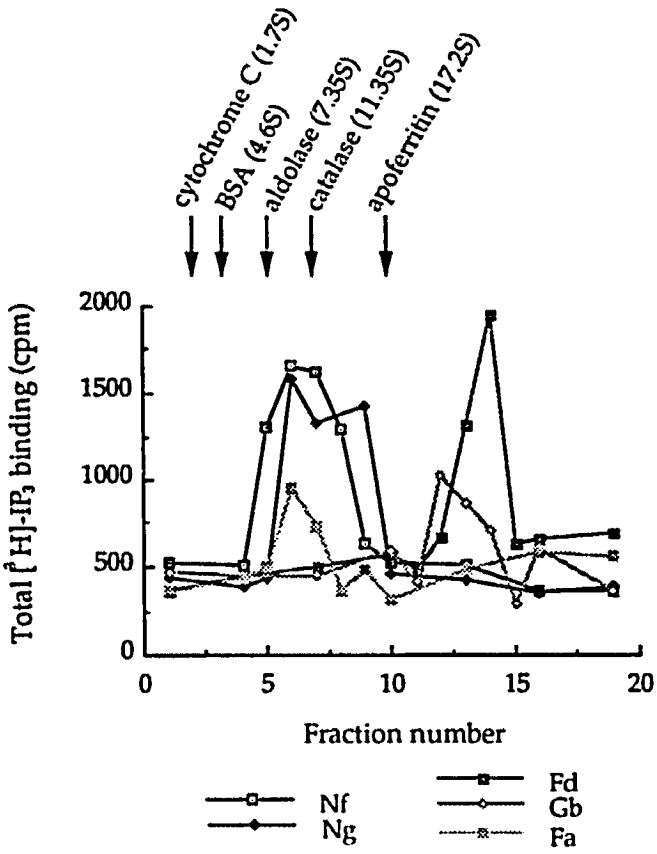

Figure 4-16. Sucrose gradient showing the [^{3}H]-IP$_3$ binding activity of collected fractions for the full-length (Fd & Gb) and truncated (Fa, Nf & Ng) receptors. Cell lysate of each was sedimented through a 5-20% linear sucrose gradient in a SW50.1 ultracentrifuge tube. 250-µl fractions were collected from the top to bottom of the tube (corresponding to fraction numbers 1-19), and 115 µl was aliquoted for assaying the IP$_3$-binding activity. A mixture of MW standards sedimented in parallel were visualized on a 4-15% linear gradient polyacrylamide gel. The peak of each standard is indicated in graph by arrow: cytochrome C (1.7 S, 13.3 kD) in fraction 2; BSA (4.6 S, 68.4 kD) in fraction 3; aldolase (7.35 S, 149.1 kD) in fraction 5; catalase (11.35 S, 221.6 kD) in fraction 7; apoferritin (17.2 S, 446.9 kD) in fraction 10.

Figure 4-17. **Studies of oligomeric association.** (a) Cotransfection and expression of paired combinations of receptor constructs were performed as described in the text. An equal amount (in microgram) of the paired cDNA constructs was used in each cotransfection. The expressed proteins were then precipitated by two different antibodies. Depending on the region of recognition, one of these antibodies would precipitate both coexpressed proteins only if there was an oligomeric association, whereas the other antibody would precipitate both non-discriminatively. All of the precipitated proteins were electrophoresed through a 4-10% gradient gel and detected by Western immunoblot with both sp2A & sp3A antibodies.

As shown here, only the antibody that recognized both constructs (e.g., sp2A directing to F & Nf in the coupling region, sp3A to F & C in the transmembrane domain) could precipitate both of the paired proteins simultaneously, indicating that there was no oligomeric association between each pair.

Ig denotes immunoglobulin used in precipitation. *C* next to the marking arrow indicates the position of the expressed C-construct. These protein bands are however not readily visualized in this exposure.

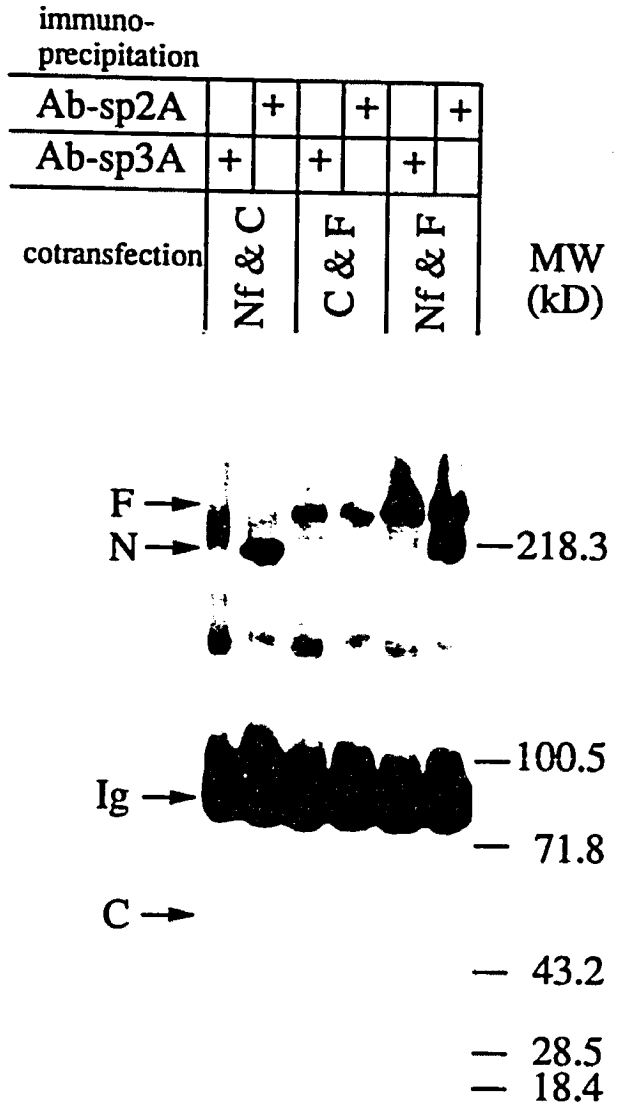

Figure 4-17. **Studies of oligomeric association.** (b) Various truncated constructs of the IP3 receptor cDNA were transfected into the stable cell line, Fd which expressed full-length receptors. The cells were lysed in the presence of 1% Triton X-100, and the lysate was subject to analytical sucrose gradient (5-20%) sedimentation. 19 fractions (250 µl each) were collected, with fraction 1 corresponding to the top of the gradient (i.e. low MW). A 50-µl sample was taken from each fraction, electrophoresed, transferred to nitrocellulose membrane, and detected by immunoreaction with a mixture of antibodies sp2A & sp3A.

Four Western blots have been aligned here for comparing the position of Fd in the sucrose gradient with or without various truncated proteins. There appears a noticeable shift of peak position of Fd proteins present in the third panel (Fd+P). This is also demonstrated below in the plot of integrated intensity (by a gel scanner) vs. fraction number. The result suggests that P fragments are capable of associating with the complementary full-length F proteins to form oligomeric complexes.

The arrow labeled C in the fourth panel points to the position of the expressed C-construct, which is not readily visualized in this exposure.

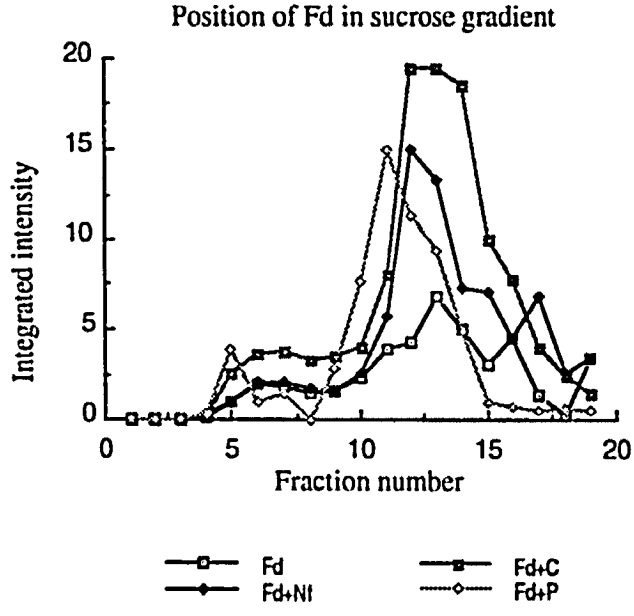

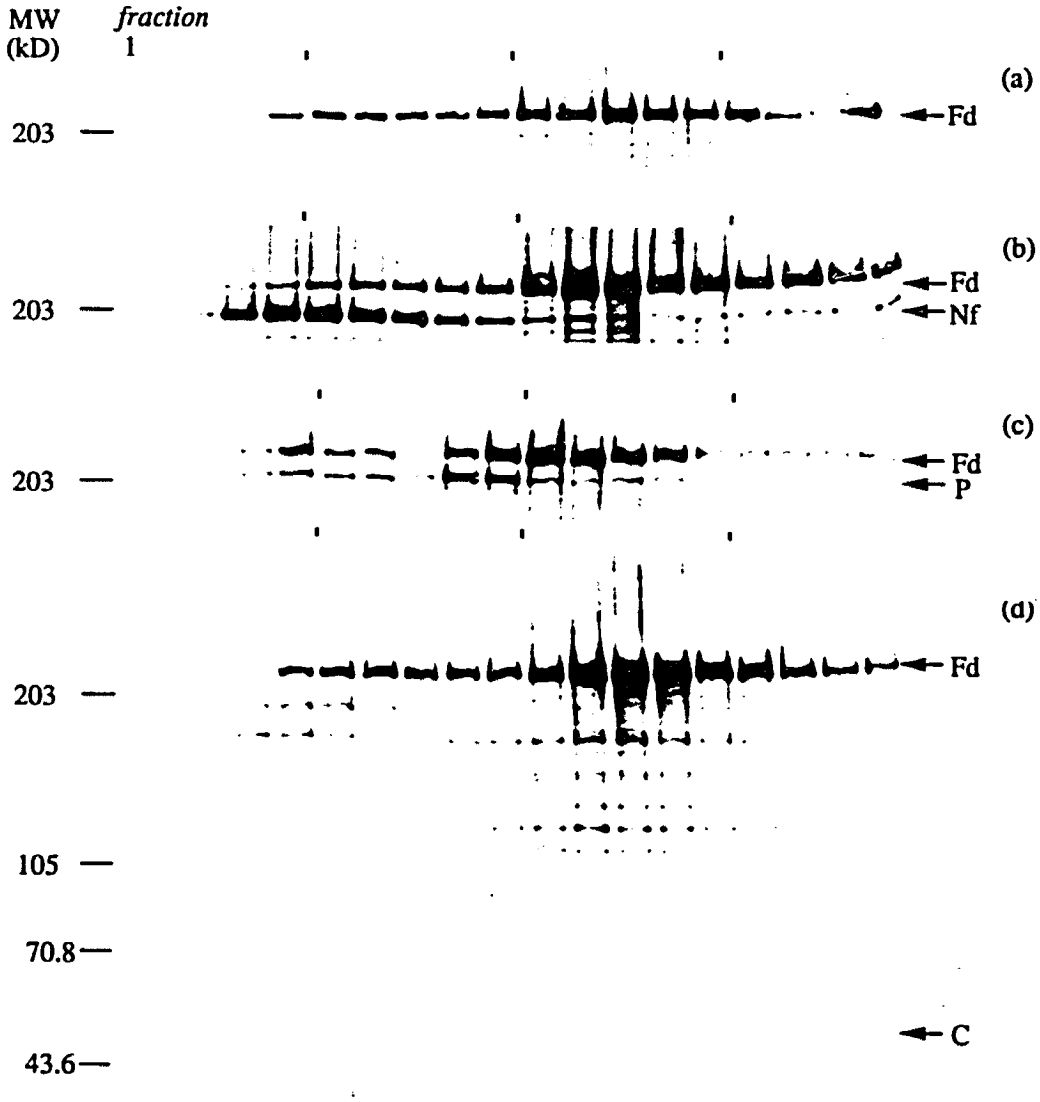

polypeptide. The complexes may include make-ups of different P to F ratios, thus cover a wide range of sedimentation indices in the sucrose gradient.

The second study confirmed the results from the co-precipitation experiment, but added that the transmembrane domain and perhaps a portion of the N-construct are necessary for oligomeric association of the receptor subunits. Both studies however have a major limitation. Since construct C did not express as well as the others, its ability of co-assembly may not have been fairly assessed.

Values of K_d altered with culture age

[^{3}H]-IP_3 binding isotherms have been repeatedly performed at different time on the same stable cell line, Fd over a period of two months. It was observed that under identical experimental conditions the apparent K_d of isolated receptors for IP_3 binding gradually rose (Figure 4-18). This obligates a cautions interpretation of the binding constants. The measurements of K_d may be compared only between two cell lines that had a similar passage number.

Discussion

I have presented in this chapter a simple expression system of the cerebellar receptor for IP_3. As anticipated, the full-length receptors synthesized in either the transient or stable expression system behaved as the native receptor: they acquired glycosylation, assembled in a higher-order oligomeric configuration, resided in the intracellular membranous compartments, and bound IP_3 with high affinity.

Expression level

Based on Western immunoblot results, the receptor expression level was similar in both transient and stable systems. The maximum binding capacity measured from the

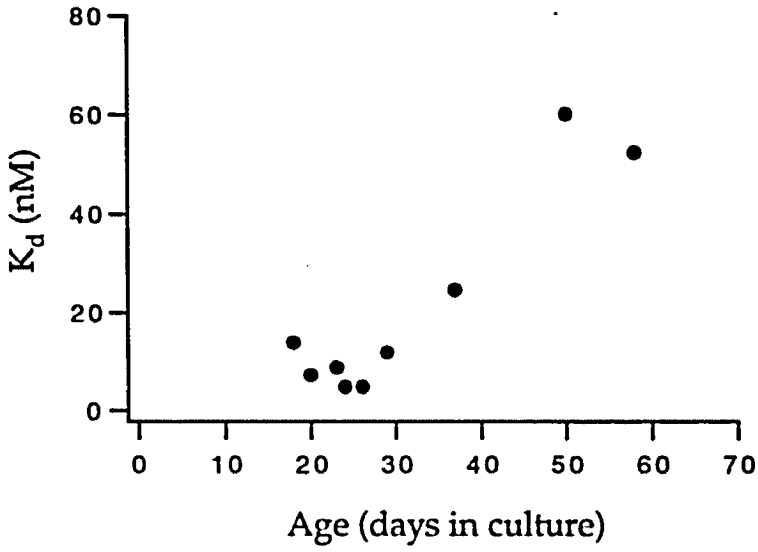

Figure 4-18. **Values of K_d altered with culture age.** $[^3H]$-IP_3 binding isotherms were performed under the same experimental conditions on membrane extracts isolated from Fd cell line, which was followed over a period of two months. From each isotherm K_d was estimated by fitting a single-site Langmuir equation and plotted against culture age (proportional to passage number).

stable cells, averaging ~20 pmole/mg total membrane protein (ranging from 13-33 pmol/mg protein, depending on the cell type), was in turn comparable to the amount of IP_3 receptors present in the richest known tissue source, cerebellum. This number could be translated into 1.08×10^5 molecules per cell, or 2.7×10^4 IP_3 receptors per cell, if each of the four subunits were assumed to bind IP_3. This calculation should reflect a more accurate estimate of receptor density than quantitation by Western (from Figure 4-9, I have estimated 2×10^7 molecules per cell). A large fraction of the immuno-reactive receptors may be non-functional. The high expression level should nevertheless facilitate the biochemical isolation of a considerable quantity of receptors for structural studies.

A major advantage of the stable expression system is that a large number of expressing cells can be grown easily by passage of the immortalized cell line without repeated transfection and without the problem of low and variable expression efficiency. Another value, in this case, is that a homogeneous population of a single receptor isoform can be isolated and studied for comparison with another.

Pulse-chase experiments have indicated that the half life of the receptor protein was much longer in the stable than in the transient expression system. Both values, ~6 hours in the transient and ~14 hours in the stable system, are notably larger than the $t_{1/2}$ of 2 hours for the μI sodium channel transiently expressed in the same HEK293 cells. This might be due to a benign nature of the IP_3 receptor, as opposed to anomalous Na^+ influx through the sodium channel which has at times been observed to be lethal. Alternatively, the stability of the protein may lie in the procurement of glycosylation or other post-translational modifications. Also, residence in distinct subcellular membrane compartments which may have different intrinsic turnover rates, or different rates of cell growth and remodeling at the time of the ^{35}S pulse may play a role. Furthermore, proper assembly of all protein components may influence the metabolic stability as well as other aspects of receptor function.

Structure and function studies

The truncated receptors lacking the membrane-spanning region (Nf, Ng and Fa) have been shown to be soluble and remain as monomers. There are two small hydrophobic regions present in these truncated constructs, but apparently they are not sufficient to provide an interaction with complementary full-length subunit to form oligomeric complexes. These monomeric proteins are capable of ligand-binding and may provide information about how each receptor subunit behaves. The construct C, which contain membrane-spanning segments, is expected to assemble by virtue of its hydrophobic sequences. The negative finding for construct C presented here may be due to its poor expression, or that additional sequences are indeed required for assembly.

The expression system may have additional use for testing whether heterotetramer is capable of forming *in vitro*. If heterotypic association among subunits of different receptor types does occur, then an enormous number of different receptor isoforms could be generated.

Binding affinity changes with the age of cells

During the course of passing the cell lines and plating them for biochemical assays, it was observed that under identical experimental conditions the apparent K_d of isolated receptors for IP_3 binding deviated from the earlier measurements. This became problematic, particularly when an accurate K_d measurement was required for the comparison of two receptor isoforms. As more is learned about the receptors, however, this property appears more intriguing than annoying. Recently a number of modulators, including calcium, redox agents and ATP, have been discovered to alter IP_3 binding affinity or channel activity (Marshall & Taylor, 1993). Any one or a combination of

these modifiers may correlate with changes in the cellular environment during growth and senescence that could form the basis for our observation.

Chapter 5.

Characterization of Two mRNA Splice Variants of the Type I IP_3 Receptor Stably Expressed in HEK293 Cells

Introduction

As for many important protein molecules which are members of a multi-gene family, an appreciation for the complexity of IP_3 receptors readily comes from molecular cloning studies. To date five different genes for the IP_3 receptor have been discovered. These genes encode receptor proteins with about 60-70% identical residues from pairs of different genes in the same species. It has been demonstrated that the type I receptor gene transcript is subject to alternative splicing, further augmenting the diversity of molecular species of the receptor. The functional receptor/channel complex is formed by assembly of four homo-, and possibly hetero-oligomeric subunits into a tetramer. Each subunit contains a ligand-binding domain which has been localized to the first 788 amino acids of the N-terminus (Mignery & Sudhof, 1990). It has been suggested that the molecular diversity accounts for the myriad functional properties observed in ligand binding and calcium release, possibly offering an explanation for the phenomenon of "quantal calcium release".

Cerebellar Purkinje cells remain the single most abundant tissue source for the IP_3 receptor, thus facilitating its first biochemical isolation and characterization. Although the type I receptors make up the majority (>90% at the mRNA level (De Smedt, 1994) and >80% at the protein level) of IP_3 binding molecules in cerebellum, the measured K_d seems to vary in different preparations (40 to 100 nM). Detailed ligand binding studies performed in our laboratory first demonstrated the existence of two distinct populations

of binding sites, one with a high affinity (K_d of 4-8 nM) and the other with a low affinity (K_d of 120 nM). They could be further distinguished by differences in calcium and temperature sensitivity. This suggests that there is indeed functional heterogeneity amid the receptors, due perhaps to multiple receptor types or to multiple binding sites on the same molecule.

Presumably a single type of receptor isolated from a heterologous expression system could clarify the issue of functional heterogeneity. The mouse type I IP_3 receptor was first expressed in fibroblast L cells by Mikoshiba *et. al.* with an estimated K_d of 19.4 nM. The same receptor of rat origin, when expressed in COS cells by Mignery *et al.*, however, had a K_d of 89.5 nM, in contrast to the similarly expressed rat type II receptor which had a higher affinity of 27 nM. Although the cause for the discrepancy is unclear, it may be appreciated in the context of a potentially enormous diversity in receptor structure generated by oligomerization of isoform subunits and their differential post-translational modification.

Two regions (*SI & SII*) of the type I receptor pre-mRNA are subject to alternative splicing. Two variations in *SI* and four in *SII* have been identified by PCR amplification, resulting in 8 possible subunit isoforms (Nakagawa, 1991b). Since 3 cassets of sequences are present in the *SII* region, there is an upper limit of 16 structural combinations if all the possible variant segments could randomly associate. On the other hand, if there exists a preferential linkage among these variant segments, a more modest number of isoforms will be generated. A number of questions follow: Do individual Purkinje cells express different variants? If they do, are hetero-oligomers capable of forming and do such hetero-oligomers occur naturally? What are the functional differences between structural variants? How could the observed receptor-channel properties be attributed to each individual receptor? Finally, which functional properties are subunit-specific and which are derived from subunit-subunit interactions?

My study aims to characterize some properties of two alternatively spliced isoforms expressed as defined, homo-oligomeric receptors, and as truncated monomeric domains from the receptor subunits. The stable HEK293 cell lines expressing a single type I receptor isoform were shown in the previous chapter to provide a useful tool for biochemical isolation and characterization. Both isoforms are found predominantly in the mammalian central nervous system. Their only structural difference lies in a stretch of 15-amino acid insert within the ligand-binding site near the amino terminus. This region contains a motif reminiscent of the loop region of an EF-hand, with carbonyl oxygen groups capable of interacting with a calcium ion in a coordinated alignment (Nakayama & Kretsinger, 1994; Persechini *et al.*, 1989). The *SII* region (in the SIIB- form) is present in both isoforms.

Because of the interesting structural difference between the two isoforms, calcium effect on the IP_3 binding was specifically tested. Calcium has been demonstrated to inhibit binding at submicromolar concentration, perhaps by interacting with another protein (e.g., calmedin) or enzyme (e.g., phospholipase C or a phosphatase). The actual mechanism is however unclear. Over-expression of the receptor in a system different from its native environment may allow a closer examination of this calcium effect.

Using the expression system, we demonstrate that each isoform alone is capable of complex ligand-binding properties, with susceptibility to modulation by various factors. The receptors are intrinsically sensitive to calcium, which behaves as an allosteric inhibitor, but the feed-back regulation by calcium may differ between the different receptor isoforms.

Results

Both receptor isoforms bind IP_3 with a high affinity

I first looked at the affinity of the two isolated receptor isoforms. Figure 4-14 in the previous chapter shows the [^{3}H]-IP_3 binding isotherm for solubilized microsomal membranes prepared from each representative cell line. Untransfected HEK293 cells, although containing endogenous IP_3 receptors detectable by sensitive immunological methods, have no significant IP_3 binding above the non-specific background. Both the F and G isoforms, on the other hand, have a high affinity for IP_3, with a $K_d \sim 20$ nM in each case. This finding is different from Mignery's K_d measurement (90 nM) for the type I receptor. The mean parameters measured in several experiments under the same conditions are summarized in Table 5-1. Therefore, contrary to a previous suggestion by Mikoshiba *et al.* (Nakagawa, 1991a), my result shows that the *SI* segment, though residing within the ligand-binding domain, does not determine the difference of binding affinity between the two isoforms.

Receptor binding is modulated by calcium

Cytosolic free calcium, a "product" of IP_3 receptor activation, has been shown to facilitate channel opening within a narrow sub-micromolar range but to inhibit ligand binding at higher concentrations. In rat cerebellum this inhibitory effect was demonstrated to be mediated by a separate membrane accessory protein named calmedin. Mignery's studies on bovine cerebellum, however, challenged the above mechanism of calcium action. Instead of direct interaction with receptor binding, calcium was proposed in the latter studies mainly to activate phospholipase C, which subsequently produces IP_3 to compete with radiolabeled ligand binding (Mignery, 1992).

Table 5-1. **Summary of K_d & B_{max}.** $[^3H]$-IP_3 binding in solubilized membranes isolated from several independent preparations of stable cell lines was performed under the same condition at 0-4°C. Binding was assayed over increasing concentrations of IP_3 ranging from 0.2 to 150 nM. The equilibrium binding parameters were estimated by fitting each individual isotherm using the Biff Plot (written by Dr. B. Forbush III, Yale University) and summarized here as averaged values. The fit has assumed a single class of binding sites that are non-interactive. All values were expressed as mean ± standard deviation, with the range given in parentheses.

Cell type	K_d (nM)	B_{max} (pmol/mg protein)
F (Fd & Fe); n=6	13 ± 6 (4-19)	29 ± 6 (18-35)
G Gb; n=3	18 ± 4 (13-21)	22 ± 4 (19-26)
Gg; n=2	18 ± 3	12 ± 1
Fa (truncated); n=3	25 ± 10 (14-38)	13 ± 4 (8-18)

Here [^{3}H]-IP$_3$ binding is performed on receptors isolated from the HEK293 expression system. Both detergent-solubilized intact receptors and a soluble form (lacking the membrane-spanning region, thus easily isolated from the cytoplasm) were susceptible to inhibition of IP$_3$ binding by calcium as shown previously in Figure 4-13. This suggests that the calcium sensitivity is intrinsic to the receptor, independent of any other membrane components such as calmedin or PLC and phospholipids.

Examination of a broad range of calcium concentrations at fixed IP$_3$ concentration (83 nM) generated a curve (Figure 5-1b & 5-2) with a sharp transition in the amount of IP$_3$ bound to the receptor. The binding profile is independent of temperature, with the maximum inhibition never reaching 100%. This curve is consistent with that obtained at 0-4^0 C with receptors in solubilized cerebellar membranes, but in contrast to the complete inhibition obtained at a higher temperature (25^0 C) with this preparation (Figure 5-1a).

This result illustrates first, that a component of calcium action on IP$_3$ binding to receptors in native cerebellar membranes is temperature-dependent. This property is separable from a second action, seen in the isolated, expressed receptors presented above, which appears to be intrinsic to the receptor.

Calcium shifts the receptor to a lower-affinity state

To elucidate the mechanism of calcium inhibition, a family of binding isotherms was produced in the presence of varying concentrations of calcium. The K_d and B_{max} were obtained for each calcium concentration by fitting the data to a single-site Langmuir binding isotherm (Figure 5-3a). While B_{max} remained relatively constant, K_d shows a stepwise change with values reaching a plateau at extremes in calcium concentrations (Figure 5-3b). This profile is consistent with a model in which the

Figure 5-1. **Calcium titration curves for IP_3 receptor.** Specific [^{3}H]-IP_3 binding in duplicates was measured in membrane extracts in the presence of increasing concentrations of calcium, and presented as percentage of the binding level at 0 Ca^{2+}. Binding assay was performed at fixed [IP_3] of 83 nM. (a) In solubilized cerebellar membranes at 0 and 25°C. (b) In solubilized membranes isolated from F and G cell lines, each at 0 and 25°C.

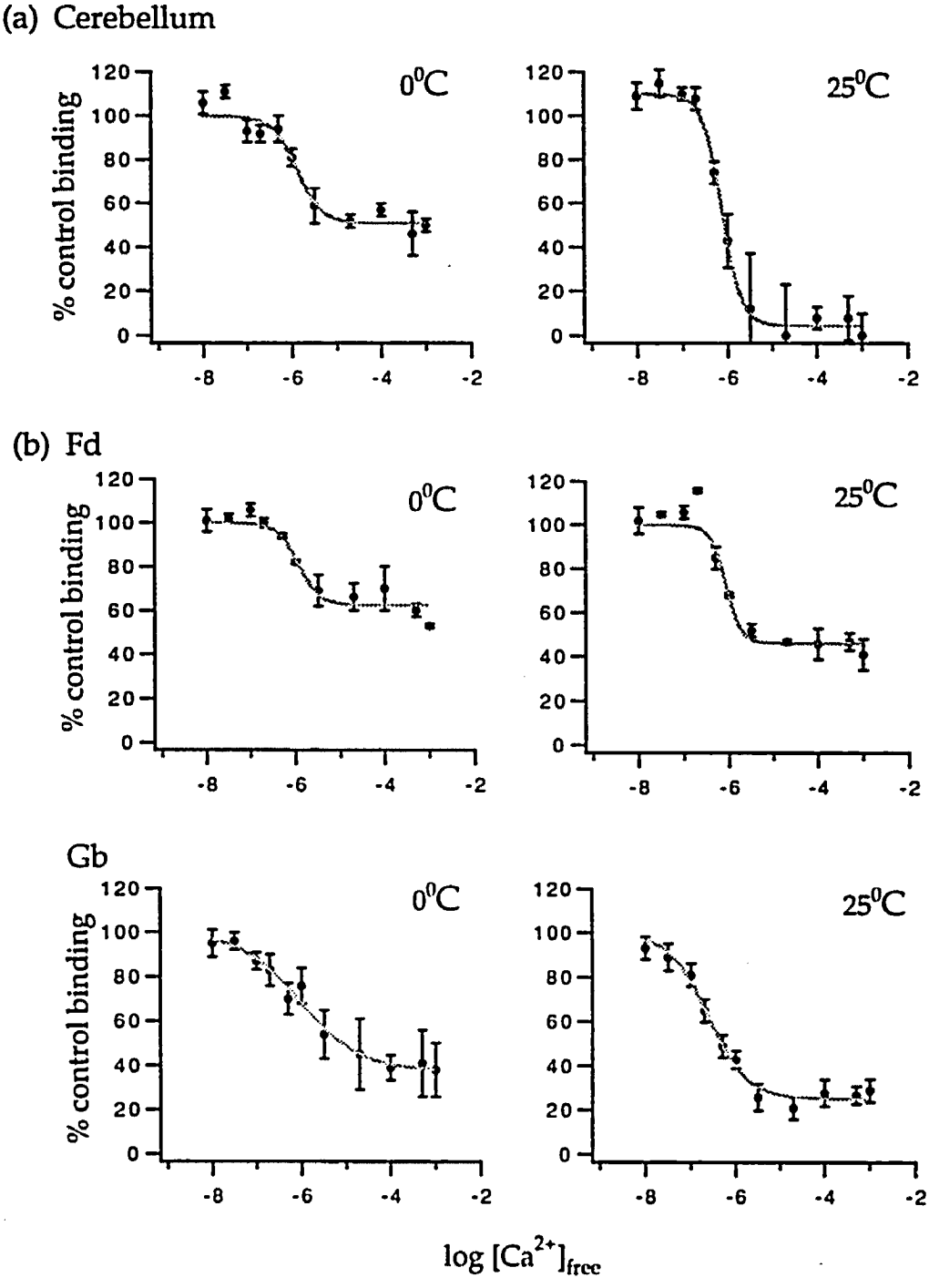

Figure 5-2. **Calcium titration curves for F and G receptors.** Soluble membrane extracts were prepared from F and G cells. [^{3}H]-IP$_3$ binding at 0-4°C was measured in increasing concentrations of calcium and at a fixed ligand concentration of 83 nM. The specific binding of [^{3}H]-IP$_3$ was presented as percentage of the binding level at 0 Ca^{2+}. Each plot was fitted with a modified Hill equation: $1-f/[1+(k/[Ca^{2+}]_{free})^n]$, where *f* is a fractional coefficient to account for the incomplete inhibition at maximum calcium concentration. *n* denotes a slope parameter or cooperativity index; k denotes the half-maximal point. The values of n obtained from these curves were compared between F and G receptors. There is a significant difference ($p<0.01$, Mann-Whitney test).

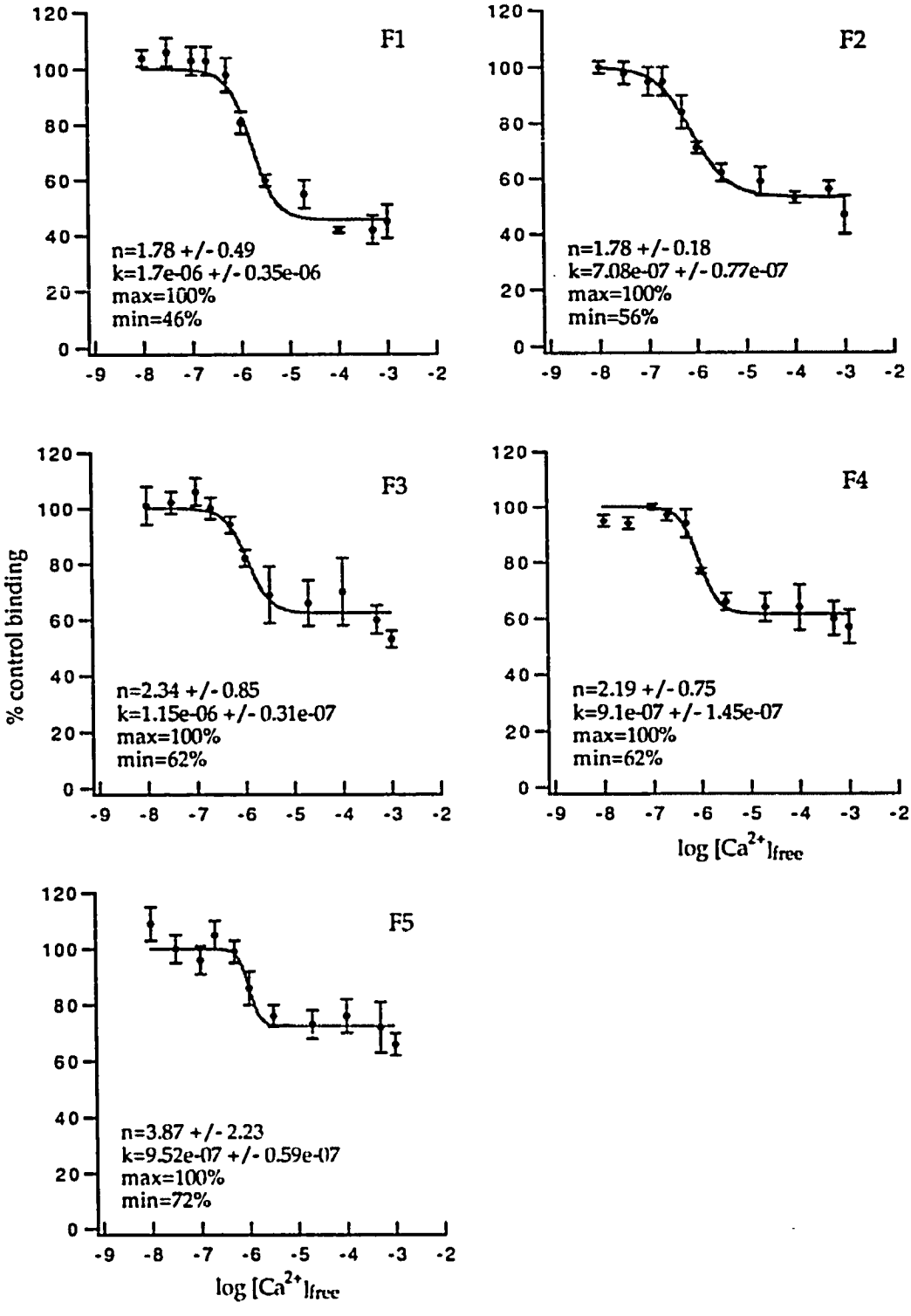

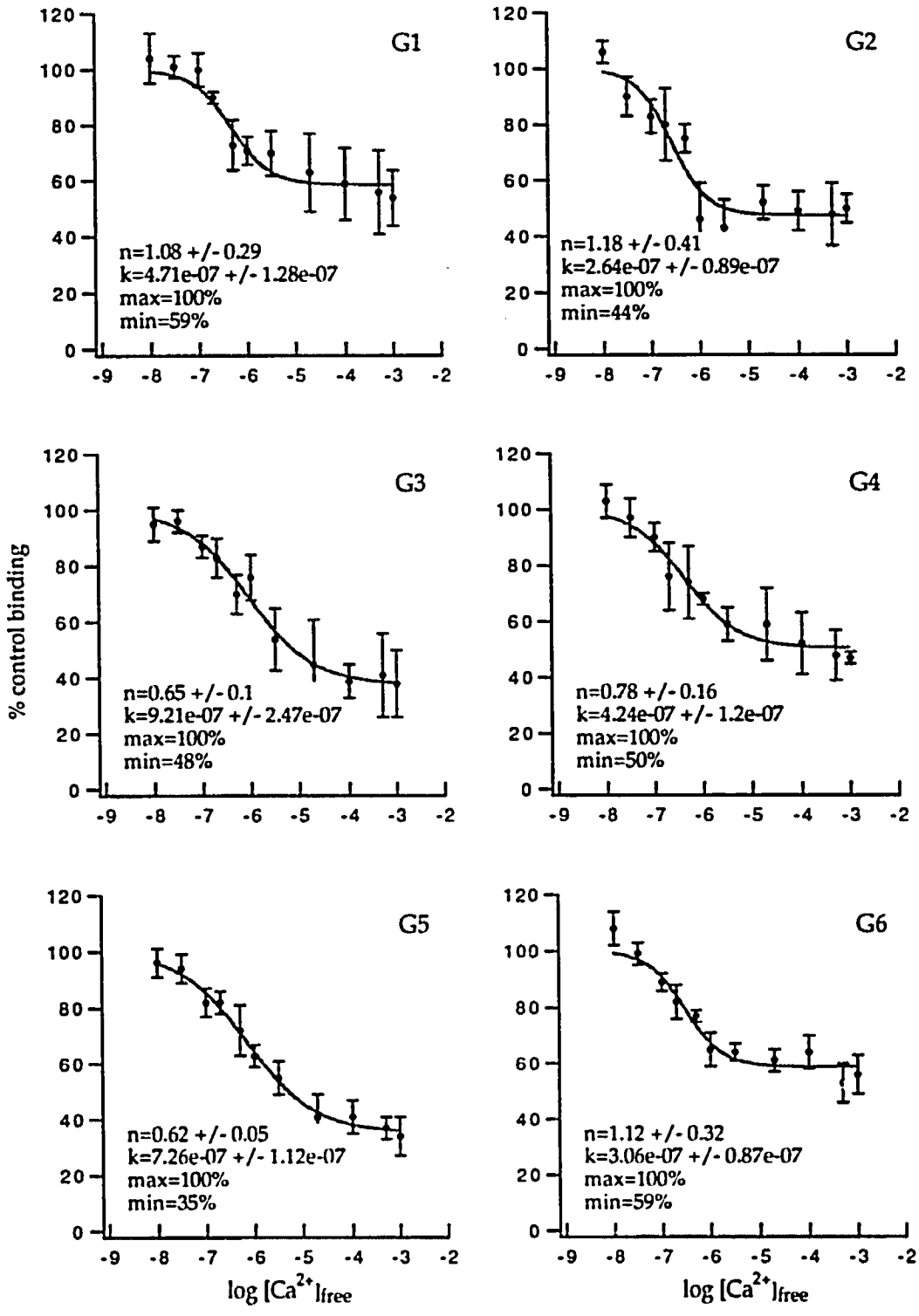

Figure 5-3. (a) **Family of calcium inhibition curves for receptors isolated from F or G cell lines. A full binding isotherm was performed on solubilized membranes from each stable cell line in the presence of a fixed concentration of free calcium as indicated on the top center of each plot.** K_d **&** B_{max} **were measured by fitting each isotherm, assuming a single class of binding sites that are non-interactive.**

F

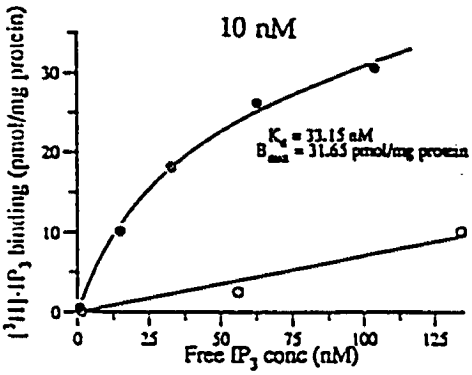

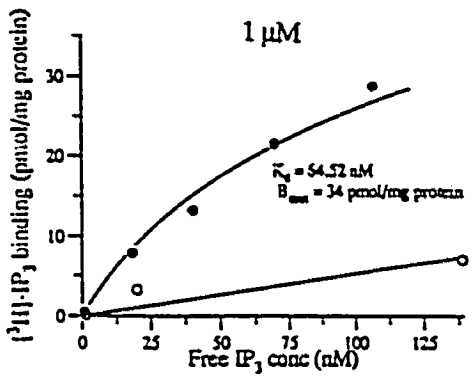

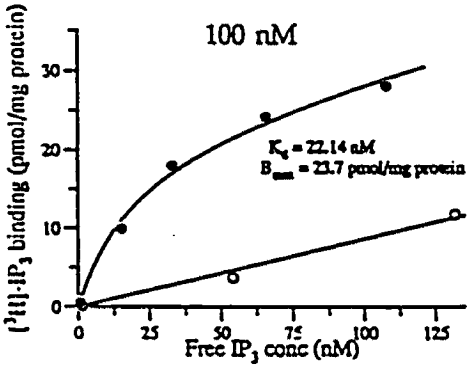

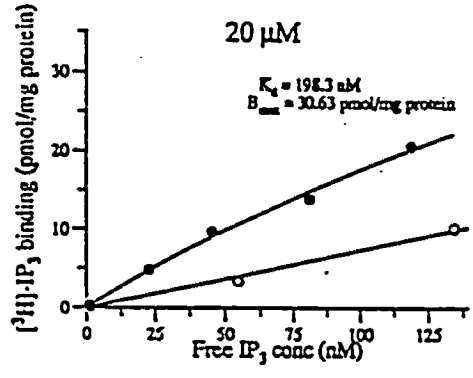

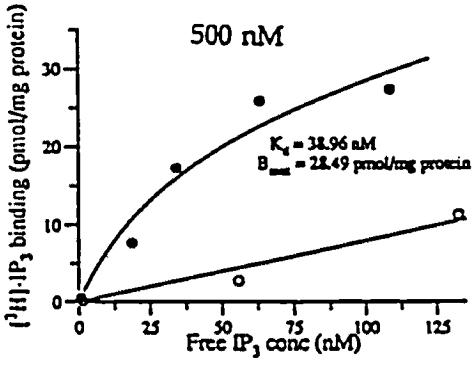

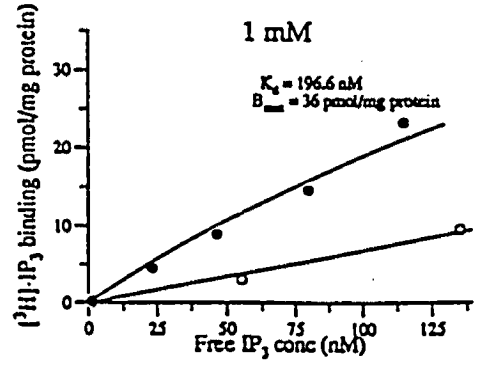

G

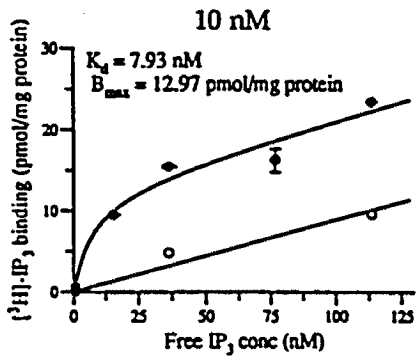

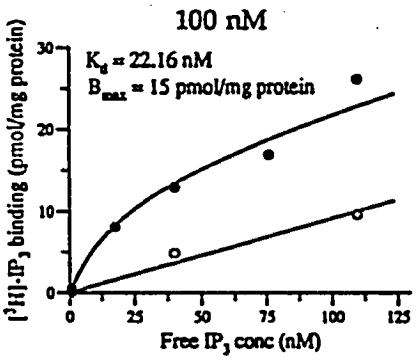

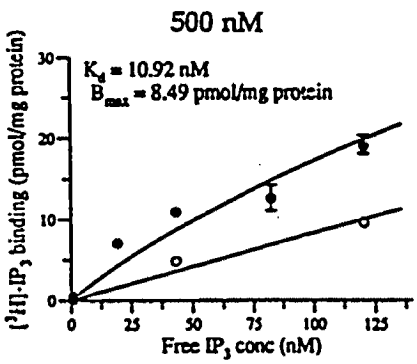

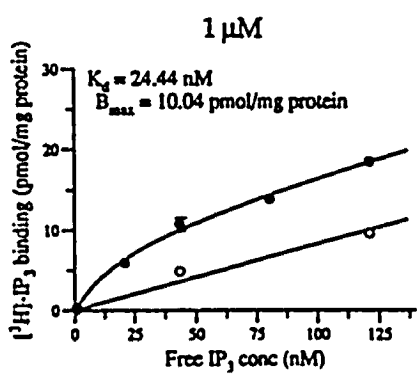

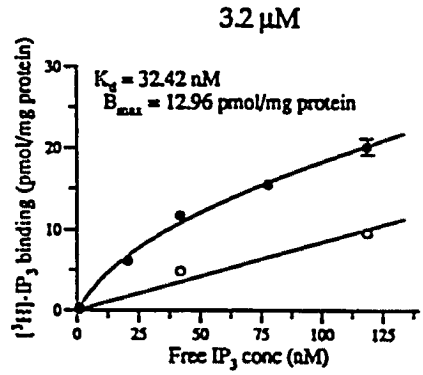

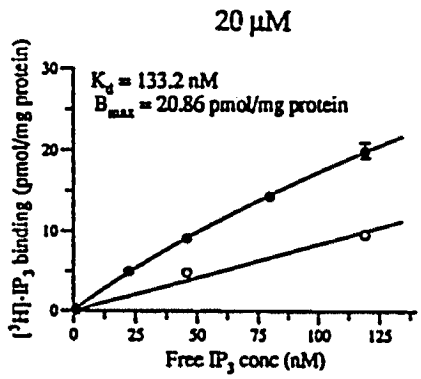

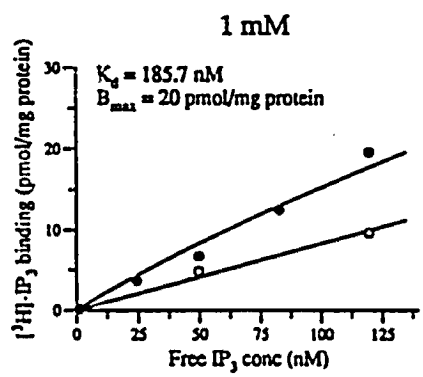

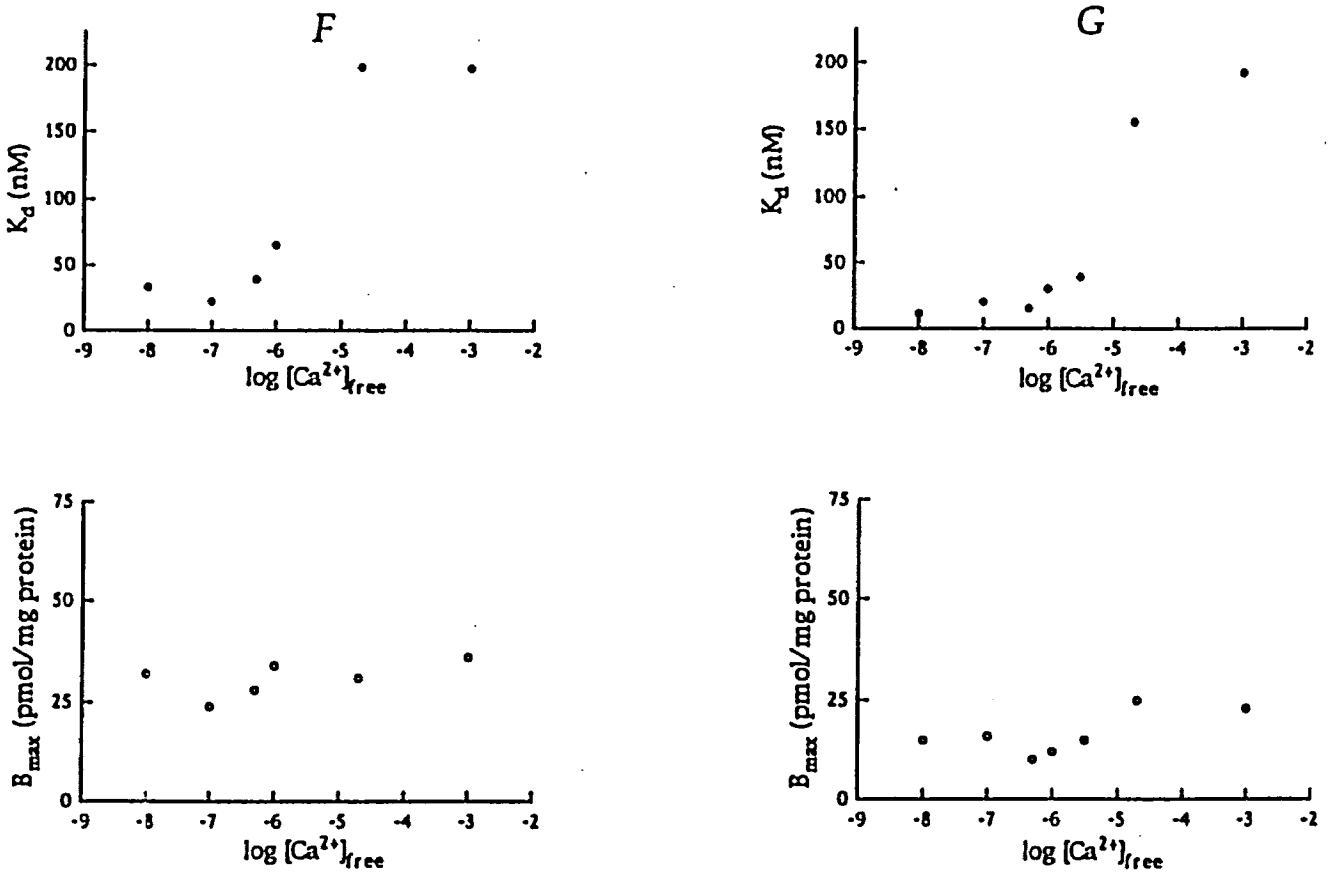

Figure 5-3. (b) K_d and B_{max} as functions of $[Ca^{2+}]_{free}$. The equilibrium binding parameters measured from the isotherms in (a) are plotted against $\log[Ca^{2+}]_{free}$. This demonstrates that calcium alters the affinity states without affecting B_{max} in both F and G receptors.

receptor can exist in at least two states with different ligand-binding affinity, and calcium acts as an allosteric modulator to stabilize the receptor in a low-affinity state.

In retrospect these family of curves were inadequately fitted by a single-site equation. Each isotherm during the receptor's transition of conformational states should be best described as summation of two components of both high- and low-binding affinities.

The F & G isoforms have different cooperativity indices for interaction with calcium

To test whether the two receptor isoforms differ in their calcium binding characteristics, solubilized receptors from each cell type, F or G, were measured for [^{3}H]-IP$_3$ binding capacity in the presence of increasing calcium. Results from 5-6 trials for each cell type are shown in Figure 5-2. Both receptor isoforms are inhibited by calcium. The profile of inhibition, however, is distinctly different: F receptors exhibit a rather sharp transition over one log unit of $[Ca^{2+}]_{free}$ between -6.5 and -5.5, whereas G receptors display a gradual decline of binding with increasing calcium concentration. Fitting the data to a pseudo-Hill equation produced a mean slope parameter (n) of 2.58 $\pm$ 0.56 (s.e.m) for F receptors, with a half-maximal change in IP$_3$ binding capacity occurring at 1.03×10^{-6} M of $[Ca^{2+}]_{free}$. For G receptors the values obtained were n = 0.85 ± 0.11 and $[Ca^{2+}]_{0.5} = 4.91 \times 10^{-7}$M. The difference in n is statistically significant ($p<0.01$).

Finally I asked if the receptor behavior could be monitored *in vivo*. To accomplish this, angiotensin II was chosen as a surface agonist to activate the phosphatidylinositide (PI) cascade in the HEK293 cells, since these cells originated from human embryonic kidney. Angiotensin II, a peptide hormone, interacts with receptors on kidney glomerular and tubular epithelium to regulate intravascular volume. These receptors are directly coupled to G proteins and PLC to produce IP$_3$. Cytoplasmic

calcium transients elicited from the activated IP_3 receptors were then monitored with the calcium-sensitive dye fluo-3 using a confocal microscope and video recorder.

Figure 5-4 summarizes the overall responses from F and G cells and the parent cell line. About 10% of the untransfected HEK293 cells responded to angiotensin II with brief but intense fluorescence transients. In both of the transfected cell lines F and G, however, on average a 3-fold higher fraction of the cells responded with fluorescence transients.

Visually, from the cinematic recording, the two cell types could be distinguished unambiguously by the pattern of their calcium transients. F cells displayed heterogeneous wave forms, with a subset of cells exhibiting disorganized fluctuations of calcium concentration or, at times, distinct, multiple spikes. The wave form of an isolated spike resembles somewhat that of the parent cells. Unlike the parent cells, however, the F cells often displayed a train of such transients. G cells, when stimulated by agonists, have a single broad transient with a sharp rise followed by a gradual fall of calcium concentration.

The fluorescence intensity within a single area (3 mm square) of each cell was quantified and plotted against time to generate calcium transient traces. When each trace was examined for the onset, peak, rising slope, and intensity of the fluorescence signal (Table 5-2), the mean value of each factor did not appear different between F and G cells. Each calcium signal had a latency of ~50 -55 seconds, a factor dependent of the length of time an effective concentration of angiotensin II was reached within the superfusion chamber. The transient rose to a peak in ~10 seconds, and the duration of signal in the transfected cells was on average significantly larger (by 2-3 fold) than that of the parent HEK293 cells. Within the population of F cells, the signal duration varied substantially, often depending on the multiplicity of calcium spikes. Both the signal

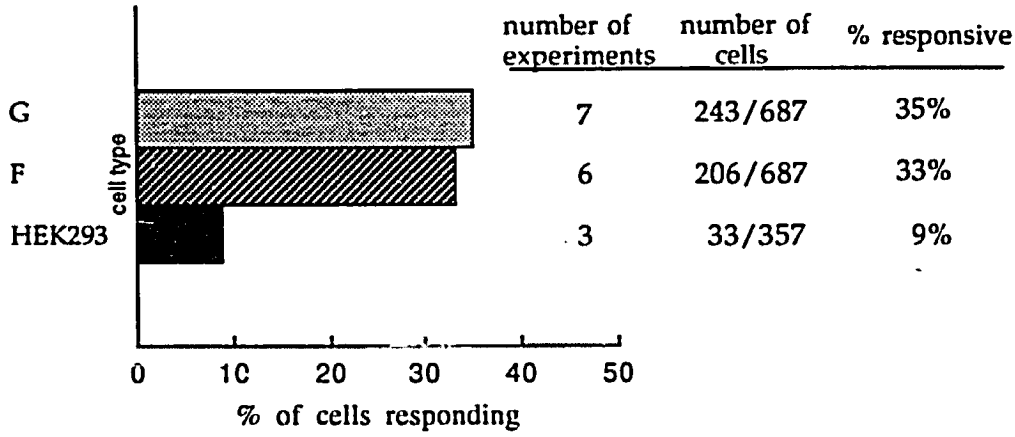

Figure 5-4. **Cell response to Angiotensin II.** The digitized records of fluorescence change of each individual cell in response to angiotensin II were compiled from all experiments within the same cell type. The cells with a positive response of calcium rise (indicated by a relative fluorescence change, $\Delta F/F$ that is at least three times the standard deviation of the baseline fluorescence level) were sorted by a computer program using IgorPro as well as by individual examination of the trace. These cells were counted, and the number used for quantifying the overall percentage of responsive cells. The number of experiments and cells examined are indicated.

Table 5-2. **Characteristics of angiotensin II-evoked calcium signals in HEK293, F, and G cells.**

	onset of signal (sec)	peak of signal (sec)	duration (sec)	intensity (ΔF/F)	slope of rise ‡	slope of fall ‡
HEK293 (n=31)	249 ± 16	257 ± 16	24 ± 2	3.7 ± 1.6	0.4 ± 0.04	0.6 ± 0.02
F (n=201)	235 ± 23	245 ± 22	49 ± 32	3.0 ± 1.6	0.3 ± 0.1	0.45± 0.16
G (n=241)	232 ± 15	248 ± 21	82 ± 28	3.1 ± 1.5	0.2 ± 0.04	0.05± 0.02

Calcium traces of relative fluorescence change, ΔF/F versus time (some of these are illustrated in Figure 5-5) were examined individually for the characteristics tabulated here. In each case 100 nM of angiotensin II was applied through either manual or electronic switch of perfusion line at time = 180 seconds.

In case there were multiple calcium spikes (which occurred in ~57% of the F cell population), the first spike was taken for measuring the occurrence of peak and the slope of rise, whereas the last spike was taken for measuring the slope of fall. The highest peak was measured for intensity. Finally, the entire span of the multiple spikes was counted as the duration of calcium signal.

All values were summarized as mean ± standard deviation within each cell type. F cells were significantly different from G cells in signal duration and slope of fall ($p<0.0001$ in each case, using either Mann-Whitney nonparametric test or unpaired t-test). No statistical significance was found in other characteristics between the two cell types. ‡Slope of rise or fall was in relative units (ΔF/F) per second.

Figure 5-5. **Representative traces of HEK293, F, and G cells, and the corresponding power spectra.** (a) The angiotensin II-evoked rise of cytosolic calcium is presented on the left as relative fluorescence change ($\Delta F/F$) versus real time in seconds. In each case 100 nM of angiotensin II was applied at time=180 sec as indicated by arrow and terminated at 540 sec as indicated by arrowhead. The corresponding power spectrum, a result of Fourier transformation, is shown on the right. For each cell type, three parameters were obtained from the individual power spectrum of every calcium trace. The bars labeled a, b, c, d mark the range of values in each power spectrum taken for the calculation of the three parameters. "d" (the mean spectral density at frequency range > 0.1 Hz) was taken as the estimated baseline noise since for the photon or thermal noise, there is roughly an equal amount of power at all frequencies underlying each power spectrum. The calculated value of "d" was subsequently subtracted from each segment of the power spectrum. *P1* ($=a-d$), the mean energy level between 0 and 0.01 Hz, quantifies the signal area. *P2* ($=\frac{b-d}{a-d}$), the ratio of (mean energy from 0.01 to 0.03 Hz) to *P1*, roughly reflects $t_{1/2}$ or the signal width in an inverse relationship. *P3* ($=\frac{c-d}{a-d}$), the ratio of (mean energy from 0.03 to 0.1 Hz) to *P1*, indicates activities of multiple spikes.

The appearance of calcium wave forms for HEK293 and G cells was consistent within each cell type. For F cells, however, the appearance was rather heterogeneous. This is shown on the bottom 5 traces (b), where different cells may have very different responses in one single experiment. The appearance ranges from (i) which resembles the untransfected HEK293 cells, (ii) which is reminiscent of some G cells, to (iii-v) which show different degrees of multiple spiking activities.

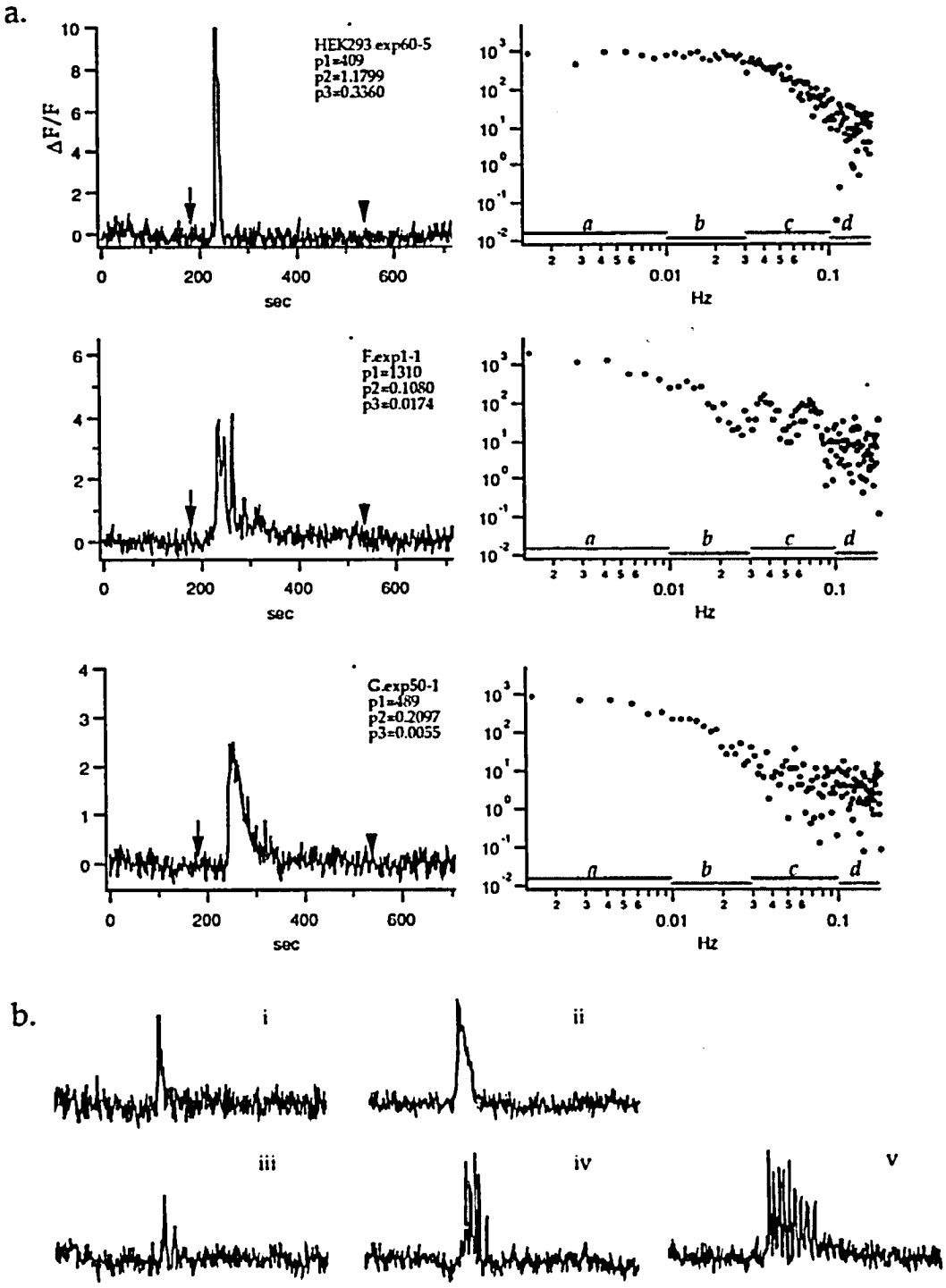

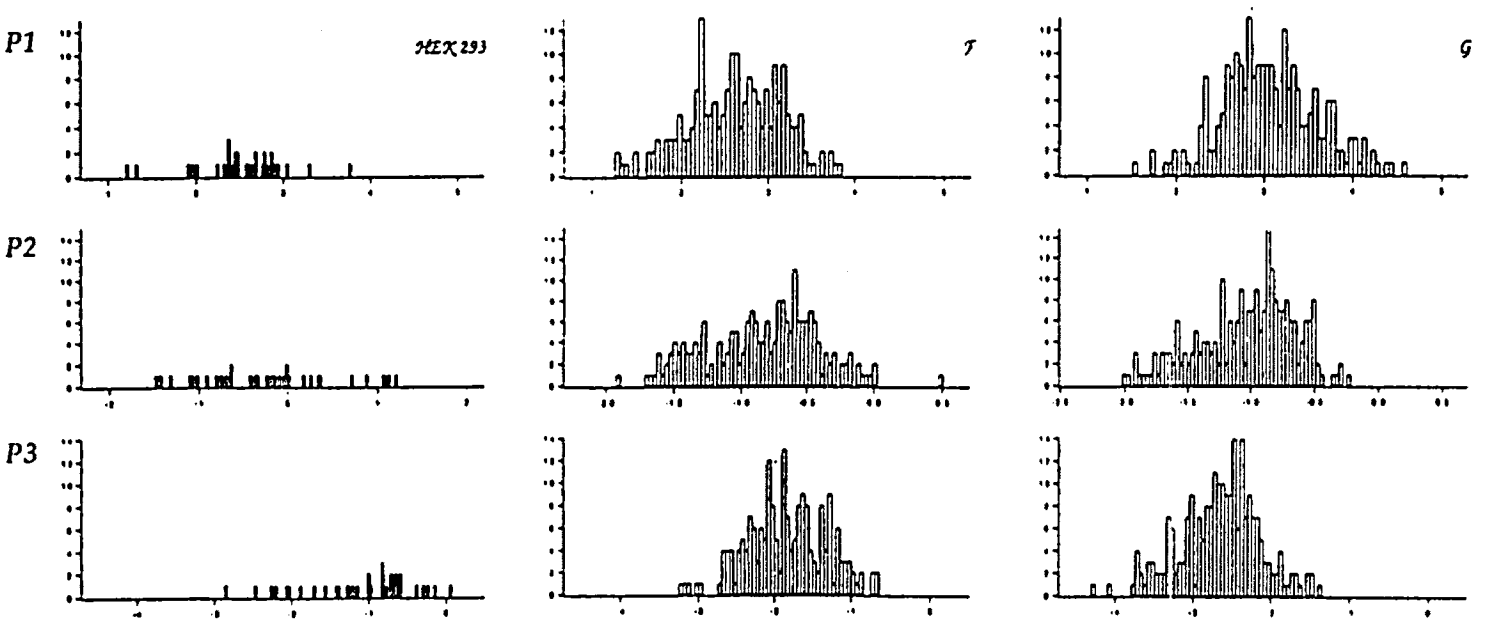

	F (n=207)	G (n=241)
P1	2.62 ± 0.53	3.05 ± 0.54
P2	-0.84 ± 0.42	-1.04 ± 0.38
P3	-1.83 ± 0.54	-2.65 ± 0.52

Figure 5-6. Histogram of measured parameters for HEK293, F, and G cells. The values of *P1*, *P2*, or *P3* were plotted in a histogram, where x-axis represents the logarithmic value of the measured parameters. Tabulated below is the mean value ± standard deviation for each log-transformed parameter derived from the histogram analysis. The distribution of all values was compared between F and G cell populations using either the non-parametric test or unpaired t-test.

duration and the slope of its falling phase were found to be significantly different between F and G cell types ($p<0.0001$, Mann-Whitney test or unpaired t-test).

The characteristics of these calcium transients were further evaluated by transformation into power spectra. In Figure 5-5 is the graphic presentation of the digitized fluorescence intensity as a time series. A representative trace from each cell type as well as their Fourier transforms are shown. The signal was transformed into a power spectrum and three parameters were derived, roughly quantifying the signal area, half-life (width of calcium signal), and oscillatory or multiple-spiking activities. Statistical analysis revealed a significant difference in all three parameters between the two cell types ($p<0.0001$, Mann-Whitney test or unpaired t-test). The difference in the third parameter, P3 was particularly prominent. The distinct calcium profiles of the two cell types likely reflected different receptor/channel kinetics.

More detailed examination of the IP_3-binding properties

From above biochemical studies it may be asserted that the IP_3 receptor fits well in the scheme of the concerted-symmetry model for an allosteric molecule proposed by Monod-Wyman-Changeux (1965). That is, the receptor exists in either a high- or a low-affinity state, with the latter state stabilized by the allosteric effector, calcium. In each state the receptor binds IP_3 in a manner that conforms to a simple Langmuir binding equation (1918), i.e. all the sites are identical and independent. A normal hyperbolic (non-cooperative) profile in response to increasing IP_3 concentrations has been described at the level of binding (Supattapone, 1988b) as well as calcium release (Ehrlich & Watras, 1988; Finch, 1991). However, a highly cooperative process of calcium release was observed in permeabilized rat Basophilic Leukemia cells (Meyer, 1988; Meyer, 1990), and yet another group reported IP_3-induced inactivation of the receptor/channel

in permeabilized hepatocytes (Hajnoczky & Thomas, 1994), suggesting perhaps a component of negative cooperativity.

Apparently the receptor behaviour in response to IP3 binding is more complex, and our understanding of just how IP3 acts to open the channel is still incomplete. The different calcium-release responses observed by various groups may well be due to the difference of cell type, or different methods of study. We believe, however, that the ligand-binding property of the IP3 receptor deserves a closer examination using the single-isoform biochemical preparation.

The same binding isotherms were performed on detergent-solubilized membranes from each stable cell line, but at more closely spaced increments of ligand concentration. These isotherms are illustrated in Figure 5-7. Each fit with gray/hatched line represents the values predicted by a Langmuir equation for non-interactive, single-class of binding sites. The apparent binding profile clearly deviates from this curve. The deviation is however not explained by the scatter of each data point. A two-component binding curve (solid line), on the other hand, provides a closer approximation of the data. each binding isotherm is best approximated by the summation of a high-affinity component with $n_H = 1$ and a second component of low-affinity with $n_H = 4$. At 0 Ca^{2+} the relative abundance of high- to low-affinity components is roughly 3:1, whereas in the presence of Ca^{2+} and in the case of a truncated receptor form (Fa), the ration is about 1:1. Calcium appears to alter the binding affinity of both components (to lower-affinity states) without changing the total binding sites. This is consistent with the notion of calcium as an allosteric inhibitor previously concluded from fitting the binding curves with single-site equations.

Figure 5-7. **A detailed look at the IP_3-binding properties of the expressed receptor isoforms.** [^{3}H]-IP_3 binding was measured as usual in solubilized membranes prepared from F & G stable cell lines. Each filled circle represents the mean of duplicate measurement of specific IP_3-binding, and the error bar indicates its range of scatter. The curve with gray/hatched line represents a fit based on the Langmuir equation for identical and independent binding sites. The solid curve represents a fit with two binding components, one of high affinity and n_H=1, the other of low affinity and n_H=4. Indicated on each graph are the equilibrium binding parameters derived from the solid curve, where K denotes the dissociation constant (nM), B denotes the number of binding sites (pmol/mg protein), and the subscript indicates either a high (H) or a low (L) binding component. The percentage of either component is provided in parentheses.

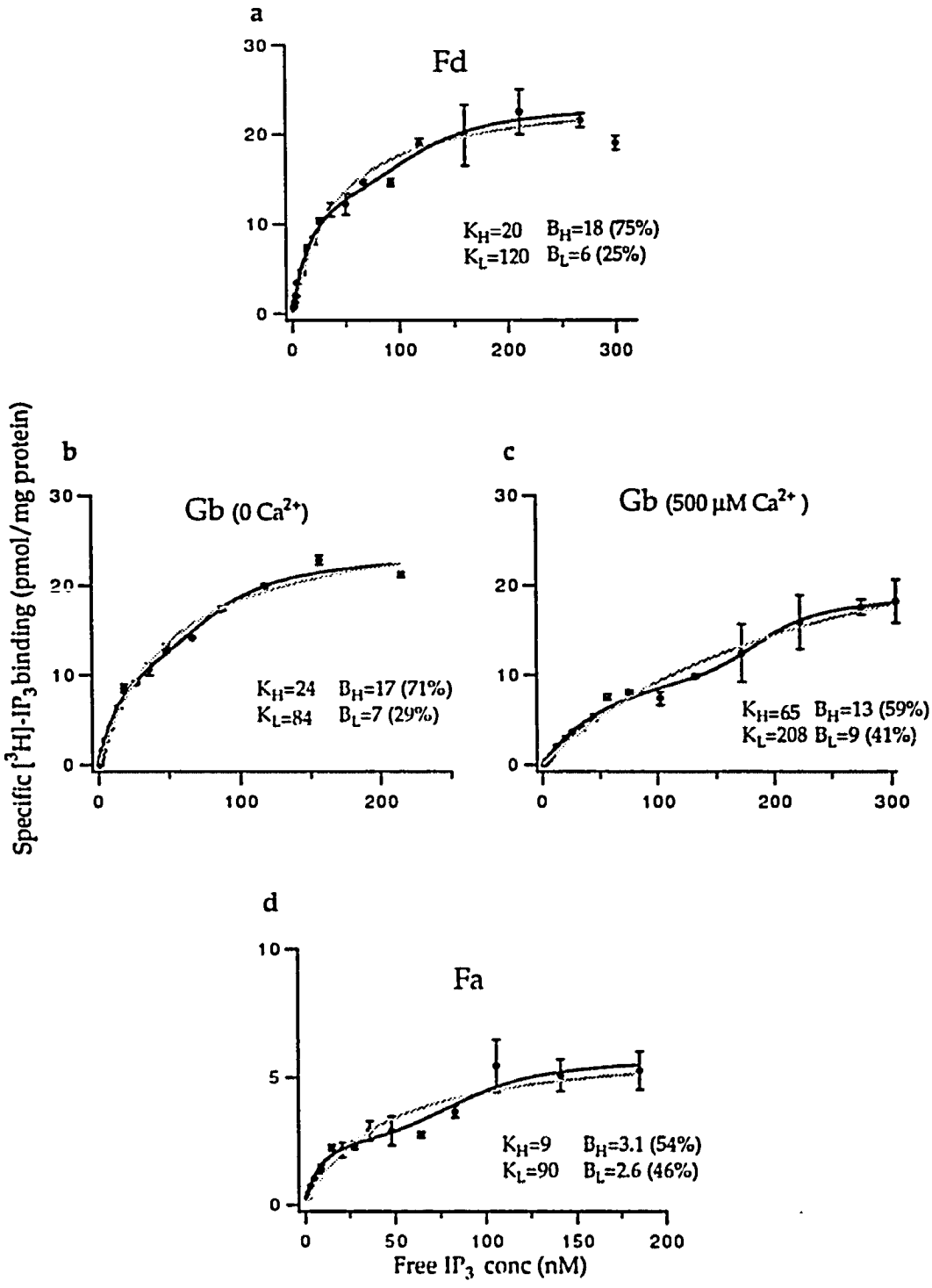

Discussion

This work presents the first detailed biochemical characterization of a single IP3 receptor isoform isolated from a homogeneous cell population. From various studies involving the native tissue preparation, it was found that the receptors displayed a complex behavior. The cause of this complexity, however, was confounded by the existence of many isoform variants within the tissue source. Over-expression of a single isoform to produce a homogeneous population of homo-tetrameric receptors allows us to simplify the system and pave the first step in understanding the function and regulation of individual form of receptor.

Ligand-binding properties of the receptor---issue of K_d

There is a controversy about the measured IP3-binding affinity for IP3 receptors, whether isolated from cerebellum or tissue-culture expression systems. It has been suggested the apparent variation be due to the mixture of various isoforms in the preparation, which has been shown by molecular cloning to be rather complex. In particular, the *SI* region has been suspected to influence IP3 binding characteristics by virtue of its residence within the IP3-binding domain. By analyzing expressed receptors with or without this 15-amino acid region, we found that the IP3 binding affinity is not influenced by *SI*.

Although both receptor isoforms have a high affinity for IP3, both are capable of adopting low-affinity states in the presence of calcium and perhaps other allosteric modulators. That calcium alters the receptor's affinity for IP3 has also been demonstrated in microsomes isolated from liver. The direction of affinity shift, however, appears opposite in the cerebellar receptor versus the hepatic type. That is, in hepatocytes, the receptor in its low-affinity (K_d=20-60 nM), activated (A) state can be

shifted by micromolar amount of calcium to a high-affinity (K_d=1-3 nM), inactive (I) state. In contrast, my studies demonstrated that the type I or cerebellar IP_3 receptor is shifted by micromolar calcium from a high-affinity (K_d=20 nM) to a low-affinity state (K_d=180 nM).

In addition to the conformational changes mediated by various modulators, each receptor isoform is capable of complex behavior in the absence of allosteric effectors, as disclosed by the shape of a single IP_3 binding isotherm. Although in the studies presented in the previous chapter each isotherm could be fitted to a first approximation by a single-site binding equation, it was noted that every isotherm displayed slight but consistent deviations from a rectangular hyperbola. The deviation is most clearly revealed in the binding isotherms plotted in Figure 5-7, in which both F and G isoforms were assayed over a wide range of closely-spaced concentrations of IP_3. Multiple inflection points are consistently observed in these plots. These inflections reflect superimposed binding processes of different affinity states, each of which is sigmoidal in shape. The occurrence of these inflections could perhaps be explained by the existence of different transition states of each receptor upon its binding of IP_3. Because only a single receptor subunit isoform is present in my expression system, and hence presumably a homogeneous population of receptors, the complex binding isotherm implies cooperative interactions among multiple IP_3 binding sites on a single receptor molecule. An allosteric inhibitor such as calcium might shift the equilibrium among receptor states with different affinities for IP_3 without altering the overall number of inflection points on the IP_3 binding isotherm or their position on the concentration axis. As revealed in Figure 5-7 b & c, a reasonable fit with the 2-component binding equation was obtained where 500 µM calcium shifted the K_d's of both components without altering the values of B_{max}. It remains to be seen whether the complex binding characteristics are due to the presence of a distinct binding site on each receptor subunit

with different affinities, or to homotropic interactions between binding sites on symmetrically arranged subunits. This can be tested readily by studying the binding profile of the monomeric, soluble domain of the molecule containing the IP3 binding site.

An important functional implication of the complex IP3 binding curve is immediately apparent. The quantal calcium release phenomenon of the IP3 receptor is an intriguing and unique property, allowing a cell to generate temporally discrete signals in response to each "quantum" of stimulus. This property describes the incomplete calcium release from stores elicited by a submaximal dose of IP3. It is explained neither by receptor desensitization, IP3 metabolism, nor by a balanced flux. In order to explain quantal release, a variety of theories have obligated a heterogeneous receptor sensitivity to IP3. Some groups proposed that discrete receptor pools are physically or functionally segregated, each releasing calcium in an all-or-none fashion but with a different sensitivity to IP3 (Ferris, 1992; Muallem, 1989). The heterogeneity of IP3 sensitivity may arise from different receptor types or differential modifications. Others have suggested that the heterogeneous response is derived from an intrinsically variable IP3 sensitivity of the receptor regulated by luminal calcium content, either through a separate protein in the ER lumen or a portion of the receptor itself (Irvine, 1990; Missiaen *et al.*, 1992a; Missiaen *et al.*, 1994). I propose an alternative model, that the heterogeneous sensitivity may arise from a homogeneous population of one single receptor isoform. The data above have shown that a single homotetrameric receptor molecule exhibits a complex binding profile which may readily form the basis for the incremental calcium release just described. These variable affinity or conformational states may overlap with some of those stabilized by various allosteric modulators including calcium, ATP, and sulfhydral reagents.

Finally, the soluble truncated receptor isolated from the stable cell line, Fa, was found to be capable of binding IP3 at a high affinity (K_d of 25 nM), similar to the full-

length receptor. It also curiously exhibited even more exaggerated inflections in the binding isotherm performed under identical experimental conditions. Immediately it suggests that there is more than one IP_3-binding site on each receptor subunit. Alternatively, this portion of the receptor undergoes conformational change and shift of various affinity states in a time-dependent fashion in response to high concentrations of IP_3, creating an apparent mixture of several affinity states within the population of single type of receptors. Conceivably the experimental condition may have allowed an equilibrium state for ligand-binding, but not necessarily for the shifts of various conformations of the receptor molecule. This suggests to us that the soluble domain of the receptor, which includes both the ligand-binding region and the so-called coupling or transducing domain, is involved directly in the interaction with different factors and the conformational shifts.

SI represents a site on the receptor directly or indirectly influenced by calcium

It remains curious, yet elusive, why so many different isoforms for IP_3 receptor exist. Above I have demonstrated that a single isoform is capable of quite complex behavior. Would cells express various receptor types only to execute a redundant function?

The expression and biochemical characterization of the two type-I receptor isoforms differing in the *SI* region was performed to correlate their function with a known structural variation. The difference in calcium inhibition profile (Figure 5-2) supports that the *SI* region indeed has a functional significance. Additional evidence is obtained from imaging the cytosolic free calcium wave forms in cells expressing each of the two isoforms.

If the *SI* region truly represents a portion of the calcium-binding motif, the observed calcium effect is then not totally fortuitous. Similar sequence motifs

representing either an EF-hand homologue or analogue are present in various ion channels including voltage-gated sodium and calcium channels (Babitch, 1990; Kretsinger *et al.*, 1991). Their function however remains unknown. This alternatively spliced segment in the IP3 receptor may have directly interacted with calcium, or it may have impeded an adjacent structure's interaction with calcium. The latter possibility is raised since a typical, functional EF-hand is composed of the calcium-binding loop flanked by two helices.

Another possibility is that the insert (together with adjacent sequences) interacts with some protein factor or other functional domain of the receptor that binds calcium. One possibility is calmedin, an integral membrane accessory protein that interacts with the IP3 receptor and confers its sensitivity to calcium. We do not anticipate calmedin to be present in an equivalent amount as the over-expressed IP3 receptors to exert its effect, unless the effect were enzymatic. We could not, however, exclude the possibility that calmedin plays a role in our expression system.

Whatever the mechanism is, my data suggest that *SI* influences the receptor's behavior vis-à-vis calcium. The F receptor, which lacks *SI*, shows a sharp reduction in IP3 binding upon encountering micromolar or sub-micromolar free calcium; i.e., the binding decreases from 90% to 10% of the binding in 0 Ca^{2+} as $[Ca^{2+}]_{free}$ increases from 0.1 to 1 μM. The receptors change conformation from a low- to a high-K_d state in a concerted, "cooperative" manner (with the cooperativity index greater than 1). The mere presence of *SI* in the same receptor (G) effectively ablated such "cooperativity". IP3 binding to the G receptor remains calcium-sensitive, but the reduction of affinity is gradual, dropping from 90% to 10% of the 0-Ca^{2+} value over approximately two logarithmic units of $[Ca^{2+}]_{free}$. Thus, calcium exerts a different form of feedback inhibition on the two IP3 receptor isoforms. Again, this description of the calcium effect on the two isoforms gives only a first approximation. There probably exist multiple

microscopic states in which the calcium-binding site interacts with the IP3-binding site to bring about the change in affinity, whereas we have observed only the "averaged" equilibrium condition.

Certainly the truncated version of the two receptor isoforms would offer additional insights as to how *SI* influences the allosteric interaction between calcium and IP3 binding. This has not been accomplished as yet, due to the lack of stable cell lines that could provide an easy preparation of these truncated receptors for similar biochemical analyses.

The calcium-inhibitory effect on IP3 binding is expected to directly influence receptor/channel inactivation. A positive cooperativity in this effect will produce a sharp termination of calcium release, whereas a negative cooperatively will allow a gradual decline in the falling phase of a calcium transient. These predictions complied exactly with the experimental outcomes in calcium-imaging of the stable cell lines. As for their activation component, the wave forms of both F and G cells were similar. Each calcium transient had a sharp threshold and a steep rise, indicative of a highly cooperative nature in channel opening as well as a positive feedback in calcium release, due perhaps to the agonistic effect of calcium at initial low concentrations.

In addition to the distinct falling phase of each calcium transient, the two cell types also differed in their oscillatory activities. A fraction of F cells exhibited multiple spikes of calcium transient, which were never observed in G cells. Although calcium oscillation is a complex process and there may be several mechanisms involved in one cell type, the different behavior observed between F and G cells could be correlated to their biochemical properties. The time period in between calcium transients is probably set by both agonist (IP3) and calcium concentrations. The application of the former remains constant during the imaging experiment, whereas the latter depends on a steady state established by calcium leak from the IP3 receptor as well as calcium reuptake via

the Ca^{2+}-ATPase. A simple explanation for the difference between the two cell lines is therefore the termination of calcium release from the IP3 receptor. In F cells this is achieved in a cooperative manner, with a rapid termination of calcium leak through the IP3 receptor, thus allowing a prompt restoration of cytosolic calcium and preparation for the next trigger of calcium release activity. The finding of a functional difference between the two alternatively spliced IP3 receptor isoforms suggests that cells may use them to generate different calcium signals. Additional diverse signals may be expected if cells allow oligomerization of dissimilar as well as similar subunits to form the functional IP3 receptors.

References

Allbritton, N.L., Meyer, T., & Stryer, L. (1992) Range of messenger action of calcium ion and inositol 1,4,5-trisphosphate. *Science*, 258(5089): 1812-5.

Anderson, K., Lai, F.A., Liu, Q.Y., Rousseau, E., Erickson, H.P., & Meissner, G. (1989) Structural and functional characterization of the purified cardiac ryanodine receptor-Ca^{2+} release channel complex. *J. Biol. Chem.*, 264(2): 1329-35.

Attree, O., Olivos, I.M., Okabe, I., Bailey, L.C., Nelson, D.L., Lewis, R.A., McInnes, R.R., & Nussbaum, R.L. (1992) The Lowe's oculocerebrorenal syndrome gene encodes a protein highly homologous to inositol polyphosphate-5-phosphatase. *Nature*, 358(6383): 239-42.

Augustine, G.J., & Neher, E. (1992) Calcium requirements for secretion in bovine chromaffin cells. *J. Physiol.*, 450(247): 247-71.

Babitch, J. (1990) Channel hands. *Nature*, 346(6282): 321-2.

Balla, T., & Catt, K.J. (1994) Phosphoinositides and calcium signaling - new aspects and diverse functions in cell regulation. *Trends Endocrinol. Metabolism*, 5250-255.

Bansal, V.S., & Majerus, P.W. (1990) Phosphatidylinositol-derived precursors and signals. *Ann. Rev. Cell Biol.*, 6(41): 41-67.

Berridge, M.J. (1987) Inositol trisphosphate as a second messenger in signal transduction. *Annals of the New York Academy of Sciences*, 494(39): 39-51.

Berridge, M.J. (1992). Inositol trisphosphate and calcium oscillations. In Advances in Second Messenger & Phosphoprotein Research (pp. 211-23). New York: Raven Press.

Berridge, M.J. (1993) Inositol trisphosphate and calcium signalling. *Nature*, 361(6410): 315-25.

Berridge, M.J., & Irvine, R.F. (1984) Inositol trisphosphate, a novel second messenger in cellular signal transduction. *Nature*, 312(5992): 315-21.

Bertolino, M., & Llinas, R.R. (1992) The central role of voltage-activated and receptor-operated calcium channels in neuronal cells. *Ann. Rev. Pharmacol. Toxicol.*, 32(399): 399-421.

Bezprozvanny, I., & Ehrlich, B.E. (1993) ATP modulates the function of inositol 1,4,5-trisphosphate-gated channels at two sites. *Neuron*, 10(6): 1175-84.

Bezprozvanny, I., Watras, J., & Ehrlich, B.E. (1991) Bell-shaped calcium-response curves of Ins(1,4,5)P_3- and calcium-gated channels from endoplasmic reticulum of cerebellum. *Nature*, 351(6329): 751-4.

Block, B.A., & Franzini, A.C. (1988) The structure of the membrane systems in a novel muscle cell modified for heat production. *J. Cell Biol.*, 107(3): 1099-112.

Blondel, O., Takeda, J., Janssen, H., Seino, S., & Bell, G.I. (1993) Sequence and functional characterization of a third inositol trisphosphate receptor subtype, IP_3R-3, expressed in pancreatic islets, kidney, gastrointestinal tract, and other tissues. *J. Biol. Chem.*, 268(15): 11356-63.

Boitano, S., Dirksen, E.R., & Sanderson, M.J. (1992) Intercellular propagation of calcium waves mediated by inositol trisphosphate. *Science*, 258(5080): 292-5.

Bootman, M.D., Berridge, M.J., & Taylor, C.W. (1992) All-or-nothing Ca^{2+} mobilization from the intracellular stores of single histamine-stimulated HeLa cells. *J. Physiol.*, 450(163): 163-78.

Chadwick, C.C., Saito, A., & Fleischer, S. (1990) Isolation and characterization of the inositol trisphosphate receptor from smooth muscle. *Proc. Natl. Acad. Sci. USA*, 87(6): 2132-6.

Chirgwin, J.M., Przybyla, A.E., MacDonald, R.J., & Rutter, W.J. (1979) Isolation of biologically active ribonucleic acid from sources enriched in ribonuclease. *Biochemistry*, 18(24): 5294-9.

Connor, J.A., Kater, S.B., Cohan, C., & Fink, L. (1990) Ca^{2+} dynamics in neuronal growth cones: regulation and changing patterns of Ca^{2+} entry. *Cell Calcium*, 11(2-3): 233-9.

Cornell-Bell, A.H., Finkbeiner, S.M., Cooper, M.S., & Smith, S.J. (1990) Glutamate induces calcium waves in cultured astrocytes: long-range glial signaling. *Science*, 247(4941): 470-3.

Cunningham, A.M., Ryugo, D.K., Sharp, A.H., Reed, R.R., Snyder, S.H., & Ronnett, G.V. (1993) Neuronal inositol 1,4,5-trisphosphate receptor localized to the plasma membrane of olfactory cilia. *Neuroscience*, 57(2): 339-52.

Danoff, S.K., Ferris, C.D., Donath, C., Fischer, G.A., Munemitsu, S., Ullrich, A., Snyder, S.H., & Ross, C.A. (1991) Inositol 1,4,5-trisphosphate receptors: distinct neuronal and nonneuronal forms derived by alternative splicing differ in phosphorylation. *Proc. Natl. Acad. Sci. USA*, 88(7): 2951-5.

Danoff, S.K., Supattapone, S., & Snyder, S.H. (1988) Characterization of a membrane protein from brain mediating the inhibition of inositol 1,4,5-trisphosphate receptor binding by calcium. *Biochem. J.*, 254(3): 701-5.

De Smedt, H., Missiaen, L., Parys, J.B., Bootman, M.D., Mertens, L., van den Bosch, L., & Casteels, R. (1994) Determination of relative amounts of inositol trisphosphate receptor mRNA isoforms by ratio polymerase chain reaction. *J. Biol. Chem.*, 269(34): 21691-8.

Ebashi, S., & Endo, M. (1968) Calcium ion and muscle contraction. *Prog. Biophys. Mol. Biol.*, 18(123): 123-83.

Ehrlich, B.E., & Watras, J. (1988) Inositol 1,4,5-trisphosphate activates a channel from smooth muscle sarcoplasmic reticulum. *Nature*, 336(6199): 583-6.

Ellisman, M.H., Deerinck, T.J., Ouyang, Y., Beck, C.F., Tanksley, S.J., Walton, P.D., Airey, J.A., & Sutko, J.L. (1990) Identification and localization of ryanodine binding proteins in the avian central nervous system. *Neuron*, 5(2): 135-46.

Emerick, M.E. (1991) Characterization of the TTX-binding site in the native membrane, and identification of endogenously phosphorylated residues on sodium channels from *Electrophorus* electroplax. Ph.D. dissertation, Yale University.

Fadool, D.A., & Ache, B.W. (1994) Inositol 1,3,4,5-tetrakisphosphate-gated channels interact with inositol 1,4,5-trisphosphate-gated channels in olfactory receptor neurons. *Proc. Natl. Acad. Sci. USA*, 919471-9475.

Ferris, C.D., Cameron, A.M., Huganir, R.L., & Snyder, S.H. (1992) Quantal calcium release by purified reconstituted inositol 1,4,5-trisphosphate receptors. *Nature*, 356(6367): 350-2.

Ferris, C.D., Huganir, R.L., Bredt, D.S., Cameron, A.M., & Snyder, S.H. (1991) Inositol trisphosphate receptor: phosphorylation by protein kinase C and calcium calmodulin-dependent protein kinases in reconstituted lipid vesicles. *Proc. Natl. Acad. Sci. USA*, 88(6): 2232-5.

Ferris, C.D., Huganir, R.L., Supattapone, S., & Snyder, S.H. (1989) Purified inositol 1,4,5-trisphosphate receptor mediates calcium flux in reconstituted lipid vesicles. *Nature*, 342(6245): 87-9.

Ferris, C.D., & Snyder, S.H. (1992) Inositol 1,4,5-trisphosphate-activated calcium channels. *Ann. Rev. Physiol.*, 54(469): 469-88.

Finch, E.A., Turner, T.J., & Goldin, S.M. (1991) Calcium as a coagonist of inositol 1,4,5-trisphosphate-induced calcium release. *Science*, 252(5004): 443-6.

Finkbeiner, S. (1992) Calcium waves in astrocytes-filling in the gaps. *Neuron*, 8(6): 1101-8.

Fleischer, S., & Inui, M. (1989) Biochemistry and biophysics of excitation-contraction coupling. *Ann. Rev. Biophys. Biophys. Chem.*, 18(333): 333-64.

Fryer, H.J., Kelly, G.M., Molinaro, L., & Hockfield, S. (1992) The high molecular weight Cat-301 chondroitin sulfate proteoglycan from brain is related to the large aggregating proteoglycan from cartilage, aggrecan. *J. Biol. Chem.*, 267(14): 9874-83.

Fujimoto, T., Nakade, S., Miyawaki, A., Mikoshiba, K., & Ogawa, K. (1992) Localization of inositol 1,4,5-trisphosphate receptor-like protein in plasmalemmal caveolae. *J. Cell Biol.*, 119(6): 1507-13.

Furuichi, T., Yoshikawa, S., Miyawaki, A., Wada, K., Maeda, N., & Mikoshiba, K. (1989) Primary structure and functional expression of the inositol 1,4,5-trisphosphate-binding protein P400. *Nature*, 342(6245): 32-8.

Galione, A. (1993) Cyclic ADP-ribose: a new way to control calcium. *Science*, 259(5093): 325-6.

Graham, F.L., Smiley, J., Russell, W.C., & Nairn, R. (1977) Characteristics of a human cell line transformed by DNA from human adenovirus type 5. *J. Gen. Virol.*, 36(1): 59-74.

Graham, F.L., & van der Eb, A.J. (1973) A new technique for the assay of infectivity of human adenovirus 5 DNA. *Virology*, 52(2): 456-67.

Hajnoczky, G., & Thomas, A.P. (1994) The inositol trisphosphate calcium channel is inactivated by inositol trisphosphate. *Nature*, 370(6489): 474-7.

Harlow, E., & Lane, D. (1988). Antibodies: A Laboraory Manual. Cold Spring Harbor Laboratory, Cold Spring Harbor, NY.

Hilly, M., Pietri, R.F., Coquil, J.F., Guy, M., & Mauger, J.P. (1993) Thiol reagents increase the affinity of the inositol 1,4,5-trisphosphate receptor. *J. Biol. Chem.*, 268(22): 16488-94.

Hingorani, S.R. (1994) Cerebellar receptors for inositol 1,4,5-triphosphate: ligand binding properties, mechanisms of feedback regulation by Ca^{2+}, and purification. Ph.D. dissertation, Yale University.

Hingorani, S.R., & Agnew, W.S. (1991) A rapid ion-exchange assay for detergent-solubilized inositol 1,4,5-trisphosphate receptors. *Anal. Biochem.*, 194(1): 204-13.

Hingorani, S.R., & Agnew, W.S. (1992) Assay and purification of neuronal receptors for inositol 1,4,5-trisphosphate. *Meth. Enzymol.*, 207(573): 573-91.

Hokin, L.E. (1985) Receptors and phosphoinositide-generated second messengers. *Ann. Rev. Biochem.*, 54(205): 205-35.

Hunkapiller, M.W., Lujan, E., Ostrander, F., & Hood, L.E. (1983) Isolation of microgram quantities of proteins from polyacrylaminde gels for amino acid sequence analysis. *Meth. Enzymol.*, 91227-36.

Huynh, T.V., Young, R.A., & Davis, R.W. (1989). Construction and screening cDNA libraries in λgt10 and λgt11. In D. M. Glover (Eds.), DNA Cloning (pp. 49-78). Oxford, UK: IRL Press.

Iino, M., & Endo, M. (1992) Calcium-dependent immediate feedback control of inositol 1,4,5-triphosphate-induced Ca^{2+} release. *Nature*, 360(6399): 76-8.

Innis, M., Gelfand, D., Sninsky, J., & White, T. (Ed.). (1990). PCR Protocols: A Guide to Methods and Applications. San Diego: Academic Press, Inc.

Irvine, R.F. (1990) 'Quantal' Ca^{2+} release and the control of Ca^{2+} entry by inositol phosphates--a possible mechanism. *FEBS Lett.*, 263(1): 5-9.

Joseph, S.K., Rice, H.L., & Williamson, J.R. (1989) The effect of external calcium and pH on inositol trisphosphate-mediated calcium release from cerebellum microsomal fractions. *Biochem. J.*, 258(1): 261-5.

Kaplin, A.I., Ferris, C.D., Voglmaier, S.M., & Snyder, S.H. (1994) Purified reconstituted inositol 1,4,5-trisphosphate receptors. Thiol reagents act directly on receptor protein. *J. Biol. Chem.*, 269(46): 28972-8.

Keller, G.H., & Manak, M.M. (1989). DNA Probes. Stockton Press, New York.

Kennedy, M.B. (1989) Regulation of neuronal function by calcium. *Trends Neurosci.*, 12(11): 417-20.

Khan, A.A., Steiner, J.P., Klein, M.G., Schneider, M.F., & Snyder, S.H. (1992a) IP_3 receptor: localization to plasma membrane of T cells and cocapping with the T cell receptor. *Science*, 257(5071): 815-8.

Khan, A.A., Steiner, J.P., & Snyder, S.H. (1992b) Plasma membrane inositol 1,4,5-trisphosphate receptor of lymphocytes: selective enrichment in sialic acid and unique binding specificity. *Proc. Natl. Acad. Sci. USA*, 89(7): 2849-53.

Kofman, O., & Belmaker, R.H. (1993) Biochemical, behavioral, and clinical studies of the role of inositol in lithium treatment and depression. *Biol. Psych.*, 34(12): 839-52.

Komalavilas, P., & Lincoln, T.M. (1994) Phosphorylation of the inositol 1,4,5-trisphosphate receptor by cyclic GMP-dependent protein kinase. *J. Biol. Chem.*, 269(12): 8701-7.

Kozak, M. (1986) Point mutations define a sequence flanking the AUG initiator codon that modulates translation by eukaryotic ribosomes. *Cell*, 44(2): 283-92.

Kretsinger, R.H., Tolbert, D., Nakayama, S., & Pearson, W. (1991). The EF-hand, homologs and analogs. In C. W. Heizmann (Eds.), Novel Calcium-Binding Proteins (pp. 17-37).

Kume, S., Muto, A., Aruga, J., Nakagawa, T., Michikawa, T., Furuichi, T., Nakade, S., Okano, H., & Mikoshiba, K. (1993) The Xenopus IP_3 receptor: structure, function, and localization in oocytes and eggs. *Cell*, 73(3): 555-70.

Lai, F.A., Misra, M., Xu, L., Smith, H.A., & Meissner, G. (1989) The ryanodine receptor-Ca^{2+} release channel complex of skeletal muscle sarcoplasmic reticulum. Evidence for a cooperatively coupled, negatively charged homotetramer. *J. Biol. Chem.*, 264(28): 16776-85.

Lee, H.C., Aarhus, R., Graeff, R., Gurnack, M.E., & Walseth, T.F. (1994) Cyclic ADP-ribose activation of the ryanodine receptor is mediated by calmodulin. *Nature*, 370(6487): 307-9.

Lerner, R.A., Green, N., Alexander, H., Liu, F.T., Sutcliffe, J.G., & Shinnick, T.M. (1981) Chemically synthesized peptides predicted from the nucleotide sequence of the hepatitis B virus genome elicit antibodies reactive with the native envelope protein of Dane particles. *Proc. Natl. Acad. Sci. USA*, 78(6): 3403-7.

Linden, D.J., & Connor, J.A. (1991) Participation of postsynaptic PKC in cerebellar long-term depression in culture. *Science*, 254(5038): 1656-9.

Linden, D.J., & Connor, J.A. (1993) Cellular mechanisms of long-term depression in the cerebellum. *Curr. Opinion Neurobiol.*, 3(3): 401-6.

Lowry, O.H., Rosenbrough, N.J., Farr, A.C., & Randal, R.J. (1951) Protein measurement with the folin phenol reagent. *J. Biol. Chem.*, 193263-275.

Maeda, N., Kawasaki, T., Nakade, S., Yokota, N., Taguchi, T., Kasai, M., & Mikoshiba, K. (1991) Structural and functional characterization of inositol 1,4,5-trisphosphate receptor channel from mouse cerebellum. *J. Biol. Chem.*, 266(2): 1109-16.

Maeda, N., Niinobe, M., Inoue, Y., & Mikoshiba, K. (1989) Developmental expression and intracellular location of P400 protein characteristic of Purkinje cells in the mouse cerebellum. *Develop. Biol.*, 133(1): 67-76.

Maeda, N., Niinobe, M., & Mikoshiba, K. (1990) A cerebellar Purkinje cell marker P400 protein is an inositol 1,4,5-trisphosphate ($InsP_3$) receptor protein. Purification and characterization of $InsP_3$ receptor complex. *EMBO J.*, 9(1): 61-7.

Maeda, N., Niinobe, M., Nakahira, K., & Mikoshiba, K. (1988) Purification and characterization of P400 protein, a glycoprotein characteristic of Purkinje cell, from mouse cerebellum. *J. Neurochem.*, 51(6): 1724-30.

Maizel, J.V. (1971) Polyacrylamide gel electrophoresis of viral proteins. *Meth. Virol.*, 5180-246.

Malviya, A.N., Rogue, P., & Vincendon, G. (1990) Stereospecific inositol 1,4,5-[32P]trisphosphate binding to isolated rat liver nuclei: evidence for inositol trisphosphate receptor-mediated calcium release from the nucleus. *Proc. Natl. Acad. Sci. USA*, 87(23): 9270-4.

Maranto, A.R. (1994) Primary structure, ligand binding, and localization of the human type 3 inositol 1,4,5-trisphosphate receptor expressed in intestinal epithelium. *J. Biol. Chem.*, 269(2): 1222-30.

Marshall, I.C., & Taylor, C.W. (1993) Regulation of inositol 1,4,5-trisphosphate receptors. *J. Exp. Biol.*, 184(161): 161-82.

Marshall, I.C., & Taylor, C.W. (1994) Two calcium-binding sites mediate the interconversion of liver inositol 1,4,5-trisphosphate receptors between three conformational states. *Biochem. J.*, 301(Pt 2): 591-8.

Masu, M., Tanabe, Y., Tsuchida, K., Shigemoto, R., & Nakanishi, S. (1991) Sequence and expression of a metabotropic glutamate receptor. *Nature*, 349(6312): 760-5.

Mauger, J.P., Lievremont, J.P., Pietri, R.F., Hilly, M., & Coquil, J.F. (1994) The inositol 1,4,5-trisphosphate receptor: kinetic properties and regulation. *Mol. Cell. Endocrinol.*, 98(2): 133-9.

Meissner, G. (1994) Ryanodine receptor/Ca^{2+} release channels and their regulation by endogenous effectors. *Ann. Rev. Physiol.*, 56(485): 485-508.

Meyer, T., Holowka, D., & Stryer, L. (1988) Highly cooperative opening of calcium channels by inositol 1,4,5-trisphosphate. *Science*, 240(4852): 653-6.

Meyer, T., & Stryer, L. (1991) Calcium spiking. *Ann. Rev. Biophys. Biophys. Chem.*, 20(153): 153-74.

Meyer, T., Wensel, T., & Stryer, L. (1990) Kinetics of calcium channel opening by inositol 1,4,5-trisphosphate. *Biochemistry*, 29(1): 32-7.

Michikawa, T., Hamanaka, H., Otsu, H., Yamamoto, A., Miyawaki, A., Furuichi, T., Tashiro, Y., & Mikoshiba, K. (1994) Transmembrane topology and sites of N-glycosylation of inositol 1,4,5-trisphosphate receptor. *J. Biol. Chem.*, 269(12): 9184-9.

Mignery, G.A., Johnston, P.A., & Sudhof, T.C. (1992) Mechanism of Ca^{2+} inhibition of inositol 1,4,5-trisphosphate ($InsP_3$) binding to the cerebellar $InsP_3$ receptor. *J. Biol. Chem.*, 267(11): 7450-5.

Mignery, G.A., Newton, C.L., Archer, B.T.I., & Sudhof, T.C. (1990) Structure and expression of the rat inositol 1,4,5-trisphosphate receptor. *J. Biol. Chem.*, 265(21): 12679-85.

Mignery, G.A., & Sudhof, T.C. (1990) The ligand binding site and transduction mechanism in the inositol-1,4,5-triphosphate receptor. *EMBO J.*, 9(12): 3893-8.

Mignery, G.A., Sudhof, T.C., Takei, K., & De Camilli, P. (1989) Putative receptor for inositol 1,4,5-trisphosphate similar to ryanodine receptor. *Nature*, 342(6246): 192-5.

Mikoshiba, K., Okano, H., & Tsukada, Y. (1985) P400 protein characteristic to Purkinje cells and related proteins in cerebella from neuropathological mutant mice: autoradiographic study by ^{14}C-leucine and phosphorylation. *Develop. Neurosci.*, 7(3): 179-87.

Missiaen, L., De, S.H., Droogmans, G., & Casteels, R. (1992a) Luminal Ca^{2+} controls the activation of the inositol 1,4,5-trisphosphate receptor by cytosolic Ca^{2+}. *J. Biol. Chem.*, 267(32): 22961-6.

Missiaen, L., De Smedt, H., Droogmans, G., & Casteels, R. (1992b) Ca^{2+} release induced by inositol 1,4,5-trisphosphate is a steady-state phenomenon controlled by luminal Ca^{2+} in permeabilized cells. *Nature*, 357(6379): 599-602.

Missiaen, L., Parys, J.B., De, S.H., Oike, M., & Casteels, R. (1994) Partial calcium release in response to submaximal inositol 1,4,5-trisphosphate receptor activation. *Mol. Cell. Endocrinol.*, 98(2): 147-56.

Miyawaki, A., Furuichi, T., Maeda, N., & Mikoshiba, K. (1990) Expressed cerebellar-type inositol 1,4,5-trisphosphate receptor, P400, has calcium release activity in a fibroblast L cell line. *Neuron*, 5(1): 11-8.

Miyazaki, S., Shirakawa, H., Nakada, K., Honda, Y., Yuzaki, M., Nakade, S., & Mikoshiba, K. (1992) Antibody to the inositol trisphosphate receptor blocks thimerosal-enhanced Ca^{2+}-induced Ca^{2+} release and Ca^{2+} oscillations in hamster eggs. *FEBS Lett.*, 309(2): 180-4.

Morgan, J.I., & Curran, T. (1986) Role of ion flux in the control of c-fos expression. *Nature*, 322(6079): 552-5.

Mourey, R.J., Estevez, V.A., Marecek, J.F., Barrow, R.K., Prestwich, G.D., & Snyder, S.H. (1993) Inositol 1,4,5-trisphosphate receptors: labeling the inositol 1,4,5-trisphosphate binding site with photoaffinity ligands. *Biochemistry*, 32(7): 1719-26.

Mourey, R.J., Verma, A., Supattapone, S., & Snyder, S.H. (1990) Purification and characterization of the inositol 1,4,5- trisphosphate receptor protein from rat vas deferens. *Biochem. J.*, 272(2): 383-9.

Muallem, S., Pandol, S.J., & Beeker, T.G. (1989) Hormone-evoked calcium release from intracellular stores is a quantal process. *J. Biol. Chem.*, 264(1): 205-12.

Nahorski, S.R., Ragan, C.I., & Challiss, R.A. (1991) Lithium and the phosphoinositide cycle: an example of uncompetitive inhibition and its pharmacological consequences. *Trends Pharmacol. Sci.*, 12(8): 297-303.

Nakade, S., Maeda, N., & Mikoshiba, K. (1991) Involvement of the C-terminus of the inositol 1,4,5-trisphosphate receptor in Ca^{2+} release analysed using region-specific monoclonal antibodies. *Biochem. J.*, 277(Pt 1): 125-31.

Nakade, S., Rhee, S.K., Hamanaka, H., & Mikoshiba, K. (1994) Cyclic AMP-dependent phosphorylation of an immunoaffinity-purified homotetrameric inositol 1,4,5-trisphosphate receptor (type I) increases Ca^{2+} flux in reconstituted lipid vesicles. *J. Biol. Chem.*, 269(9): 6735-42.

Nakagawa, T., Okano, H., Furuichi, T., Aruga, J., & Mikoshiba, K. (1991a) The subtypes of the mouse inositol 1,4,5-trisphosphate receptor are expressed in a tissue-specific and developmentally specific manner. *Proc. Natl. Acad. Sci. USA*, 88(14): 6244-8.

Nakagawa, T., Shiota, C., Okano, H., & Mikoshiba, K. (1991b) Differential localization of alternative spliced transcripts encoding inositol 1,4,5-trisphosphate receptors in mouse cerebellum and hippocampus: *in situ* hybridization study. *J. Neurochem.*, 57(5): 1807-10.

Nakanishi, S. (1994) Metabotropic glutamate receptors: synaptic transmission, modulation, and plasticity. *Neuron*, 13(5): 1031-7.

Nakayama, S., & Kretsinger, R.H. (1994) Evolution of the EF-hand family of proteins. *Ann. Rev. Biophys. Biomol. Struct.*, 23(473): 473-507.

Neher, E. (1993) Spatial and temporal aspects of Ca^{2+} changes in secretion control. *Biochemical Society Transactions*, 21(2): 420-3.

Nelson, W.J., & Hammerton, R.W. (1989) A membrane-cytoskeletal complex containing Na^+,K^+-ATPase, ankyrin, and fodrin in Madin-Darby canine kidney (MDCK) cells: implications for the biogenesis of epithelial cell polarity. *J. Cell Biol.*, 108(3): 893-902.

Newton, C.L., Mignery, G.A., & Sudhof, T.C. (1994) Co-expression in vertebrate tissues and cell lines of multiple inositol 1,4,5-trisphosphate $InsP_3$ receptors with distinct affinities for $InsP_3$. *J. Biol. Chem.*, 269(46): 28613-9.

Nicotera, P., Bellomo, G., & Orrenius, S. (1992) Calcium-mediated mechanisms in chemically induced cell death. *Ann. Rev. Pharmacol. Toxicol.*, 32(449): 449-70.

Otsu, H., Yamamoto, A., Maeda, N., Mikoshiba, K., & Tashiro, Y. (1990) Immunogold localization of inositol 1, 4, 5-trisphosphate $InsP_3$ receptor in mouse cerebellar Purkinje cells using three monoclonal antibodies. *Cell Struct. Funct.*, 15(3): 163-73.

Peng, Y.W., Sharp, A.H., Snyder, S.H., & Yau, K.W. (1991) Localization of the inositol 1,4,5-trisphosphate receptor in synaptic terminals in the vertebrate retina. *Neuron*, 6(4): 525-31.

Persechini, A., Moncrief, N.D., & Kretsinger, R.H. (1989) The EF-hand family of calcium-modulated proteins. *Trends Neurosci.*, 12(11): 462-7.

Pietri, F., Hilly, M., & Mauger, J.P. (1990) Calcium mediates the interconversion between two states of the liver inositol 1,4,5-trisphosphate receptor. *J. Biol. Chem.*, 265(29): 17478-85.

Ross, C.A., Danoff, S.K., Schell, M.J., Snyder, S.H., & Ullrich, A. (1992) Three additional inositol 1,4,5-trisphosphate receptors: molecular cloning and differential localization in brain and peripheral tissues. *Proc. Natl. Acad. Sci. USA*, 89(10): 4265-9.

Rossier, M.F., & Putney, J.J. (1991) The identity of the calcium-storing, inositol 1,4,5-trisphosphate-sensitive organelle in non-muscle cells: calciosome, endoplasmic reticulum ... or both? *Trends Neurosci.*, 14(7): 310-4.

Saito, A., Inui, M., Radermacher, M., Frank, J., & Fleischer, S. (1988) Ultrastructure of the calcium release channel of sarcoplasmic reticulum. *J. Cell Biol.*, 107(1): 211-9.

Sambrook, J., Fritsch, E., & Maniatis, T. (1989). Molecular Cloning: A Laboratory Manual (2nd ed.). Cold Spring Harbor Laboratory, Cold Spring Harbor, NY.

Sambrook, J.F. (1990) The involvement of calcium in transport of secretory proteins from the endoplasmic reticulum. *Cell*, 61(2): 197-9.

Sanderson, M.J., Charles, A.C., Boitano, S., & Dirksen, E.R. (1994) Mechanisms and function of intercellular calcium signaling. *Mol. Cell. Endocrinol.*, 98(2): 173-87.

Satoh, T., Ross, C.A., Villa, A., Supattapone, S., Pozzan, T., Snyder, S.H., & Meldolesi, J. (1990) The inositol 1,4,5,-trisphosphate receptor in cerebellar Purkinje cells: quantitative immunogold labeling reveals concentration in an ER subcompartment. *J. Cell Biol.*, 111(2): 615-24.

Shirakawa, H., & Miyazaki, S. (1994) Evidence for inositol tetrakisphosphate-activated Ca^{2+} influx pathway refilling inositol trisphosphate-sensitive Ca^{2+} stores in hamster eggs. *Cell Calcium*, 171-13.

Smith, D.B., & Johnson, K.S. (1988) Single-step purification of polypeptides expressed in *Escherichia coli* as fusions with glutathione S-transferase. *Gene*, 6731-40.

Sudhof, T.C., Newton, C.L., Archer, B.T.I., Ushkaryov, Y.A., & Mignery, G.A. (1991) Structure of a novel $InsP_3$ receptor. *EMBO J.*, 10(11): 3199-206.

Sullivan, K.M.C., Lin, D., Agnew, W., & Wilson, K.L. (1995) IP_3 receptor activation is required for nuclear vesicle fusion. *(manuscript submitted to PNAS).*

Supattapone, S., Danoff, S.K., Theibert, A., Joseph, S.K., Steiner, J., & Snyder, S.H. (1988a) Cyclic AMP-dependent phosphorylation of a brain inositol trisphosphate receptor decreases its release of calcium. *Proc. Natl. Acad. Sci. USA*, 85(22): 8747-50.

Supattapone, S., Worley, P.F., Baraban, J.M., & Snyder, S.H. (1988b) Solubilization, purification, and characterization of an inositol trisphosphate receptor. *J. Biol. Chem.*, 263(3): 1530-4.

Takei, K., Mignery, G.A., Mugnaini, E., Sudhof, T.C., & De Camilli, P. (1994) Inositol 1,4,5-trisphosphate receptor causes formation of ER cisternal stacks in transfected fibroblasts and in cerebellar Purkinje cells. *Neuron*, 12(2): 327-42.

Taylor, C.W., & Potter, B.V. (1990) The size of inositol 1,4,5-trisphosphate-sensitive Ca^{2+} stores depends on inositol 1,4,5-trisphosphate concentration. *Biochem. J.*, 266(1): 189-94.

Terasaki, M., Slater, N.T., Fein, A., Schmidek, A., & Reese, T.S. (1994) Continuous network of endoplasmic reticulum in cerebellar Purkinje neurons. *Proc. Natl. Acad. Sci. USA*, 91(16): 7510-4.

Trimmer, J.S. (1991) Immunological identification and characterization of a delayed rectifier K^+ channel polypeptide in rat brain. *Proc. Natl. Acad. Sci. USA*, 88(23): 10764-8.

Tsien, R.W., & Tsien, R.Y. (1990) Calcium channels, stores, and oscillations. *Ann. Rev. Cell Biol.*, 6(715): 715-60.

Ukomadu, C. (1993) Functional expression of the μI sodium channel in HEK 293 cells: biophysical and biochemical properties. Ph.D. dissertation, Yale University.

Walton, P.D., Airey, J.A., Sutko, J.L., Beck, C.F., Mignery, G.A., Sudhof, T.C., Deerinck, T.J., & Ellisman, M.H. (1991) Ryanodine and inositol trisphosphate receptors coexist in avian cerebellar Purkinje neurons. *J. Cell Biol.*, 113(5): 1145-57.

Worley, P.F., Baraban, J.M., & Snyder, S.H. (1989) Inositol 1,4,5-trisphosphate receptor binding: autoradiographic localization in rat brain. *J. Neurosci.*, 9(1): 339-46.

Worley, P.F., Baraban, J.M., Supattapone, S., Wilson, V.S., & Snyder, S.H. (1987) Characterization of inositol trisphosphate receptor binding in brain. Regulation by pH and calcium. *J. Biol. Chem.*, 262(25): 12132-6.

Yamada, N., Makino, Y., Clark, R.A., Pearson, D.W., Mattei, M.G., Guenet, J.L., Ohama, E., Fujino, I., Miyawaki, A., Furuichi, T., & et, a.l. (1994) Human inositol 1,4,5-trisphosphate type-1 receptor, $InsP_3R1$: structure, function, regulation of expression and chromosomal localization. *Biochem. J.*, 302(Pt 3): 781-90.

Yamamoto, H.M., Sugiyama, T., Hikichi, K., Mattei, M.G., Hasegawa, K., Sekine, S., Sakurada, K., Miyawaki, A., Furuichi, T., Hasegawa, M., & et, a.l. (1994) Cloning and characterization of human type 2 and type 3 inositol 1,4,5-trisphosphate receptors. *Receptors & Channels*, 2(1): 9-22.

Appendix. Protein biosynthesis:

$$X \xrightarrow{k_0} N \xrightarrow{k_1} P$$

where k_0 = rate of synthesis, k_1 = rate of degradation,

N denotes synthesized proteins, X denotes precursor molecules, and P denotes degraded products.

$$\frac{dN}{dt} = k_0 - k_1 N$$

$$\frac{dN}{k_0 - k_1 N} = dt$$

$$\int \frac{dN}{k_0 - k_1 N} = \int dt$$

$$\ln(k_0 - k_1 N) = -k_1 t + \alpha$$

at t=0, $\alpha = \ln(k_0 - k_1 N_0)$

$$\therefore \ln \frac{k_0 - k_1 N_t}{k_0 - k_1 N_0} = -k_1 t$$

$$k_0 - k_1 N_t = (k_0 - k_1 N_0) e^{-k_1 t}$$

$$N_t = \frac{k_0}{k_1} - (\frac{k_0}{k_1} - N_0) e^{-k_1 t}$$

$$\equiv N_\infty - (N_\infty - N_0) e^{-k_1 t}$$

In general, at t=∞, $N_t = N_\infty = B_{max} = \frac{k_0}{k_1}$

For pulse-chase experiments, as $t \to \infty$, $N_\infty \to 0$

$$\therefore N_t = N_0 e^{-k_1 t}$$

$$\frac{N_t}{N_0} = e^{-k_1 t}$$

$$\ln \frac{N_t}{N_0} = -k_1 t \equiv -\frac{t}{\tau}$$